

POLITECNICO DI TORINO

Corso di Laurea Magistrale in
Ingegneria meccanica

Tesi di Laurea Magistrale
Analysis of Young's modulus of turbine steels



Relatore
prof.ssa Raffaella Sesana

Candidato
Davide D'Alfonso

Anno Accademico 2020/2021

Contents

Contents	3
Introduction	5
Chapter 1	6
1.1 Young's modulus	6
1.2 Experimental technique to measure Young's modulus	10
1.2.1 Static Young's modulus: tensile test	12
1.2.2 Dynamic Young's modulus: Impact excitation technique	14
1.2.3 Other techniques to measure the static and dynamic modulus	23
1.2.3.1 Three-point bending test	23
1.2.3.2 Nanoindentation testing	25
1.2.3.3 Sonic resonance technique	26
Chapter 2	31
2.1 Materials	31
2.1.1 Steel 1	32
2.1.2 Steel 2	35
2.1.3 Steel 3	36
2.2 Measurements techniques	38
2.2.1 Technique to measure static Young's modulus at room temperature	38
2.2.2 Technique to measure the static Young's modulus at high temperatures	40
2.2.3 Technique to measure the dynamic Young's modulus at room temperature	41
2.2.4 Technique to measure the dynamic Young's modulus at high temperature	42
2.3 Testing equipment and devices	43
2.3.1 Tensile test	43
2.3.1.1 Axial extensometer MTS 634.12F-25	46
2.3.1.2 Axial extensometer Epsilon model 3549	47
2.3.1.3 Thermometer GHM 3251 and Thermocouple	48
MTC11-00-700-200-10	
2.3.2 Dynamic modulus at room temperature	50
2.3.3 Dynamic modulus at high temperatures	52
2.4 Specimens	55
2.4.1 Specimens for tensile tests	55
2.4.2 Specimens for impulse excitation	57

2.5 Test plan and experimental set-up	59
2.5.1 Test plan and experimental set-up to measure static Young's modulus at room temperature	59
2.5.2 Test plan and experimental set-up to measure static Young's modulus at high temperatures	60
2.5.3 Experimental set-up and test plan to measure dynamic Young's modulus at room temperature	61
2.5.4 Experimental set-up and test plan to measure dynamic Young's modulus at high temperature	62
2.6 Data analysis	64
2.6.1 Analysis of the data of the tensile tests	64
2.6.2 Analysis of the data of impulse excitation tests	72
2.6.3 Procedure to find the relationship between static and dynamic Young's modulus	73
Chapter 3	74
Results	74
3.1 Results of the static Young's modulus for steel 1	74
3.2 Results of the static Young's modulus for steel 2	91
3.3 Results of the static Young's modulus for steel 3	107
3.4 Results of the dynamic Young's modulus at room temperature	123
3.5 Results of the dynamic Young's modulus at high temperatures	125
3.6 Comparison between static and dynamic modulus and between dynamic Young's modulus of small and full size specimen	130
3.7 Relationships between dynamic and static Young's moduli for small and full size	136
Conclusion	140
Bibliography	141

Introduction

This work focuses on the study of the three turbine steels, in particular, to find a relationship between Young's modulus and temperature and a correlation between static and dynamic Young's modulus.

The dissertation is divided in 3 chapters. In the first, after the definitions of static and dynamic Young's modulus, 5 experimental techniques (tensile test, impact excitation technique, three-point bending test, sonic resonance method and nanoindentation) to measure this characteristic are presented.

The second chapter contains the description of the experimental activity, in particular: the select materials and their properties found in the literature, the two techniques used in this work and the chosen parameters, the devices adopted, the testing equipment and devices, the specimens, the test plan the experimental set-up and the way to analyze the data.

In the third chapter, the results are presented and discussed.

The conclusions summarizes what in done in this work and explains how to continue this work.

Chapter 1

1.1 Young's modulus

Young's modulus describes the elastic properties of a solid undergoing tension or compression monotonic testing in only one direction.

Sometimes referred to as the modulus of elasticity, Young's modulus is equal to the longitudinal stress divided by the strain [1], where stress and strain may be described as follows in the case of a metal bar under tension (figure 1):

- Stress = Force/cross sectional area;
- Strain = change in length/original length.

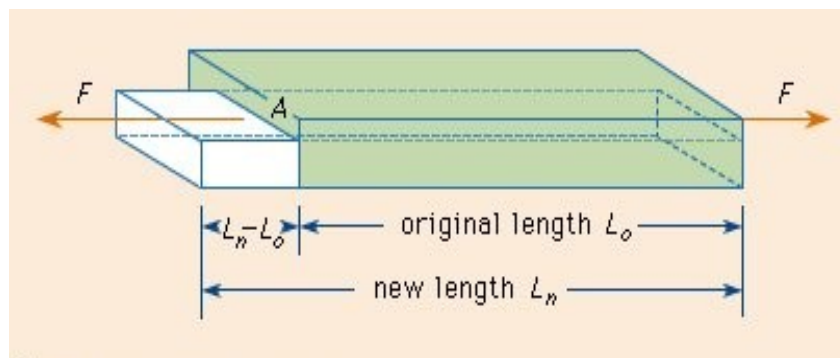


Figure 1: Generic specimen under stress

The SI unit of Young's modulus is Pascal and the common symbol is “ E ”. In general, when we talk about Young's modulus we are referring to static Young's modulus which is obtained by quasi-static tests (as tensile test, three-point bending test and nanoindentation test).

Differently to the static Young's modulus, the dynamic Young's modulus is defined as the ratio of stress to strain under vibratory conditions. In this case, a specimen is exposed to a cyclic stress ($\sigma = \sigma_0 \sin(\omega t)$) which involves a cyclic strain with the same frequency but with a phase lag ($\varepsilon = \varepsilon_0 \sin(\omega t + \delta)$). [2]

Static Young's modulus enables the calculation of the change in the dimension of a bar made of an isotropic elastic material under tensile or compressive loads. For instance, it predicts how much a material sample extends under tension or shortens under compression. Young's modulus is

also used in order to predict the deflection that will occur in a beam when a load is applied at a point in between the beam's supports. There are also multiple other reasons which have led to the study of this magnitude. Scientists and engineers have felt the need to measure the Young's modulus of the materials.

In the table 1 are listed mechanical properties of common materials including static Young's modulus. [3]

Material	Yield Strength [MPa]	UTS [MPa]	Young's Modulus [GPa]
Aluminum	35	90	69
Copper	69	200	117
Brass	75	300	120
Iron	130	262	170
Nickel	138	480	210
Steel	180	380	200
Titanium	450	520	110
Molybdenum	565	655	330
Zirconium alloy (typical cladding)	380	510	99
08Kh18N10T stainless steel	216	530	196
Alloy 304L stainless steel	241	586	193
SA-508 Gr.3 Cl.2 (low-alloy ferritic steel)	500	700	210
15Kh2NMFA (low-alloy ferritic steel)	490	610	220

Table 1: mechanical properties of common elements

For example, Young's modulus of the steel is about three times greater than that of aluminum, which means that it takes three times as much force to stretch a steel bar the same amount as a similarly shaped aluminum bar.

Young's modulus is a not constant and depends on the following factors: temperature, chemical composition, crystalline anisotropy, hardening, and heat treatments.

In general, as the temperature increases, Young's modulus decreases. The figure 2 shows the experimental behavior of elastic modulus for some metal alloys. [4]

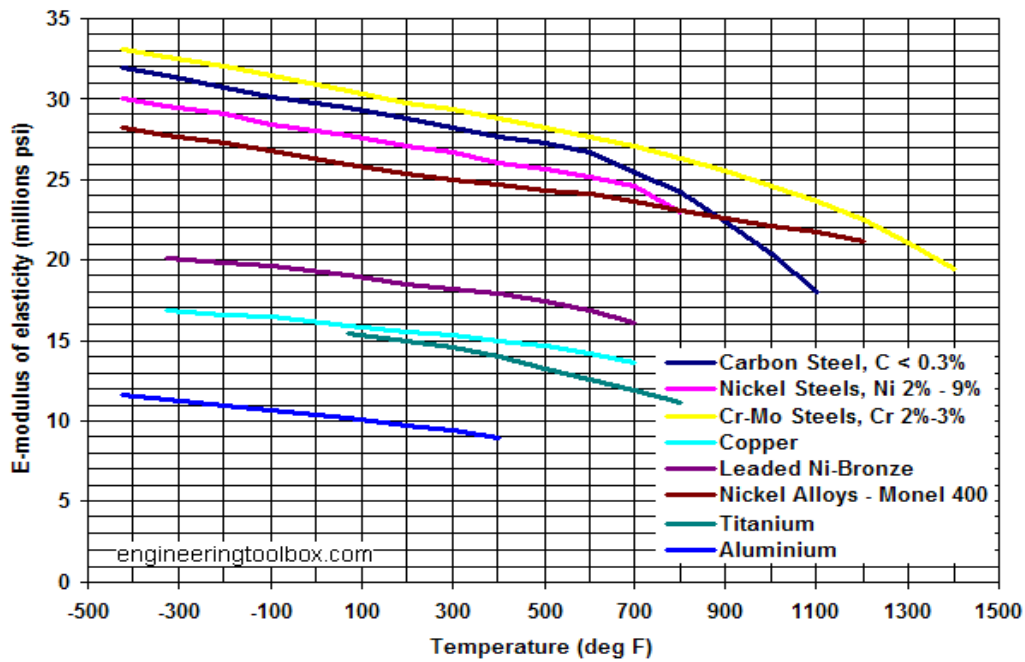


Figure 2: General trend of Young's modulus of some metal alloys with temperature

For the steels, the alloy elements inserted in a metal matrix change the distance between the atoms altering in this way the force of the atomic bonds and therefore the mechanical properties. The table 2 shows this phenomenon, indicating how Young's modulus of the steel changes with some alloy elements (10^6 psi = 6,8948 GPa). [4]

Steel alloys	Young's modulus (10^6 psi)
Carbon steel C \leq 0.3%	29.5
Carbon steel C \geq 0.3%	29.3
Carbon-molybdenum steels	29.2
Nickel steels Ni 2% - 9%	27.8
Cr-Mo steels Cr 1/2% - 2%	29.7
Cr-Mo steels Cr 2 1/4% - 3%	30.6
Cr-Mo steels Cr 5% - 9%	30.9
Chromium steels Cr 12%, 17%, 27%	29.2
Austenitic steels (TP304, 310, 316, 321, 347)	28.3

Table 1: General trend of Young's modulus of some metal alloys with temperature

Another factor which affects Young's modulus is the crystalline anisotropy. It is here reported as an example of some tensile tests performed in the company Comtes which show how the elastic modulus changes with the orientation of crystalline grains. For this purpose, 12 specimens of the same steel alloy, with the same initial dimensions but different orientation of

crystalline grains, obtained by rolling, have been analyzed. 4 specimens with 0 degrees orientation, 4 specimens with 45 degrees orientation and 4 specimens with 90 degrees orientation underwent tensile monotonic testing. The resulting stress-strain curves are in the figure 3 and the results in the table 3.

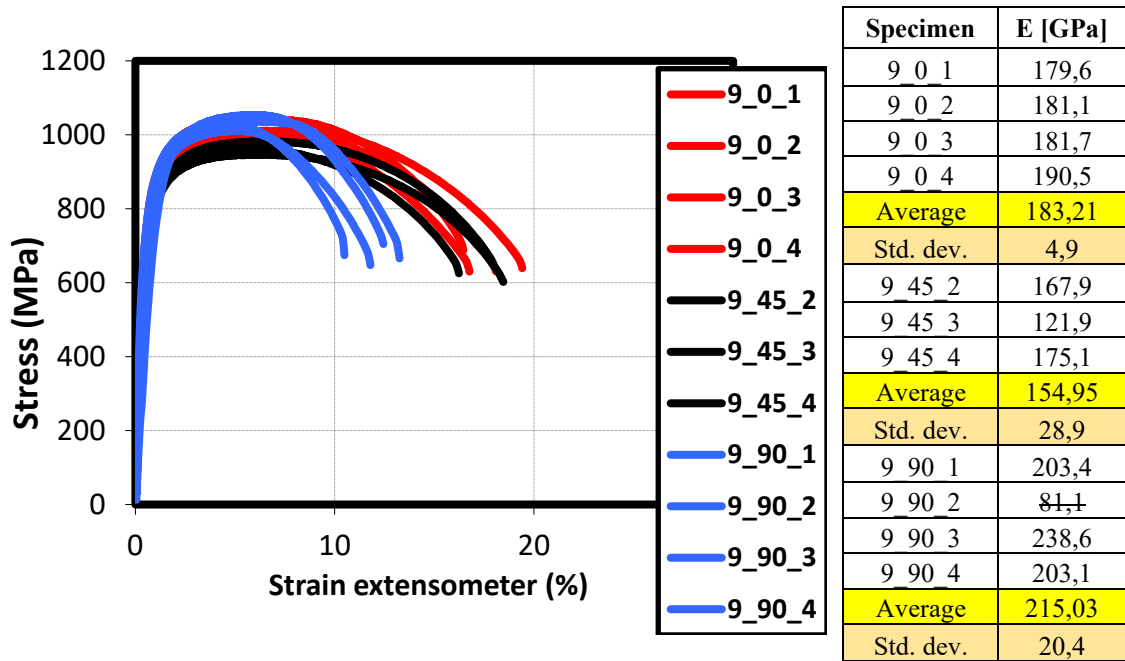


Figure 3: Stress-strain curves for different orientations

Table 2: Results tesile tests

The specimens with an orientation of crystalline grains of 0° provided an average elastic modulus of 183,21 GPa; the specimens with 45° have an average Young’s modulus of 154,95 GPa and those with 90° of orientation have an average elastic modulus of 215,03 GPa.

The thermo-mechanical processing affects Young’s modulus too as in the case of the hardening which increases Young’s modulus. [5]

1.2 Experimental technique to measure Young's modulus

The literature offers different techniques to measure Young's modulus; the most commonly used are tensile test, impact excitation technique, three-point bending test, sonic resonance method and nanoindentation. The table 4 indicates the standards which these techniques follow.

Technique	Static Young's modulus	Dynamic Young's modulus	Standard
Tensile test	✓		BN EN ISO 6892-1: 2016
Impact excitation		✓	ASTM E1876-15
Three-point bending	✓		ASTM E 2769-18
Sonic resonance		✓	ASTM E1875-20a
Nanoindentation	✓		The IBIS Handbook of Nanoindentation

Table 4: Techniques to measure Young's modulus and relative standards

The table 5 summarizes the advantages and the disadvantages of the tensile test and the dynamic methods.

Tensile Test	Dynamic Methods
<p>Advantages:</p> <ul style="list-style-type: none"> • “Engineering value” for modulus • Generation of stress-strain curve • Widely available test equipment 	<p>Advantages:</p> <ul style="list-style-type: none"> • Quick, simple, non-destructive • Good accuracy • Uses small specimens • High temperature measurement • Can readily measure shear modulus and Poisson’s ratio
<p>Disadvantages:</p> <ul style="list-style-type: none"> • High accuracy strain measurement required • Needs for extensometers • Specialized test • Larger specimens required • Large interlaboratory scatter • Accurate high temperature measurements are difficult 	<p>Disadvantages:</p> <ul style="list-style-type: none"> • Relevance of dynamic modulus to engineering applications and design • Sensitive to dimensional tolerances • Methods do not always work well for some materials and composites • Calculations require some knowledge of other material parameters • Equipment not widely available

Table 5: advantages and disadvantages of the tensile test and the dynamic methods

In this work, comparisons between static and dynamic Young’s modulus are made on three turbine steels using tensile test and impact excitation technique. The exact procedure will be explained in the following.

1.2.1 Static Young's modulus: tensile test

The tensile test is a quasi-static test which leads to the determination of static Young's modulus.

According to the standard BS EN ISO 6892-1:2016, the tensile test consists in an uniaxial force applied to a standard specimen.

The applied force and the strain of the specimen are measured through load cells and strain gauges. The axial stress is determined by dividing the measured force by the original cross-sectional area of the specimens. The stress and the strain are reported in a plot and the slope of the elastic zone of the stress-strain curve is identified as Young's modulus. [6]

The determination of Young's modulus is influenced by several parameters; these include characteristics of the specimen such as orientation of grains relative to the direction of the stress, grain size, residual stress, previous strain history, dimensions, and eccentricity; testing conditions, such as alignment of the specimen, speed of testing, temperature, temperature variations, condition of test equipment, ratio of error in applied force to the range in force values, and ratio of error in extension measurement to the range in extension values used in the determination and interpretation of data. [7]

The literature suggests different ways to calculate the elastic modulus and the laboratories have the possibilities to choose which one to use since there is not one universally correct.

For materials with linear elastic behavior, the slope of the elastic zone is Young's modulus.

For materials with nonlinear elastic behavior, it is possible to use one of the following methods: [7]

- initial tangent modulus which considers Young's modulus equivalent to the slope of the tangent in the origin of stress-strain curve;
- tangent modulus: the considered value is the slope of the stress-strain curve at any specified stress or strain in the elastic zone;
- secant modulus which uses the slope of the secant drawn from the origin to any specified point on stress-strain curve;
- the chord modulus takes in consideration the slope of the chord drawn between any two specified points on the stress-strain curve below the elastic limit of the material.

In the specific case in which the tensile test is adopted just to measure Young's modulus, it is appropriate to perform a minimum of 3 cycles from the preload stress to a maximum stress without exceeding the elastic region. [6]

Regarding the tensile tests at high temperature, it needs of furnaces and suitable devices that withstand high temperatures, but this leads to less precise results. [8]

1.2.2 Dynamic Young's modulus: Impact excitation technique

The dynamic Young's modulus is based on the analysis of the vibrations of the test specimens.

The two main methods to measure the dynamic Young's modulus are the impact excitation method and resonance technique; in this paragraph the first method is described while the second in the paragraph 1.2.3.3.

The special equipment RFDA (Resonant Frequency and Damping Analysis) from the company IMCE allows to correlate the free vibrations of the test specimens to their Young's modulus. The equipment RFDA works following the standard ASTM E1876-15.

The standard ASTM E1876-15 permits to use parallelepiped or a disk specimens without indicating standard dimensions. However, the minimum length of the rectangular specimens has to be 20 mm at room temperature and 30 mm at high temperature while the disk specimens must have a minimum diameter of 20 mm at room temperature and 30 mm at high temperature to measure Young's modulus.

The impact excitation method consists of 3 steps (as show in the figure 4): excitation of the specimen, detection of free vibration and signal analysis.

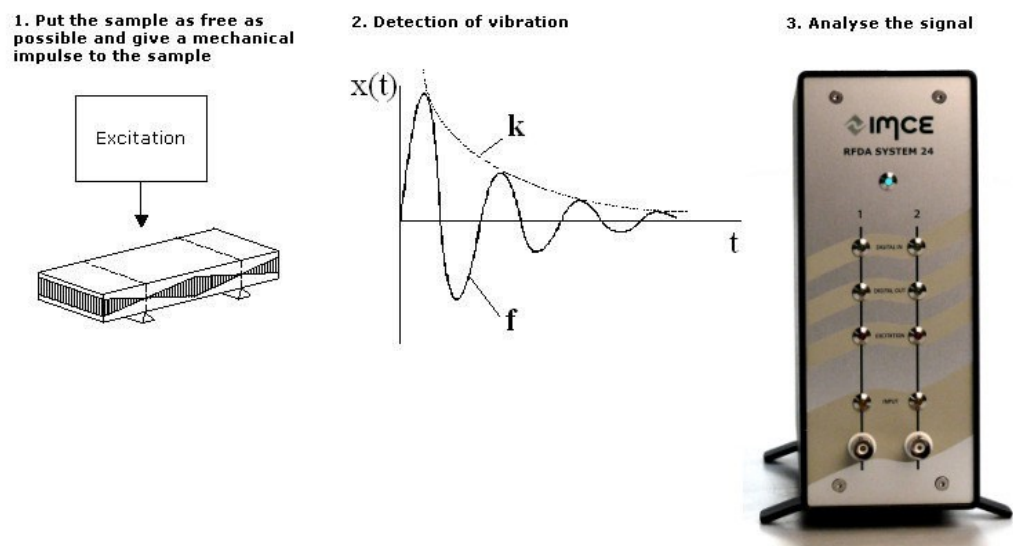


Figure 4: Rfda (Resonant Frequency and Damping Analysis) operating principle

The figures 5, 6, 7 and 8 show the main types of vibration of a rectangular and disk specimens when they are hit by an automatic or manual tapping device. [9]

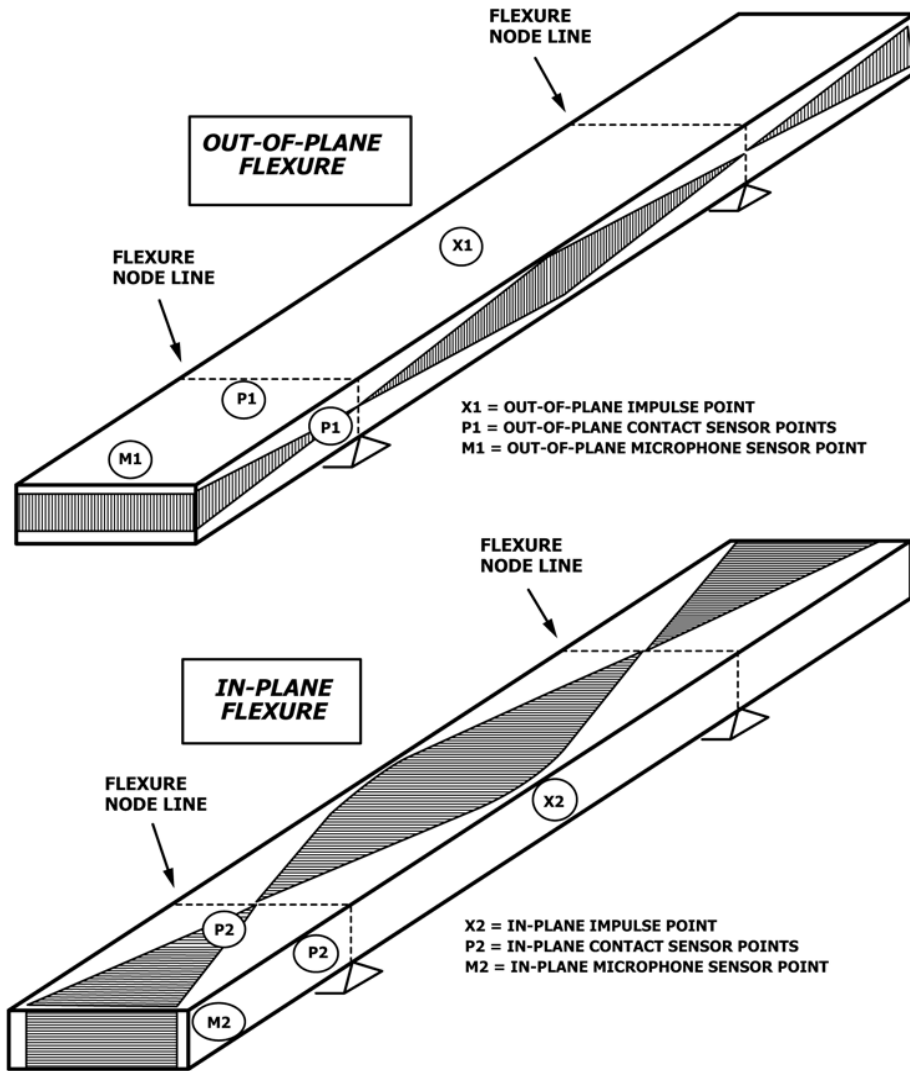


Figure 5: Flexural vibrations for rectangular samples

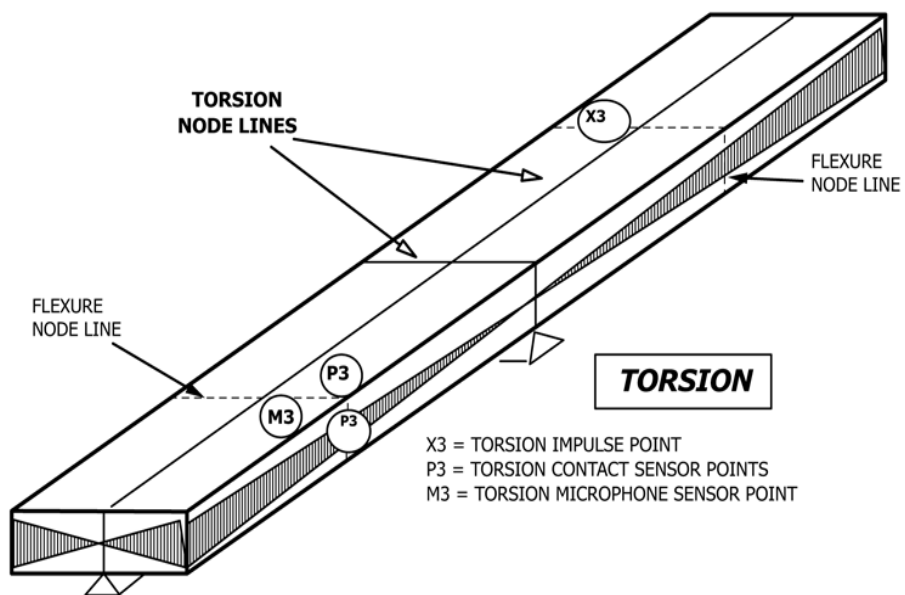


Figure 6: torsional vibration for rectangular samples

The rectangular specimens can vibrate in flexural (out-of-plane and in plane) and in torsion modes. The out-of-plane flexural vibration is indicated how the fundamental flexural resonant frequency and is used to calculate the dynamic Young's modulus while the fundamental torsional resonant frequency is used to calculate the dynamic shear modulus. The figure 5 and 6 show how to strike the samples to get the flexural and torsional resonant frequencies and where place the supports and the microphone. [9]

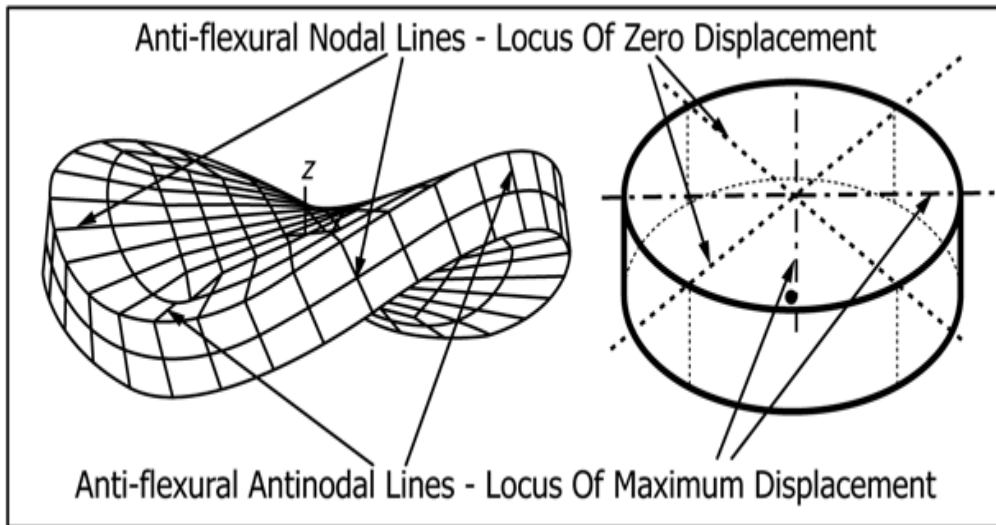


Figure 7: first natural vibration

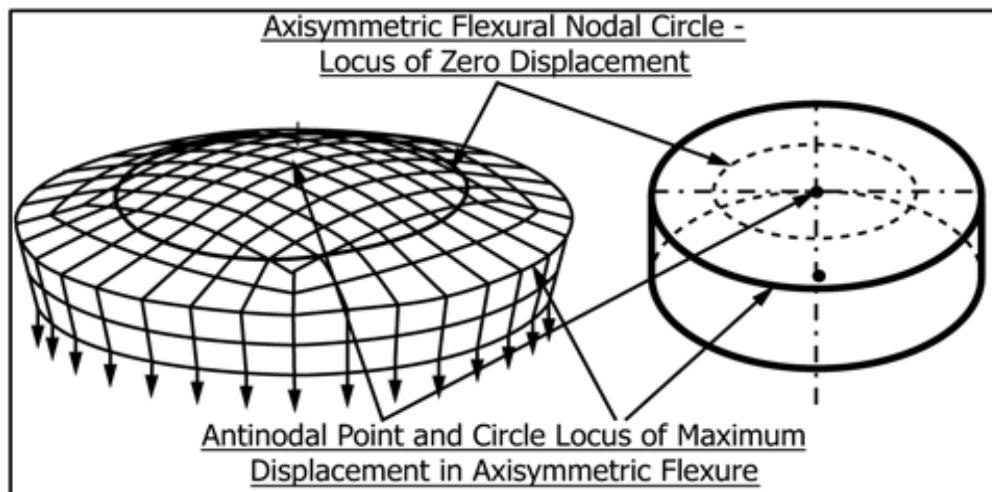


Figure 8: second natural vibration

The first and second natural vibrations of the disks are both important to arrive to dynamic Young's modulus.

The figures 9 show where to strike the specimens, where to place the supports and the microphone to get the resonant frequencies. [9]

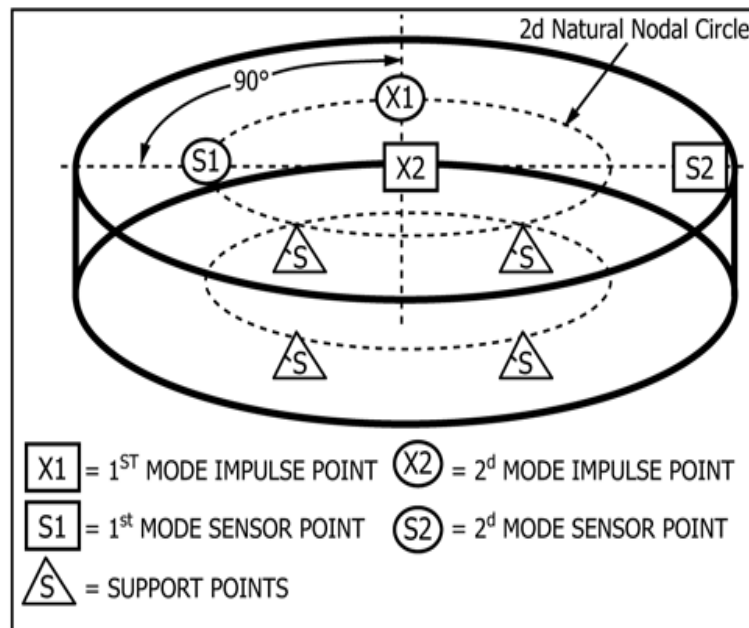


Figure 9: impulse and sensor points and supports for first and second resonant frequencies.

When the specimen (a parallelepiped or a disk) is excited by a small mechanical impulse through a tapping device, the energy of the impulse is dissipated by the material into a vibration. This vibration has a frequency spectrum according to specimen resonant frequencies which are related to the elastic properties of the material, the geometry and the density. The damping of every frequency depends on the type of material. [10]

The vibration is detected by a microphone which produces an electrical signal which is sent to the electrical part of the RFDA equipment.

The signal is amplified, conditioned and sent to the computer where it is analyzed by the RFDA software program.

The specially developed mathematical algorithm of RFDA software program calculates each frequency and damping from the detected frequency spectrum assigning to each frequency a sinusoidal and damped vibration similar to that in figure 10. [10]

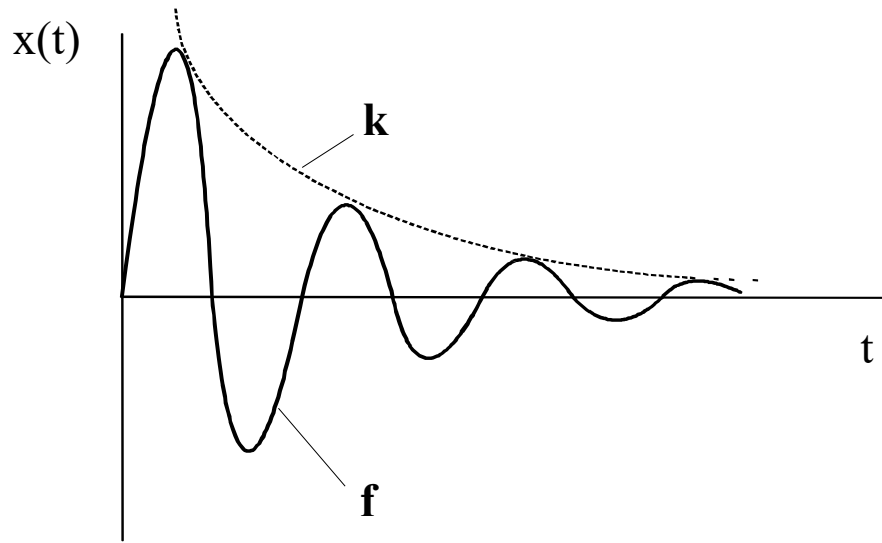


Figure 10: Sinusoidal damped vibration

where:

$$x(t) = Ae^{-kt} \sin(\omega t + \Phi) \quad (1)$$

For each ω the corresponding frequency is calculated as $f = \frac{\omega}{2\pi}$.

For the rectangular specimens, the fundamental flexural and the torsional resonant frequencies are used respectively for the determination of dynamic Young's modulus and dynamic shear modulus.

For the disks, the first and the second natural resonant frequencies are important to calculate the dynamic Young's modulus.

The block diagram which summarizes this procedure is in figure 11.

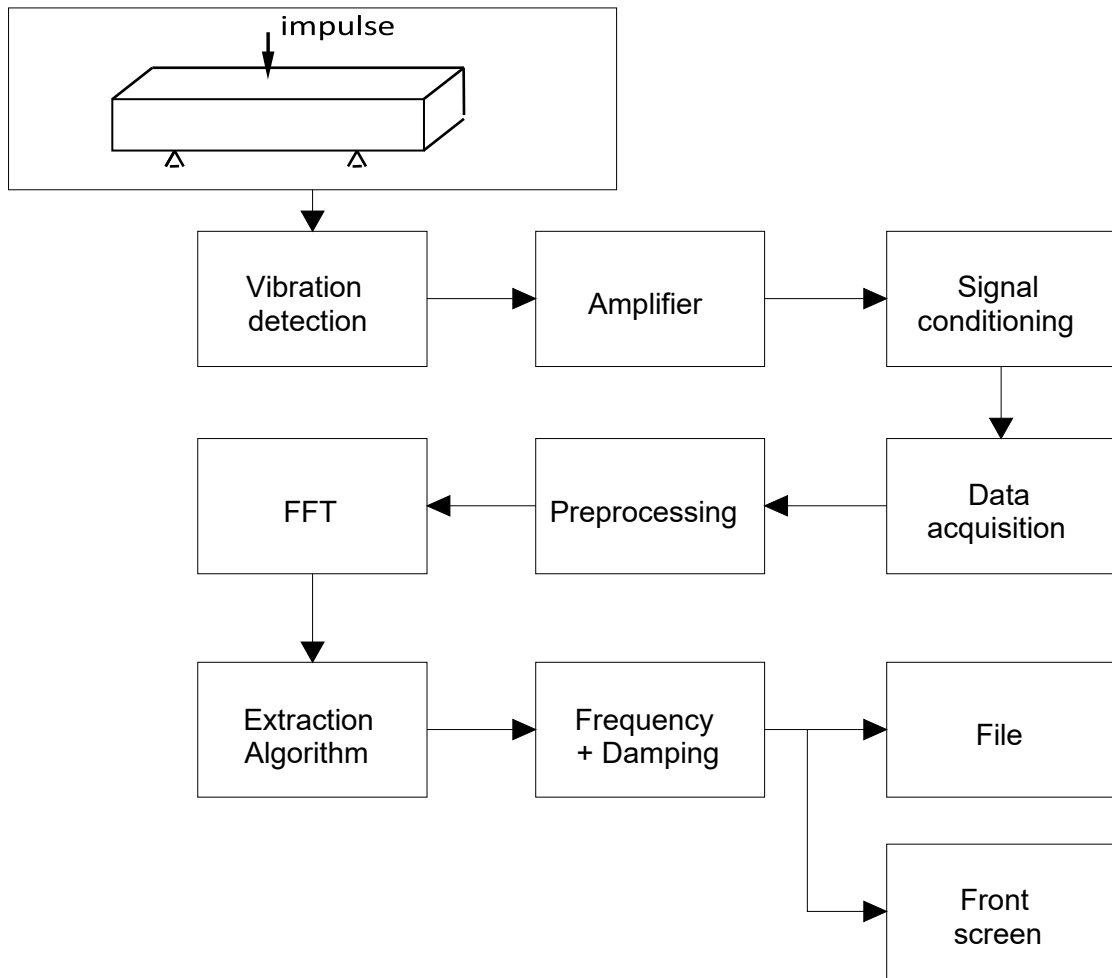


Figure 11: Block diagram of the RFDA (Resonant Frequency and Damping Analysis)

For dynamic Young's modulus of a rectangular bars: [9]

$$E = 0,9465 \left(\frac{mf_f^2}{b} \right) \left(\frac{L^3}{t^3} \right) T_1 \quad (2)$$

where:

E = Young's modulus (Pa);

m = mass of the bar (g);

b = width of the bar (mm);

L = length of the bar (mm);

t = thickness of the bar (mm);

f_f = fundamental flexural resonant frequency of bar (Hz);

T_1 is a correction factor for fundamental flexural mode to account for finite thickness of bar, Poisson's ratio and so forth. [9]

$$T_1 = 1 + 6,585(1 + 0,0752\mu + 0,8109\mu^2) \left(\frac{t}{L}\right)^2 - 0,868 \left(\frac{t}{L}\right)^4 - \left[\frac{8,340(1 + 0,2023\mu + 2,173\mu^2) \left(\frac{t}{L}\right)^4}{1 + 6,338(1 + 0,1408\mu + 1,536\mu^2) \left(\frac{t}{L}\right)^2} \right]$$

If $L/t \geq 20$, T_1 can be simplified to the following:

$$T_1 = \left[1 + 6,585 \left(\frac{t}{L}\right)^2 \right] \quad (3)$$

Dynamic shear modulus of a rectangular bars is: [9]

$$G = \frac{4Lmf_t^2}{bt} R \quad (4)$$

where:

G = shear modulus (Pa);

f_t = fundamental torsional resonant frequency of bar (Hz);

R is a geometrical correction factor. [9]

Poisson's ratio is: [9]

$$\mu = \left(\frac{E}{2G}\right) - 1 \quad (5)$$

where:

μ = Poisson's ratio;

G = shear modulus (Pa);

E = Young's modulus (Pa).

The uncertainties of dynamic Young's modulus, dynamic shear modulus and Poisson's ratio are calculated in according with "Standards Measurement & Testing Project No. SMT4-CT97-2165":

$$U(E)\% = \left[(U(m)\%)^2 + (2U(f_f)\%)^2 + (U(b)\%)^2 + (3U(L)\%)^2 + (3U(t)\%)^2 \right]^{0,5} \quad (6)$$

$$U(G)\% = \left[(U(m)\%)^2 + (2U(f_t)\%)^2 + (U(b)\%)^2 + (U(L)\%)^2 + (U(t)\%)^2 \right]^{0,5} \quad (7)$$

$$U(\mu)\% = [(U(E)\%)^2 + (U(G)\%)^2]^{0.5} \quad (8)$$

where $U(a)\%$ represents the percentage uncertainty of the magnitude a (eg. $U(E)\% = 100\% \times U(E)/E$). [11]

For the disks dynamic Young's modulus E is the average of E_1 and E_2 . [9]

$$E = \frac{E_1 + E_2}{2} \quad (9)$$

where

$$E_1 = \frac{[37,6991f_1^2D^2m(1 - \mu^2)]}{(K_1^2t^3)} \quad (10)$$

and

$$E_2 = \frac{[37,6991f_2^2D^2m(1 - \mu^2)]}{(K_2^2t^3)} \quad (11)$$

E_1 = first natural calculation of dynamic Young's modulus (MPa);
 E_2 = second natural calculation of dynamic Young's modulus (MPa);
 f_1 = first natural resonant frequency of the disk (Hz);
 f_2 = second natural resonant frequency of the disk (Hz);
 D = diameter of the disk (mm);
 m = mass of the disk (g);
 μ = Poisson's ratio;
 K_1 = first natural geometric factor;
 K_2 = second natural geometric factor;
 t = thickness of the disk (mm);
 r = radius of the disk (mm).

How to calculate K_1 , K_2 and μ is indicated in ASTM E 1876 – 15.

Dynamic shear modulus for disk is calculated from Young's modulus and Poisson's ratio: [9]

$$G = \frac{E}{[2(1 + \mu)]} \quad (12)$$

1.2.3 Other techniques to measure the static and dynamic elastic modulus

In this paragraph, the techniques that can be used to calculate Young's modulus but not used in this work are briefly described. Regarding the static modulus, the methods which will be discussed are the four-point bending test and nanoindentation, while for dynamic modulus, the resonant ultrasound spectroscopy.

1.2.3.1 Three-point bending test

This test method, in accordance with the standard ASTM E 2769–18, describes the use of linear controlled-rate-of-loading in three-point bending to determine the static elastic modulus of isotropic specimens in the form of rectangular bars.

A specimen of rectangular cross section is tested in three-point bending (flexure) as a beam. The specimens used in this test method are ordinarily in the form of rectangular beams with a dimensional ratio of 1:3:12.

The beam rests on two supports and is loaded midway between the supports as in figure 12.

The procedure of the test consists of the following steps: [12]

- 1) Measure the test length (L) of the test specimen as the distance between the two support points of the flexure fixture;
- 2) Measure the width (b) and thickness (d) of the specimen midway along its length;
- 3) Center the specimen on the supports of the flexure fixture, with the long axis of the specimen perpendicular to the loading nose and supports;
- 4) Place the furnace around the test specimen and program the temperature to the desired isothermal test temperature;
- 5) Preload the test specimen with $0.01 \text{ N} \pm 1 \%$ of full scale. Set the displacement-axis signal to be zero;
- 6) Apply a linearly increasing force at a rate of 0.1 N/min up to the maximum applicable load while recording the applied force (or calculated stress) and specimen displacement (or calculated strain) as a function of time.
- 7) Terminate the test if the maximum strain reaches 30 mm/m (3 %) or the proportional limit, the yield force, the rupture force or the

maximum force of the analyzer has been reached, whichever occurs first.

- 8) Once maximum force is achieved, terminate the force program and remove the load from the test specimen. Cool the apparatus to ambient temperature;
- 9) Display the thermal curve with stress or force on the Y-axis and strain or deflection on the X-axis such as that in figure 13.

Determine the slope of the linear portion of the curve which is between the upper limit of the toe and the proportional limit.

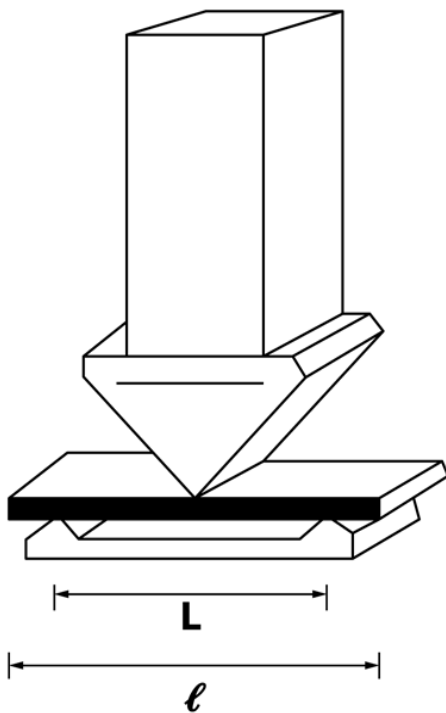


Figure 12: Flexure support geometry

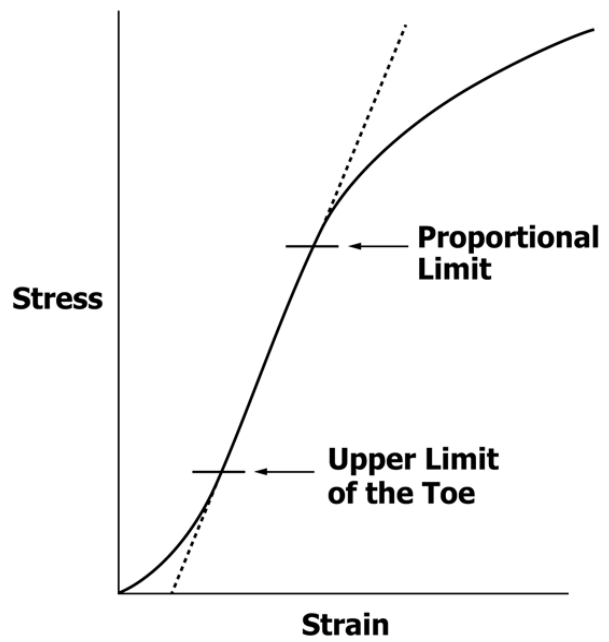


Figure 13: Stress- strain curve

The static elastic modulus E is the ratio of stress with respect to strain within the elastic limit of the stress-strain curve: [9]

$$E = \frac{\sigma}{\varepsilon} \quad (13)$$

where:

$$\sigma = \frac{3FL}{2bd^2} \quad (14)$$

$$\varepsilon = \frac{6Dd}{L^2} \quad (15)$$

σ = stress (MPa);
 ε = strain;
 b = beam width (mm);
 d = beam thickness (mm);
 D = beam displacement (mm) ;
 F = force (N);
 L = support span (mm).

1.2.3.2 Nanoindentation testing

Indentation at the nanometer scale with a nanoindenter (figure 14) using a diamond indenter is a widely used technique to determine mechanical properties of materials during indentation and therefore static Young's modulus . [13]

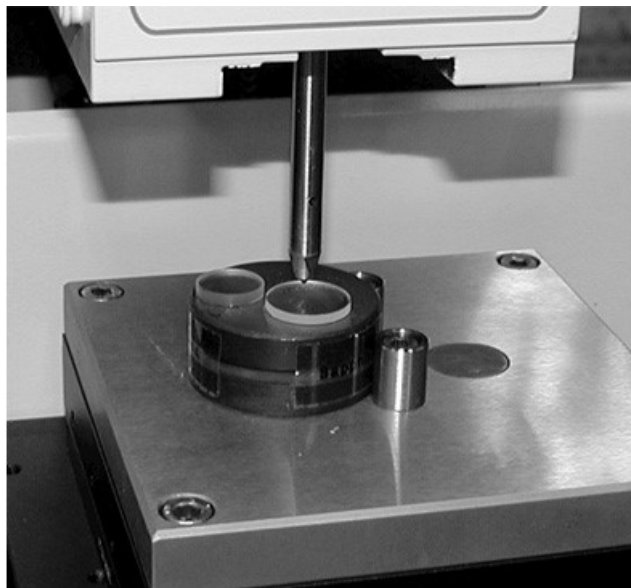


Figure 14: Schematic of nanoindentation test

The position of the indenter relative to the test surface of the specimen is constantly measured with a sensitive capacitance gage. The load (P) applied to make the indent is monitored and recorded continuously as a function of displacement (z). A typical indentation load-displacement curve is shown in figure 15.

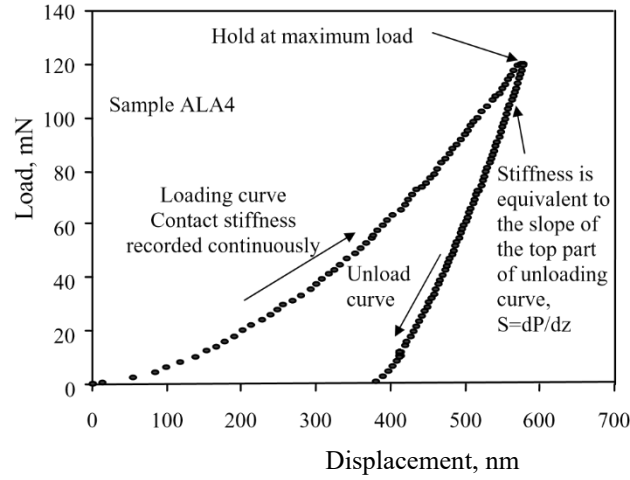


Figure 15: Typical indentation load–displacement curve

The stiffness (S) of the specimen is continuously detected or calculated as the slope of the top part of the unloading curve of the load-displacement cycle. The relationship between stiffness and Young’s modulus is defined in following equation: [13]

$$S = \frac{2\beta}{\sqrt{\pi}} \sqrt{AE_r} \quad (16)$$

where S is the stiffness, A is the contact area, E_r the reduced modulus and β an indenter geometry dependent constant.

E_r is defined as: [13]

$$\frac{1}{E_r} = \frac{1 - \nu^2}{E} + \frac{1 - \nu_0^2}{E_0} \quad (17)$$

where E and E_0 are the Young’s modulus of the sample and the indenter, and ν and ν_0 the Poisson’s ratio of the test material and the indenter, respectively.

1.2.3.3 Sonic resonance technique

This technique is used to determinate dynamic Young’s modulus of elastic materials following the standard E1875-20a.

The specimens of elastic materials possess specific mechanical resonant frequencies that are determined by the modulus of elasticity, mass, and geometry of the test specimen. Therefore, the dynamic elastic properties of a material can be computed if the geometry, mass, and mechanical resonant frequencies of a suitable test specimen of that material can be measured. The dynamic Young’s modulus is determined using the fundamental flexural

resonant frequency. The dynamic shear modulus, or modulus of rigidity, is found using the fundamental torsional resonant frequency. Dynamic Young's modulus and dynamic shear modulus are used to compute Poisson's ratio.

This test method is specifically appropriate for materials that are elastic, homogeneous, and isotropic.

The test apparatus is shown in figure 16. It consists of a variable-frequency audio oscillator, used to generate a sinusoidal voltage, and a power amplifier and suitable driving transducer to convert the electrical signal to a mechanical driving vibration. A frequency meter, which should be digital, monitors the audio oscillator output to provide an accurate frequency determination. A suitable suspension-coupling system supports the test specimen. A detecting transducer senses the mechanical vibration in the specimen and to convert it into an electrical signal that is passed through an amplifier and displayed on an indicating meter. The meter may be a voltmeter, microammeter, or oscilloscope. An oscilloscope should be used, because it enables the operator to positively identify resonances, including higher order harmonics, by Lissajous figure analysis. If a Lissajous figure is desired, the output of the audio oscillator should be displayed on the horizontal axis of the oscilloscope. If temperature-dependent data are desired, a suitable furnace or cryogenic chamber shall be used.

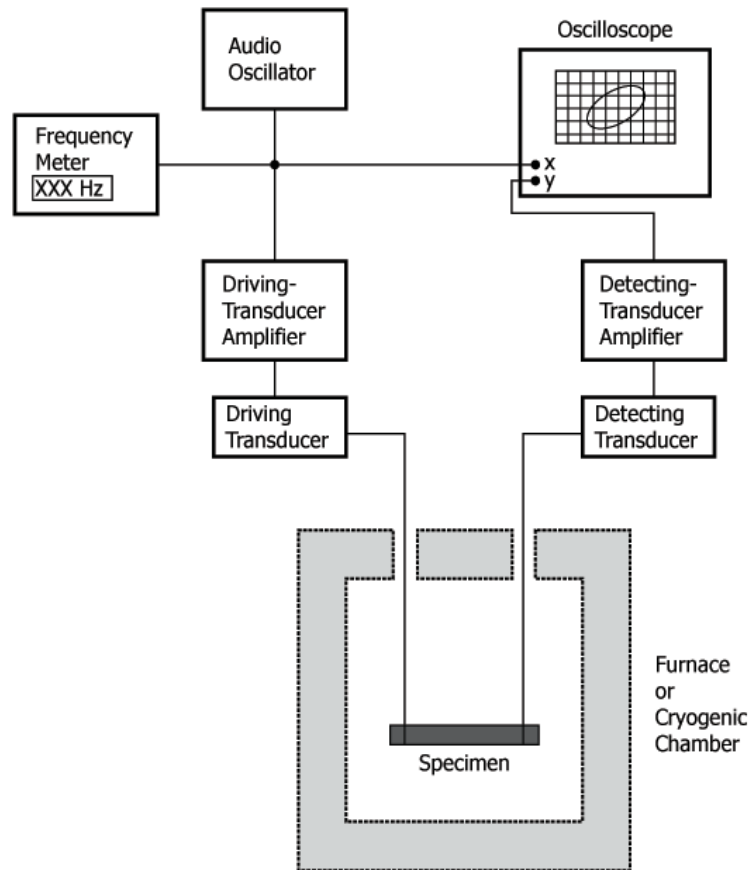


Figure 16: Block diagram of a typical test apparatus for sonic resonance tests

If the specimen is supported on direct contact supports, the supports shall permit the specimen to oscillate without significant restriction in the desired mode. In flexural modes, the specimen should be supported at its transverse fundamental node locations ($0.224 L$ from each end). In torsional modes the specimen should be supported at its center point (as in figure 17). The supports should have minimal area in contact with the specimen and shall be cork, rubber, or similar material. In order to properly identify resonant frequencies, the transducers should be movable along the total specimen length and width. The transducer contact pressure should be consistent with good response and minimal interference with the free vibration of the specimen.

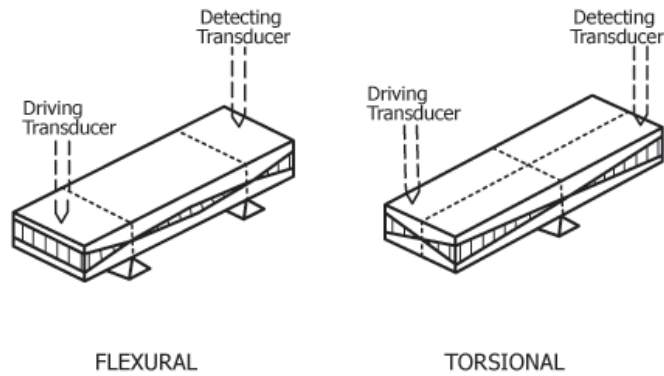


Figure 17: Specimen positioned for measurement of flexural and torsional resonant frequencies using direct support and direct contact transducers

The specimens have to be rectangular or circular in cross section. A slender specimen with a ratio of length to minimum cross-sectional dimension greater than 5 and approximately 25 should be used for ease in calculation. For dynamic shear modulus measurements of rectangular specimens, a ratio of width to thickness of 5 should be used to minimize experimental difficulties. Specimens shall have a minimum mass of 5 g to avoid coupling effects.

The procedure of this test consists in the following steps:

1. Support the specimen properly along the nodes.
2. Activate the equipment so that power adequate to excite the specimen is delivered to the driving transducer.
3. Set the gain of the detector circuit high enough to detect vibration in the specimen and to display it on the oscilloscope screen with sufficient amplitude to measure accurately the frequency at which the signal amplitude is maximized.
4. Scan frequencies with the audio oscillator until specimen resonance is indicated by a sinusoidal pattern of maximum amplitude on the oscilloscope or by a single closed loop Lissajous pattern.
5. Find the fundamental flexural resonant frequency.
6. The dimensions and mass of the specimen may be measured before or after the test.

Dynamic Young's modulus of rectangular bars is calculated as follows:
[14]

$$E = 0,9465 \left(\frac{mf_f^2}{b} \right) \left(\frac{L^3}{t^3} \right) T_1$$

where:

E = Young's modulus (MPa);

m = mass of the bar (g);

b = width of the bar (mm);

L = length of the bar (mm);

t = thickness of the bar (mm);

f_f = fundamental flexural resonant frequency of bar (Hz);

T_1 is a correction factor for fundamental flexural mode to account for finite thickness of bar, Poisson's ratio and so forth. [14]

$$T_1 = 1 + 6,585(1 + 0,0752\mu + 0,8109\mu^2) \left(\frac{t}{L}\right)^2 - 0,868 \left(\frac{t}{L}\right)^4 - \left[\frac{8,340(1 + 0,2023\mu + 2,173\mu^2) \left(\frac{t}{L}\right)^4}{1 + 6,338(1 + 0,1408\mu + 1,536\mu^2) \left(\frac{t}{L}\right)^2} \right]$$

If $L/t \geq 20$, T_1 can be simplified to the following:

$$T_1 = \left[1 + 6,585 \left(\frac{t}{L}\right)^2 \right]$$

For cylindrical specimens, dynamic Young's modulus E is: [14]

$$E = 1,6067(mf_f^2) \left(\frac{L^3}{D^4}\right) T_1 \quad (18)$$

where:

m = mass of the bar (g);

f_f = fundamental flexural resonant frequency of bar (Hz);

L = length of the bar (mm);

D = diameter of the bar (mm);

f_f = fundamental flexural resonant frequency of bar (Hz);

T_1 is a correction factor for fundamental flexural mode to account for finite diameter of bar, Poisson's ratio and so forth. [14]

Chapter 2

This work is focused on the correlation between static and dynamic Young's modulus for selected materials. The selected materials are turbine steels which will be indicated as steel 1, steel 2 and steel 3 because it prefers to keep hidden the chemical composition.

The measurements of static Young's modulus from tensile tests are performed from room temperature to operating temperature of steam turbines (approximately 650°C).

The dynamic Young's modulus is based on the analysis of vibrations of the selected materials. The special equipment RFDA from the company IMCE allows to correlate the free vibrations of the specimens to their Young's modulus.

The tests are done on different size specimens (standard and miniature specimens) from RT to operating temperature of steam turbines.

In this chapter, the materials and their mechanical characteristics useful to this work, the measurements techniques of static and dynamic Young's modulus, the test equipment and the devices, the specimens, the experimental set-up, the procedure for data analysis are shown.

2.1 Materials

The providers of the three different alloys of steel did not give the authorization to reveal their chemical composition hence they will be called steel 1, steel 2 and steel 3 throughout the dissertation. However, it is known that they from turbine components like discs and shafts.

Static Young's modulus of these steels, found in literature and obtained by laboratories, are taken in consideration to have a comparison with the results of this work. Another important parameter which is used in this work is the yield strength used to estimate the maximum stresses to perform the tensile tests. This procedure will be better explained in the paragraph 2.5.1 and 2.5.2 while in the paragraphs 2.1.1, 2.1.2 and 2.1.3 the steels 1, 2 and 3 are described.

2.1.1 Steel 1

The alloy of the steel 1 in the quenched and tempered condition is used for turbine and generator installations, in particular shafts and discs. The steel is weldable if the relevant measures required are observed.

The behaviors of static Young's modulus and yield strength with temperature found in literature are here reported and will be compared with the final results of this work.

Regarding Young's modulus, the figure 18 shows the trend of elastic modulus with temperature according to the materials search platform Matmatch. [15]

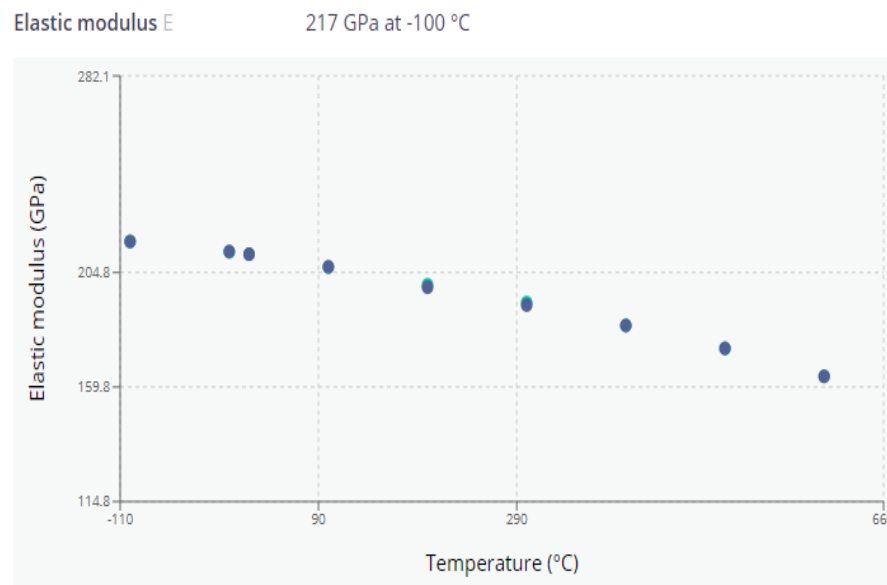


Figure 18: Elastic modulus - temperature (Matmatch)

From the plot, the Young's modulus at room temperature can be estimated in a range between 217 GPa (at $-100\text{ }^{\circ}\text{C}$) and 205 GPa. It can be visually estimated at a value of about 200 GPa at $200\text{ }^{\circ}\text{C}$, at about 185 GPa at $400\text{ }^{\circ}\text{C}$ and between 160 GPa and 165 GPa at $600\text{ }^{\circ}\text{C}$.

The trend of yield strength according to the materials search platform Matmatch is plotted in figure 19. [15]

Yield strength Rp0.2 Rp0.2 0 - 525 MPa at 100 °C

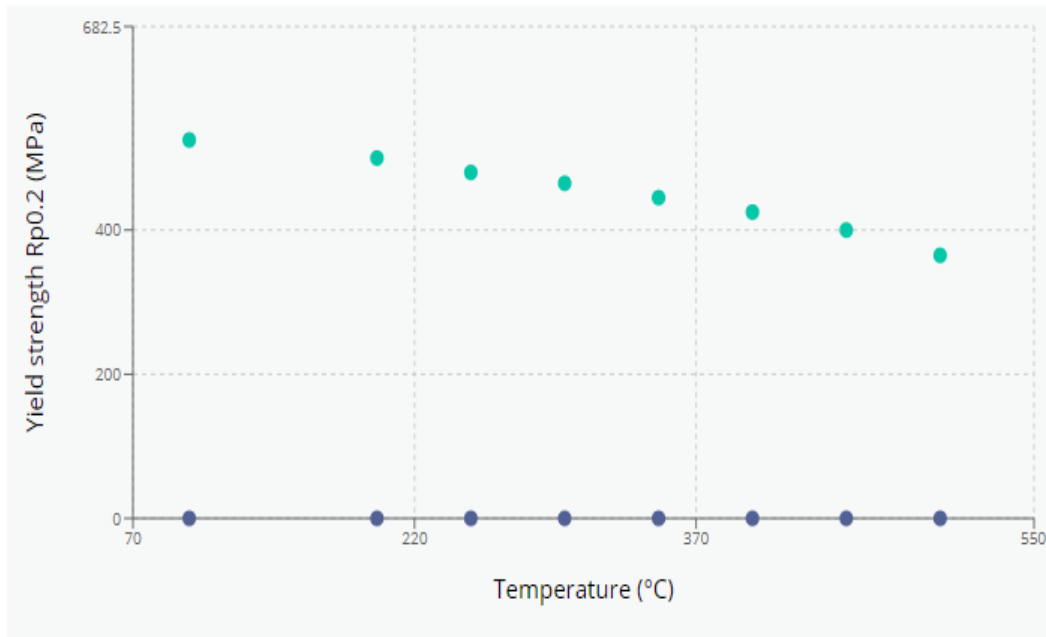


Figure 19: yield strength - temperature (Matmach)

The relevant data of this plot for this work are the yield strength is higher than 400 MPa at room temperature, at 200 °C and 400 °C.

The figure 20 shows the curve stress – strain at 20 °C according to the materials database Total materia. [16]

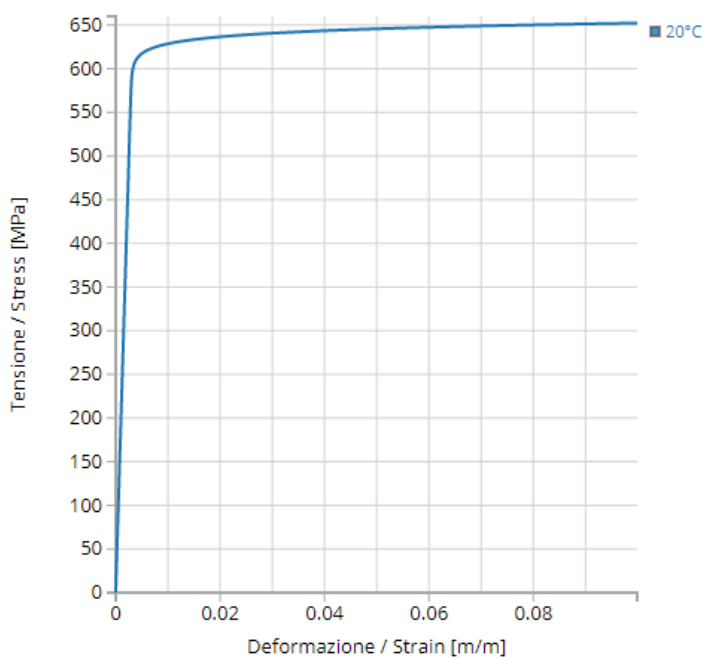


Figure 20: Stress – strain at room temperature (Total materia)

Deformazione / Strain	Tensione / Stress (MPa)
0	0
0.002	395
0.0049	617
0.0098	628
0.0147	633
0.0196	636
0.0245	639
0.0294	640
0.0343	642
0.0392	643
0.0441	644
0.049	646
0.0539	646
0.0588	647

Table 6: Table stress-stain

Since the first part of curve is linear is possible to calculate Young's modulus at room temperature dividing the stress by strain. For this calculation, the data in the second row of the table 6 are used: $E = \frac{395 \text{ MPa}}{0,002} = 197,5 \text{ GPa}$.

Static Young's modulus at room temperature, at 200 °C, 400 °C and 600°C obtained by the company Comtes FHT after tensile tests of 12 specimens till the failure is given in the table 7.

Specimens	T [°C]	D ₀ [mm]	D _u [mm]	L ₀ [mm]	L _U [mm]	E [GPa]
T1	23	9,99	5,55	50,00	60,67	179,0
T2	23	10,00	5,45	50,00	61,18	186,2
T3	23	9,97	5,51	50,00	60,27	198,1
Average	-	-	-	-	-	188
T4	200	9,99	5,58	50,00	59,14	248,6
T5	200	9,98	5,63	50,00	58,46	218,6
T6	200	10,00	5,50	50,00	59,15	217,8
Average	-	-	-	-	-	228
T7	400	9,96	5,24	50,00	60,06	201,7
T8	400	9,98	5,37	50,00	59,51	200,0
T9	400	9,98	5,78	50,00	59,44	198,6
Average	-	-	-	-	-	200
T10	600	9,96	3,21	50,00	62,90	170,6
T11	600	9,97	3,14	50,00	62,76	131,4
T12	600	9,95	3,17	50,00	61,84	134,6
Average	-	-	-	-	-	146

Table 7: Static Young's moduli for steel 1 (Comtes)

It is important to underline that the estimated Young's modulus by the three sources, Matmatch, Total materia and Comtes, is respectively between 205 GPa and 217 GPa in the first case, 197,5 GPa in the second and 188 GPa in the third; this indicates that the results obtained by different laboratories variate because of several factors which influence the tests (operator, adopted devices, followed standards, ...).

2.1.2 Steel 2

The alloy of the steel 2 is used in turbine and generator installations. Also for this steel, the searched parameters are Young's modulus and the yield strength.

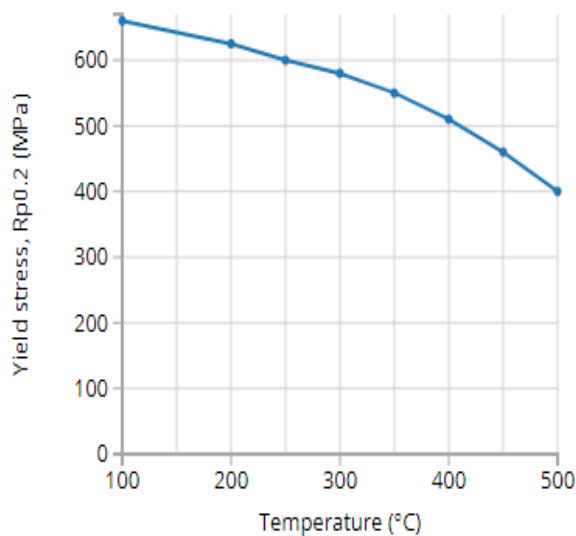
On the website of the company WIAM the behavior of Young's modulus as function of the temperature of the steel 2 is reported in the table 8. [17]

Temperature [°C]	Density [g/cm ³] ☑	Young's Modulus [kN/mm ²] ☑
-100		217.00
0		213.00
20	7.800	212.00
100		207.00
200		199.00
300		192.00
400		184.00
500		175.00
600		164.00

Table 8: Young's modulus – temperature (WIAM)

Regarding the yield strength, the trend with temperature is shown in the figure 21.(Source: materials database Total materia) [18]

Yield stress, $R_{p0,2}$ (MPa) 



Temperature (°C)	Value (MPa)
100	660
200	625
250	600
300	580
350	550
400	510
450	460
500	400

Figure 21: yield strength - temperature (Total materia)

2.1.3 Steel 3

The alloy of the steel 3 in the quenched and tempered condition is used for turbine and generator installations, in particular shafts and discs. The temperatures up to the steel may be used depend on the total stressing of the component. The steel is weldable if the relevant measures required are observed.

The trend of yield strength with temperature derives from the materials database Total materia (figure 22). [19]

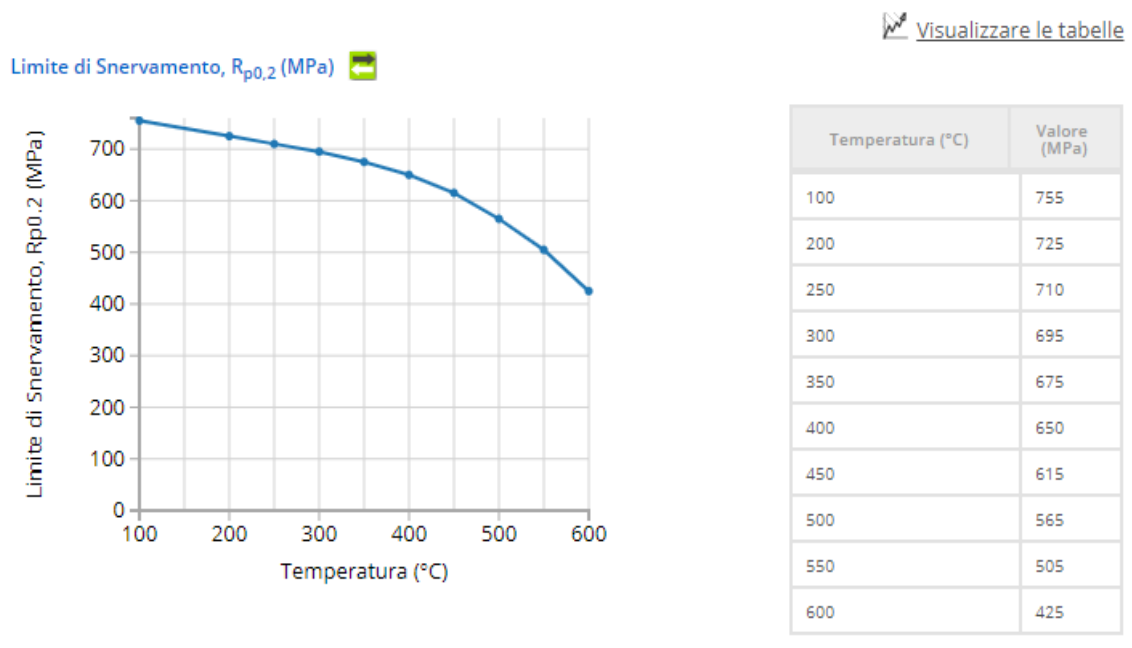


Figure 22: yield strength – temperature (Total materia)

Static Young's moduli at room temperature, at 200 °C, 400 °C and 600°C obtained by the company Comtes FHT after tensile tests till the failure are given in the table 9.

Specimens	T [°C]	D₀ [mm]	D_u [mm]	L₀ [mm]	L_u [mm]	E [GPa]
T1_20C	20	9,99	5,56	50,00	60,25	213,0
T2_20C	20	9,98	5,56	50,00	60,18	209,8
T3_20C	20	9,98	5,23	50,00	60,56	224,4
Average	-	-	-	-	-	215,7
T4_200C	200	9,99	5,61	50,00	58,54	231,1
T5_200C	200	9,99	5,38	50,00	58,64	222,7
T6_200C	200	9,98	5,45	50,00	58,39	205,2
Average	-	-	-	-	-	219,7
T7_400C	400	10,00	5,47	50,00	58,91	196,4
T8_400C	400	9,98	5,99	50,00	58,01	177,4
T9_400C	400	10,00	5,41	50,00	58,54	205,4
Average	-	-	-	-	-	193,1
T10_600C	600	9,99	3,22	50,00	62,65	146,0
T11_600C	600	9,99	3,11	50,00	63,06	139,9
T12_600C	600	9,98	3,14	50,00	63,38	162,5
Average	-	-	-	-	-	149,5

Table 9: Static Young's moduli for steel 3 (Comtes)

2.2 Measurements techniques

In this paragraph the techniques and the procedures adopted to measure the static and dynamic Young's modulus are described.

2.2.1 Technique to measure static Young's modulus at room temperature

The tensile test is the technique performed to obtain static Young's modulus. The tensile tests are carried out in accordance with the standard BS EN ISO 6892-1:2016.

This standard indicates the testing rate can be based on the control of the strain rate (method A) or the stress rate (method B).

Two different types of strain rate control are possible:

- The method A1 is in closed loop and involves the control of the strain through an extensometer;
- The method A2 is in open loop and involves the control of the estimated strain rate over the parallel length which is achieved by using the crosshead separation rate calculated by multiplying the required strain rate by the parallel length.

The method adopted in this work is A1. The strain rate is $0,000278 \text{ s}^{-1}$ which corresponds to a crosshead separation rate of 1 mm/min.

The preload is 0,2 kN.

The data sampling frequency shall be chosen in a way that a minimum of 50 measured values is obtained in the range between the minimum and maximum stresses.

The minimum data sampling frequency can be calculated by following formula:

$$f_{min} = \frac{N \cdot E \cdot \dot{\epsilon}_{Lc}}{\sigma_2 - \sigma_1} \quad (19)$$

where:

- N is the number of measured values in the relevant range (minimum 50);
- E is Young's modulus;
- $\dot{\epsilon}_{Lc}$ is the estimated strain rate over the parallel length;
- σ_2 is the maximum stress;
- σ_1 is the minimum stress.

σ_1 and σ_2 are chosen in such a way that the curve stress-strain is visually as straight as possible in this range.

In this case the piston speed v_c is 1 mm/min and the parallel length L_c is 60 mm so the estimated strain rate over the parallel length $\dot{\epsilon}_{L_c}$ is 0,000278 s⁻¹ ($\dot{\epsilon}_{L_c} = \frac{v_c}{L_c}$).

To estimate the minimum data sampling frequency, a Young's modulus of 210 GPa is considered, and σ_1 and σ_2 are estimated, for a first approximate calculation, respectively of 80 MPa and 120 MPa; the result is $f_{min} = 72,92$ Hz.

The data sampling of the devices is set to 100 Hz so there are at least 50 measured values between σ_1 and σ_2 .

The measured room temperatures at which the tests are performed are: 26,5 °C for steel 1, 27,9 °C for steel 2 and 27,4 °C for steel 3.

2.2.2 Technique to measure the static Young's modulus at high temperatures

The tensile tests at high temperature are performed following the procedure suggested by the standard BS EN ISO 6892-2:2015.

When the specimen is heated and reaches the temperature at which to carry out the test, it remains at that temperature for 10 minutes before to apply the load (soaking time).

The crosshead speed is 1 mm/min, the preload is 0,2 kN and the estimated minimum data sampling frequency is 72,92 Hz.

The maximum difference between the nominal temperature at which the test should be performed (T) and the measured temperature on the surface of the parallel length of the test piece (T_i) must be $\pm 3^\circ\text{C}$ for tests at 600°C or less. The measured temperatures on the surfaces of the test pieces at the start and the end of the cycles of tensile are reported in the table 10:

	T_i start [$^\circ\text{C}$]	T_i end [$^\circ\text{C}$]
Steel 1 200 $^\circ\text{C}$	198,5	200,0
Steel 1 400 $^\circ\text{C}$	401,0	404,0
Steel 1 600 $^\circ\text{C}$	600,9	601,0
Steel 2 200 $^\circ\text{C}$	204,5	204,5
Steel 2 400 $^\circ\text{C}$	400,1	402,2
Steel 2 600 $^\circ\text{C}$	600,0	601,0
Steel 3 200 $^\circ\text{C}$	200,0	202,2
Steel 3 400 $^\circ\text{C}$	298,4	401,1
Steel 3 600 $^\circ\text{C}$	600,8	598,7

Table 10: initial and final temperature on the surface of the test pieces

2.2.3 Technique to measure the dynamic Young's modulus at room temperature

Dynamic Young's modulus has been calculated following the standard ASTM E 1876-15.

The machine suitable for the measure of this magnitude is RFDA Professional. It receives as inputs the geometrical dimensions (length, width and thickness) and the mass of the specimens and measures the fundamental flexural resonant frequency of the sample when it is hit by a tapping device. It is possible calculate dynamic Young's modulus by means of these data ($E = 0,9465 \left(\frac{mf_f^2}{b} \right) \left(\frac{L^3}{t^3} \right) T_1$).

To measure Young's modulus at room temperature, using the impulse excitation method, the minimum length indicated by the standard ASTM E1876-15 is of 20 mm.

Smaller specimens can lead to large relative dimensional errors during the measurements and so involve errors in the final result of Young's modulus; moreover, too light specimens shift and jump during the test.

The specimens are supported with the wires that are located at $0,224 L$ from the edge of the rectangular bars (L is the length of the bar). In the nodes, the displacements are always zero when the bar is in resonance.

2.2.4 Technique to measure the dynamic Young's modulus at high temperature

The operating principle and formulas used for rectangular bars are the same as dynamic Young's modulus at room temperature.

To measure Young's modulus at high temperatures the minimum length indicated by the standard ASTM E1876-15 is of 30 mm.

RFDA HT1050 has been used to measure dynamic Young modulus at high temperature.

The supports for the small and full size specimens are different as shown in the figures 23 and 24; anyway, they are supported along the nodes which are distant $0,224L$ from the edge.

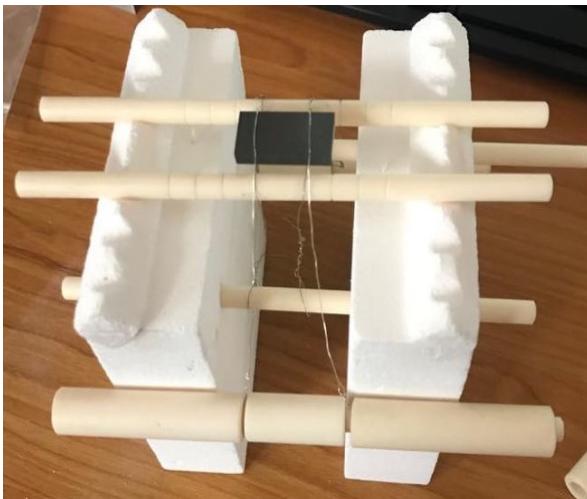


Figure 23: Support adopted for small specimens

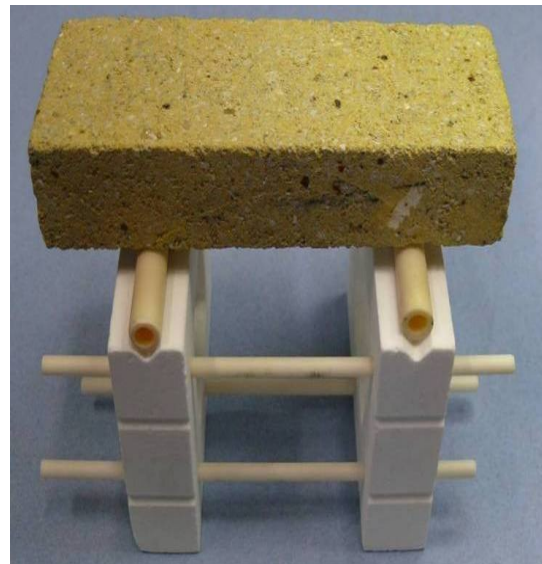


Figure 24: example of support adopted for full size specimens

2.3 Testing equipment and devices

2.3.1 Tensile test

UFP400 and Inova are the tensile testers adopted to perform the two sets of the tests.

The equipment used for the first set of tensile tests consists of (figure 25):

- tensile tester UFP400;
- Furnace KVSP 0,2.0,3-13;
- Axial extensometer MTS 634.12F-25;
- Axial extensometer Epsilon model 3549;
- Thermometer GHM 3251;
- Thermocouple MTC11-00-700-200-10.

For the second set of tensile tests, the equipment is (figure 26):

- tensile tester Inova;
- Furnace;
- Axial extensometer Epsilon model 3549;
- Thermometer GHM 3251;
- Thermocouple MTC11-00-700-200-10.

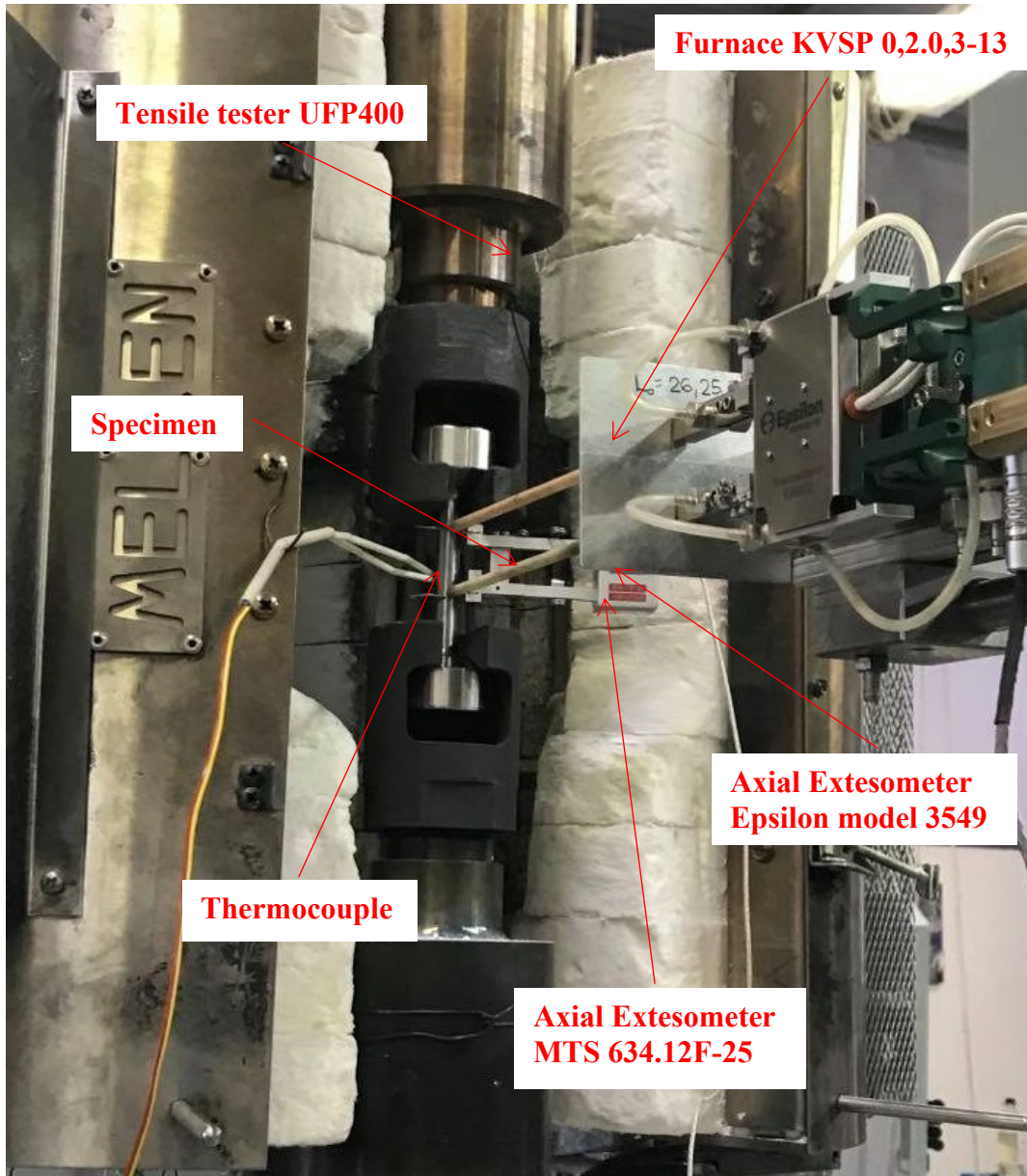


Figure 25: Equipment for the first set of tensile tests



Figure 26: Inova

The specifications for the Furnace KVSP 0,2.0,3-13 are:

- Intended use: electric furnace with divided chamber intended for laboratory purposes;
- Electric power: 4 kVA;
- Rated heating output: 3,8 kW;
- Operating voltage:
 - main circuits: 230 V / 20 V / 32 V AC;
 - control circuits: 230 V;

- Nominal temperature: 1300 °C;
- Weight of furnace/ el. control box: 50 kgs / 120 kgs;
- Indoor atmosphere: oxidative;
- External dimensions (diameter x length): 400 x 500 mm;
- Internal dimensions (diameter x length): 100 x 280 mm.

2.3.1.1 Axial extensometer MTS 634.12F-25

The MTS 634.12F-25 axial extensometer (figures 27 and 28) is used just for the tests at room temperature to have a confirm of the goodness of the second extensometer which is used during all tests.



Figure 27: Axial extensometers MTS 634.12F-25

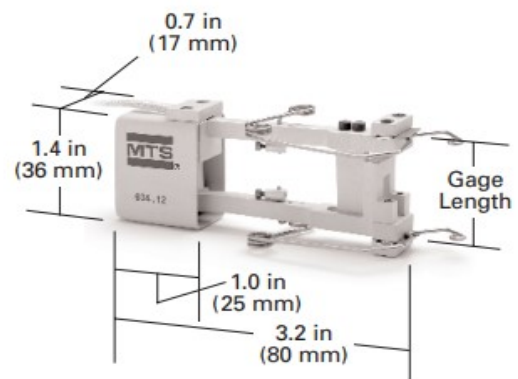


Figure 28: Dimensions of MTS 634.12 Axial extensometers

The specifications of MTS 634.12F-25 axial extensometer are:

- gage length of 25 mm and a travel of 0 to +12,5 mm or -2,5 to +12,5 mm;
- Accuracy: meets or exceeds ASTM E83 Class B1 and ISO 9513 Class 0,5 standards; [19]
- Nonlinearity:
 - Typical: 0,18% of range;
 - Maximum: 0,25% of range;
- Hysteresis (is measured over the \pm maximum travel range and is specified as a percent of this full range):
 - Typical: 0,07%;
 - Maximum: 0,1%;
- Maximum Operating Frequency: 50 Hz (at small displacements with sinusoidal waveform)
- Quick Attach Specimen Size Limits:

- Diameter: 0,10 to 0,56 in (2,5 to 14 mm);
- Flat width: 0,4 to 1,0 in (10,5 to 26 mm);
- Thickness: 0.01 to 0,5 in (0,3 to 12,5 mm);
- Bridge Resistance: 350 Ω ;
- Unit Weight (unit weight includes extensometer and Quick-Attach springs, does not include cable and connector): 37 grams;
- Shipping Weight: 1,3 lb (0,6 kg).

2.3.1.2 Axial extensometer Epsilon model 3549

The axial extensometer Epsilon model 3549 (figure 29) is adopted for the tests at room and elevated temperatures (max. 1600 °C) and is supplied with alpha grade silicon carbide rods.

This extensometer mounts on a slide bracket that can attach to the load frame of the test system. The gauge length for the 3549 is automatically set prior to mounting on the test specimen, which allows for hot mounting after thermal equilibrium has been reached.

The specifications are here listed:

- Accuracy: meets ASTM Class B1 and ISO 9513 Class 0,5 standards; [19]
- Linearity: $\leq 0.15\%$ of full scale measuring range;
- Bridge Resistance: 350 Ω ;
- Unit Weight: < 30 grams;
- Contact Force: adjustable up to 400 g;
- Excitation: 5 to 10 VDC recommended, 12 VDC or VAC max;
- Output: 1.5 to 2 mV/V.



Figure 29: Axial extensometer Epsilon model 3549

2.3.1.3 Thermometer GHM 3251 and Thermocouple MTC11-00-700-200-10

The thermometer GHM 3251 and its specifications are in the figures 30 and 31.



Figure 30: Thermometer GMH 3251

Specifications:	GMH 3211	GMH 3221	GMH 3231	GMH 3251
Thermocouples:	K, J, T, N, S, E, B	K	K, J, T, N, S, E, B	K, J, T, N, S, E, B
Measuring channels:	1 thermocouple input (type K balancing material)		2 thermocouple inputs (type K balancing material)	
Measuring ranges				
type K:	-220.0 ... +1372.0 °C	-220.0 ... +1372.0 °C	-220.0 ... +1372.0 °C	-220.0 ... +1372.0 °C
type J:	-200.0 ... +1100.0 °C	-	-200.0 ... +1100.0 °C	-200.0 ... +1100.0 °C
type T:	-200.0 ... +400.0 °C	-	-200.0 ... +400.0 °C	-200.0 ... +400.0 °C
type N:	-200.0 ... +1300.0 °C	-	-200.0 ... +1300.0 °C	-200.0 ... +1300.0 °C
type S:	-50.0 ... +1768.0 °C	-	-50.0 ... +1768.0 °C	-50.0 ... +1768.0 °C
type E:	-60.0 ... +850.0 °C NEW	-	-60.0 ... +850.0 °C NEW	-60.0 ... +850.0 °C NEW
type B:	+300 ... +1750 °C NEW	-	+300 ... +1750 °C NEW	+300 ... +1750 °C NEW
Accuracy: (at nominal temperature)	±(0.5 °C + 0.2 % of m.v.) (J, K, N, T, E) ±(0.8 °C + 0.4 % of m.v.) (S, B)	±(0.5 °C + 0.2 % of m.v.)		±(0.5 °C + 0.2 % of m.v.) (J, K, N, T, E) ±(0.8 °C + 0.4 % of m.v.) (S, B)
Analog output:	no	no	no	0 ... 1 V
Alarm:	no	no	no	CH1, CH2, CH1+2, DIF
Data logger:	no	no	no	manual: 1.000 data sets cyclic: 10.000 data sets
Probe connections (miniature flat plug):	1	2	2	2
Serial interface:	3-pin jack connector Ø 3.5 mm	-	3-pin jack connector Ø 3.5 mm	3-pin jack connector Ø 3.5 mm
Difference measurement:		Temperature difference probe 1 - probe 2 can be displayed if 2 probes are connected.		
Compensation value for surface measurements:	adjustable	-	adjustable	adjustable
Power supply:	9 V battery, d.c. connector	9 V battery	9 V battery, d.c. connector	9 V battery, d.c. connector
Battery life:	approx. 500 h	approx. 300 h	approx. 300 h	approx. 300 h

Figure 31: Thermometer specifications

Specifications of the thermocouple:

- Material: Inconel
- Type of thermocouple: K
- Diameter: 3 mm
- Length (N in the figure): 700 mm
- type of insulation: silicon ($T_{\max} = 200^{\circ}\text{C}$)



Figure 32: thermocouple welded to the specimen

The figure 32 shows the thermocouple welded to the specimen.

2.3.2 Dynamic modulus at room temperature

The RFDA Professional system (figure 33) has been used for measuring dynamic Young's modulus at room temperature. Its functioning is based on impulse excitation method and consists of the following items:

- Computer system;
- RFDA System 24 (figure 34);
- Transducer (IMCE microphone);
- Sample support system;
- Automatic tapping device. [10]

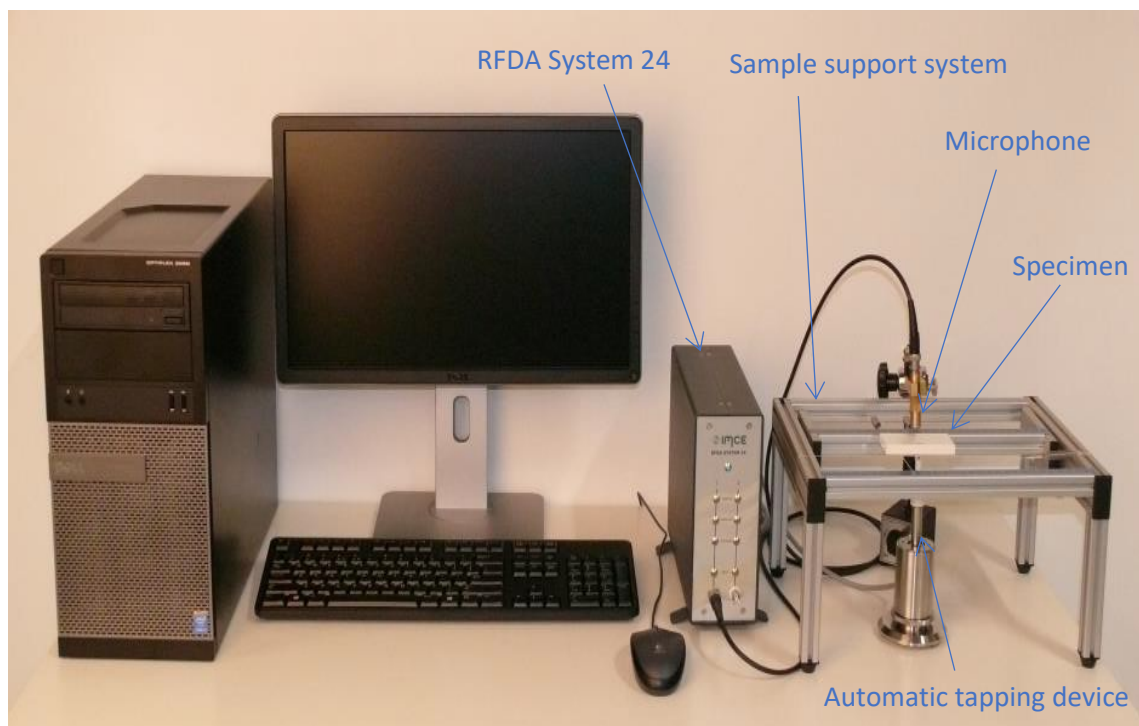


Figure 33: RFDA professional system

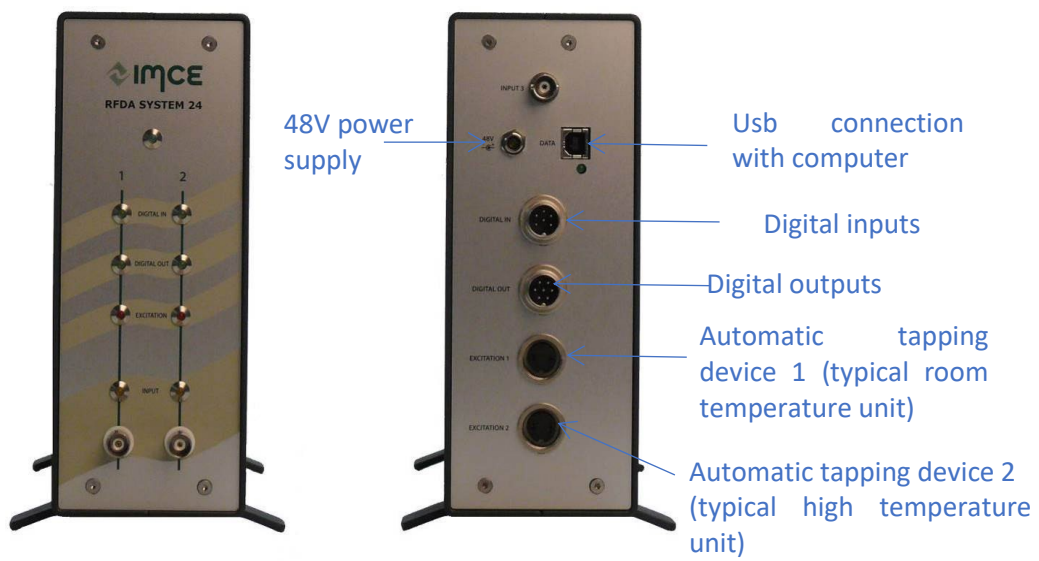


Figure 34: RFDA System 24

2.3.3 Dynamic modulus at high temperatures

RFDA HT1050 has been used for measuring dynamic Young's modulus at high temperature. The RFDA HT1050 system consists out of the following items (figures 35 and 36):

- Furnace;
- Furnace control unit;
- Computer system;
- RFDA System 24;
- Transducer (microphone);
- Sample support system;
- Automatic tapping device. [20]

The RFDA HT1050 system allows a protective gas to flow in the chamber at high temperature to prevent the oxidation.

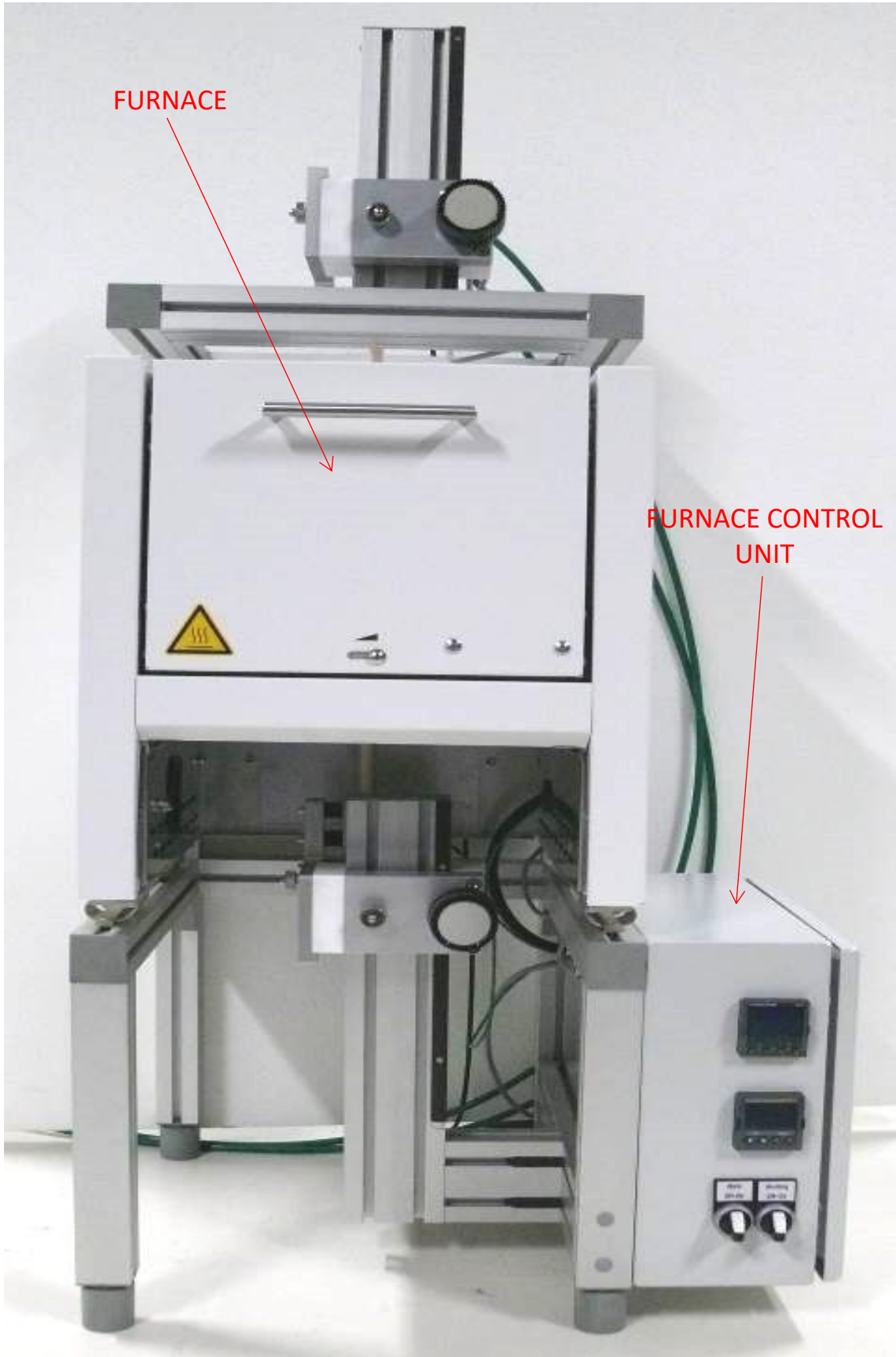


Figure 35: General overview RFDA HT1050

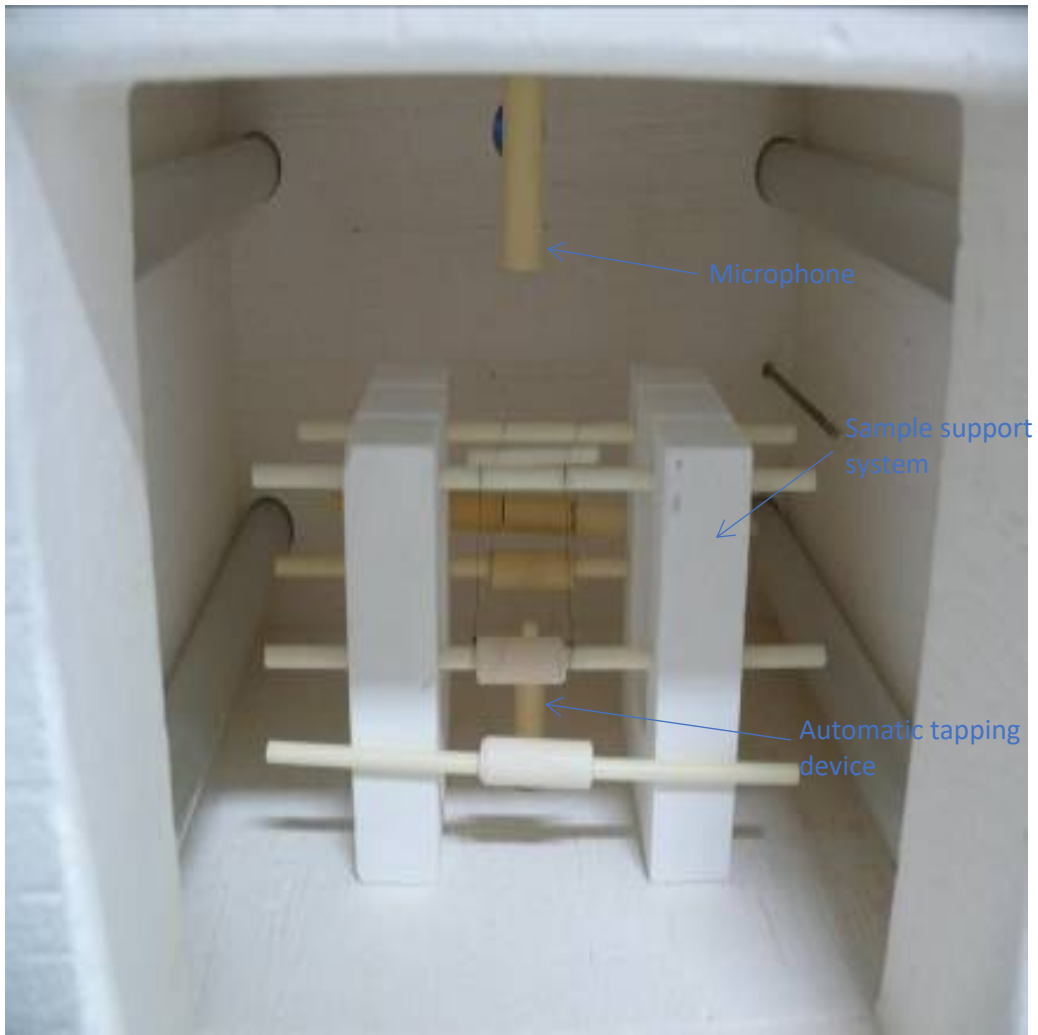


Figure 36: sample and supports placed in the furnace

2.4 Specimens

2.4.1 Specimens for tensile tests

3 standard specimens (1 specimen for every kind of steel) with a nominal diameter of 10 mm have been employed for the tensile tests at room temperature, at 200 °C, 400 °C and 600 °C in accordance with the standards BS EN ISO 6892-1:2016 and BS EN ISO 6892-2:2015.

The figure 37 shows the nominal dimensions of the specimens while the figures 38, 39 and 40 show the three specimens used in the tests.

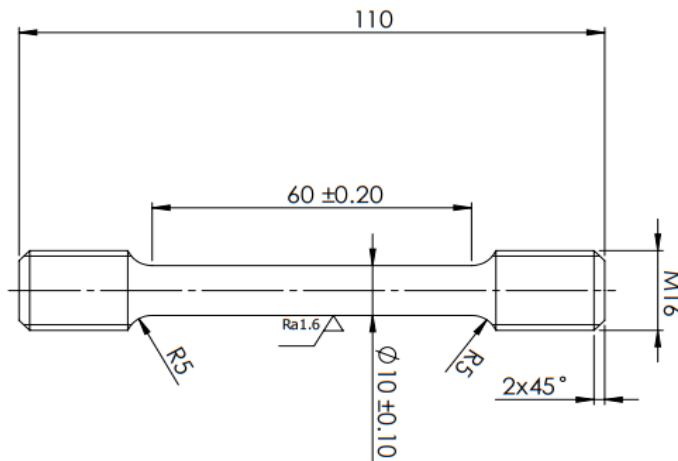


Figure 37: Standard specimen for tensile test



Figure 38: Steel 1 - Specimen A



Figure 39: Steel 2 - Specimen B



Figure 40: Steel 3 - Specimen C

The three standard tensile test specimens derive from the turbines shaft and disks illustrated in the figures 41, 42 and 43.



Figure 41: Steel 1



Figure 42: Steel 2

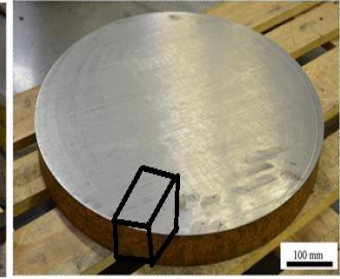


Figure 43: Steel 3

The real diameter of every specimen is the average of 5 measurements on the central cross-section performed with a caliber (table 11).

Specimen	D1 [mm]	D2 [mm]	D3 [mm]	D4 [mm]	D5 [mm]	D average [mm]
A	10,01	10,01	10,01	10	10,01	10,008
B	10,02	10,03	10,02	10,02	10,02	10,022
C	10,05	10,06	10,04	10,04	10,05	10,048

Table 11: Average diameters of tensile test specimens

2.4.2 Specimens for impulse excitation

For the impulse excitation tests from room temperature to 600 °C, 9 specimens (3 specimens for every kind of steel) are used in accordance with the standard ASTM E1876-15.



Figure 44: Specimen D



Figure 45: Specimen E



Figure 46: Specimen F



Figure 47: Specimen G



Figure 48: Specimen H



Figure 49: Specimen I



Figure 50: Specimen J



Figure 51: Specimen K



Figure 52: Specimen L

The 9 test specimens for impulse excitation derive from the turbines shaft and disks illustrated in the figures 41, 42 and 43.

The material, the shape, the dimensions (length, width and thickness) and the mass of the 9 specimens for the impulse excitation tests are listed in the table 12.

The length, width, thickness and the mass of the table 12 are the average of 5 measurements.

Specimens	Materials	Shape	L [mm]	W [mm]	T [mm]	m [g]
D (figure 44)	Steel 1	rectangular	20,016	10,005	2,992	4,690
E (figure 45)	Steel 2	rectangular	20,008	10,009	3,006	4,718
F (figure 46)	Steel 3	rectangular	20,015	10,007	2,997	4,717
G (figure 47)	Steel 1	rectangular	29,982	9,995	3,013	7,057
H (figure 48)	Steel 2	rectangular	29,992	9,994	3,016	7,062
I (figure 49)	Steel 3	rectangular	29,934	9,991	3,011	7,069
J (figure 50)	Steel 1	rectangular	80,056	35,036	9,096	198,062
K (figure 51)	Steel 2	rectangular	80,000	35,046	9,049	198,817
L (figure 52)	Steel 3	rectangular	69,988	34,998	9,096	170,638

Table 12: Dimensions of the specimens for impulse excitation test

The last three specimens of the table 12 are larger than previous ones and are used to understand if a variation of the sizes can influence the results.

2.5 Test plan and experimental set-up

2.5.1 Test plan and experimental set-up to measure static Young's modulus at room temperature

One specimen for every kind of steel has been tested.

The average diameter of every specimen is the average of 5 measurements on the central cross-section performed with a caliber.

5 cycles of tensile are performed on every specimen of the three steels from the preload to a stress lower than half of yield strength, to be sure to stay in the elastic zone (recommended procedure by the annex G of the standard BS EN ISO 6892-1:2016). The yield strength of the 3 steels at different temperatures have been found in literature (paragraph 2.1).

The maximum stresses at which the 5 cycles of tensile are performed are listed in the table 13.

	Steel 1	Steel 2	Steel 3
RT	200 MPa	250 MPa	200 MPa

Table 13: Maximum stresses at which the cycles of tensile are performed

The experimental set-up is in figure 25. It consists in:

- tensile tester UFP400;
- Axial extensometer MTS 634.12F-25;
- Axial extensometer Epsilon model 3549;
- Thermometer GHM 3251;
- Thermocouple.

The axial extensometers Epsilon model 3549 and MTS 634.12F-25 are used simultaneously at room temperature to verify the goodness of the first extensometer which is used alone at high temperature. This procedure consists in comparing the results of Young's modulus coming from the two devices.

2.5.2 Test plan and experimental set-up to measure static Young's modulus at high temperatures

The average diameter of every specimen is the average of 5 measurements on the central cross-section performed with a caliber.

5 cycles of tensile are performed on every specimen of the three steels at 200 °C, 400 °C and 600 °C from the preload to a stress lower than half of yield strength, to be sure to stay in the elastic zone.

UFP400 and Inova are the tensile testers adopted to perform the two sets of the tests.

First, all the cycles of the tensile were carried out with UFP400 but since the results are different from those expected, the tests for the steels 1 and 2 at 400°C and 600°C are repeated with the machine Inova.

The yield strength of the 3 steels at different temperatures have been found in literature (paragraph 2.1).

The maximum stresses at which the 5 cycles of tensile are performed are listed in the table 14.

	Steel 1	Steel 2	Steel 3
200°C	200 MPa	250 MPa	200 MPa
400°C	180 MPa	200 MPa	200 MPa
600°C	120 MPa	120 MPa	120 MPa

Table 14: Maximum stresses at which the cycles of tensile are performed

The experimental set-up is in figures 25 and 26. It consists in:

- tensile tester UFP400 and Inova;
- Furnace;
- Axial extensometer Epsilon model 3549;
- Thermometer GHM 3251;
- Thermocouple.

2.5.3 Experimental set-up and test plan to measure dynamic Young's modulus at room temperature

In the figure 53 the experimental set-up for measuring dynamic Young's modulus, dynamic shear modulus and Poisson's ratio at room temperature is shown.



Figure 53: Set-up for dynamic Young's modulus, dynamic shear modulus and Poisson's ratio at room temperature

To get these 3 parameters, the microphone and the tapping devices have to be placed at the opposite corners of the rectangular bar, while, to obtain just the dynamic Young's modulus with a more accuracy of the result, they have to be placed at the center of the specimen.

5 measurement for every specimen are executed.

2.5.4 Experimental set-up and test plan to measure dynamic Young's modulus at high temperature

The equipment RFDA HT1050 is used to measure dynamic Young modulus at high temperature.

The experimental set-up is shown in the figure 54 where the supports and the test specimen are displaced in the furnace.

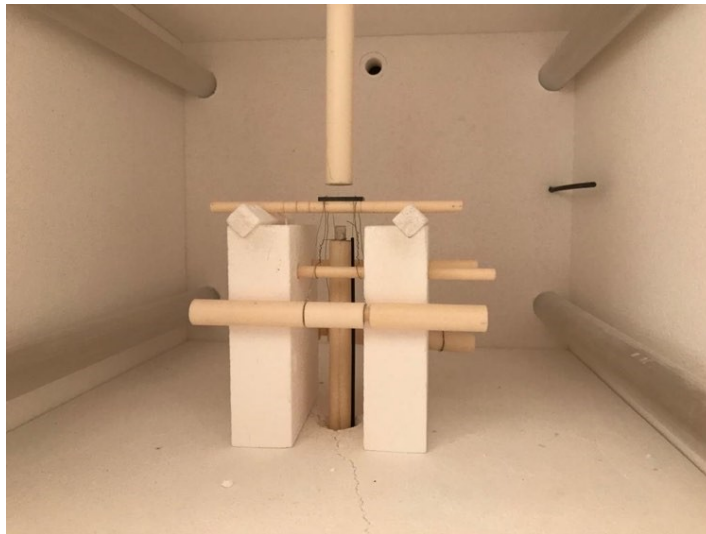


Figure 54: Support placed in the furnace

The trend of the temperature set for the furnace is shown in figure55:

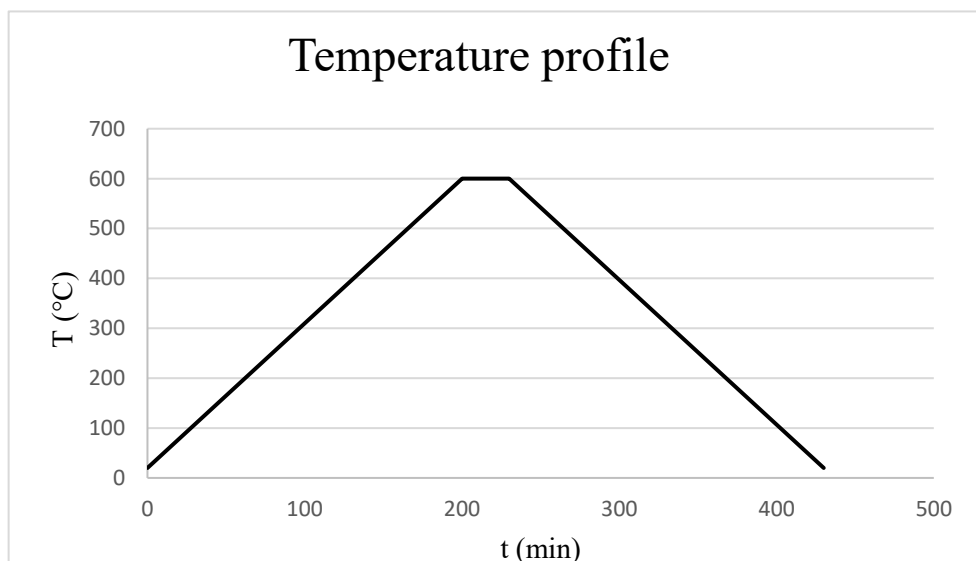


Figure 55: Temperature profile

The first part of the temperature profile is a ramp from the ambient condition up to 600 °C with a slope of 3 °C per minute; this choice was made to have a difference of temperature between the internal part and the surface smallest possible. In the second part the temperature is constant at 600 °C for 30 minutes. The third part is a ramp with a negative slope of -3 °C per minutes. The specimens are hit by the projectile every two minutes at the center of the lower surface instead of the corner because hitting the small specimens in the corner causes major stability problems (the specimens can jump or, in the worst case, fall from the supports).

2.6 Data analysis

2.6.1 Analysis of the data of the tensile tests

After the tests, it is adopted the least squares method for the evaluation of the recorded data. (method recommended by standard BS EN ISO 6892-1:2016 annex G).

The line between the points in which you want to calculate the elastic modulus is:

$$\sigma = E \cdot \varepsilon + b \quad (20)$$

where:

- σ is the stress in MPa;
- E is the modulus of elasticity in MPa;
- ε is the strain;
- b is the stress offset in MPa.

The match between the straight line and the data points is evaluated visually and through the coefficient of correlation R^2 , which must be as close as possible to 1.

To be clearer the procedure is explained step by step for the steel 1 at 400 °C.

- 1) The load cell and the ceramic axial extensometer (Epsilon model 3549) provide respectively, instant by instant, the force and the elongation (table 15).

Time [s]	Displacement of the crossbar [mm]	Force [N]	Elongation ΔL [mm]
0,011719	0,003	-3,5	-0,002016
0,021484	0,003	-3	-0,002016
0,03125	0,003	-3,5	-0,002316
0,041016	0,003	-3,5	-0,00246
0,050781	0,003	-4	-0,002388
...
457,021	0,812	195	0,12846

Table15: Force and elongation

- 2) The force is divided by the cross-section area to determinate the stress and the elongation is divided by the original gauge length to have the

strain (Table 16). The cross-section area of the specimens is calculated as $\frac{\pi \cdot d^2}{4}$ where the diameter derives from the average of 5 measurements; in this case, the diameter is 10,008 mm and so the area results 78,62565 mm.

Stress [MPa]	Strain
-0,04451	-0,0000768
-0,03816	-0,0000768
-0,04451	-8,8229E-05
-0,04451	-9,3714E-05
-0,05087	-9,0971E-05
...	...
2,480107	0,004893714

Table 16: Stress and strain

- 3) Using the stresses and the strains, the curves of the 5 cycles are plotted as in figure 56 :

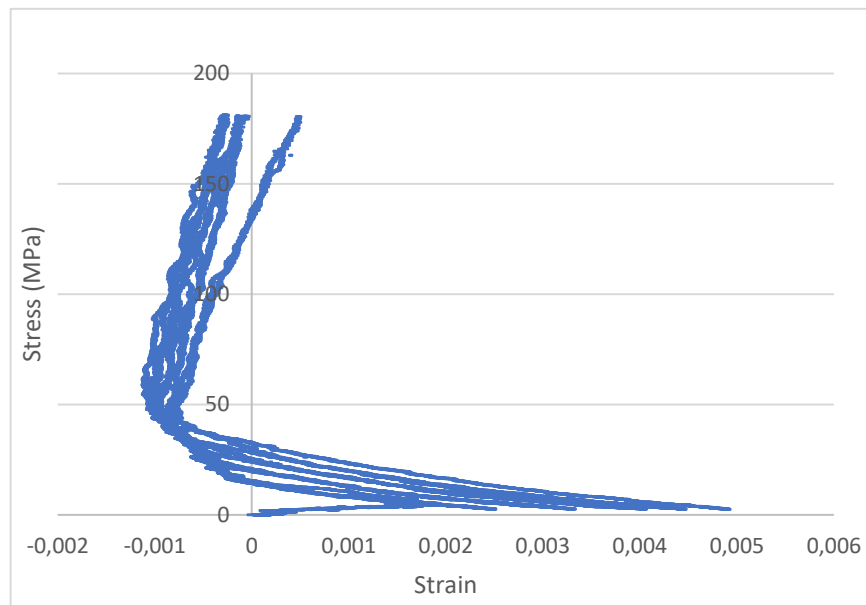


Figure 56: Stress- strain curves of the 5 cycles

- 4) The parts of the plot useless to determinate the elastic modulus are cut (figure 57):

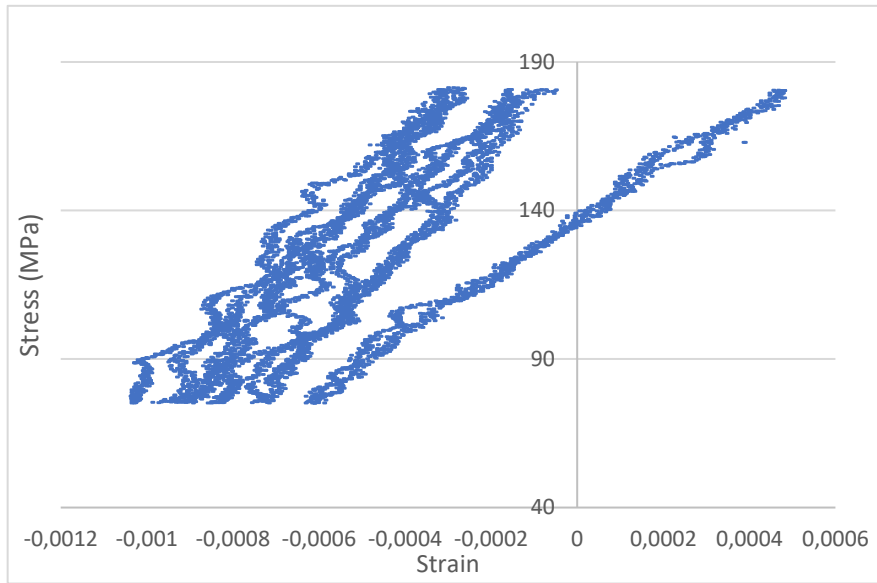


Figure 57: Lineae part of stress- strain curves of the 5 cycles

- 5) The 5 cycle are divided in 5 plots and the trendlines during the increment loading and the decrement unloading are drawn figures 58, 59, 60, 61 and 62:

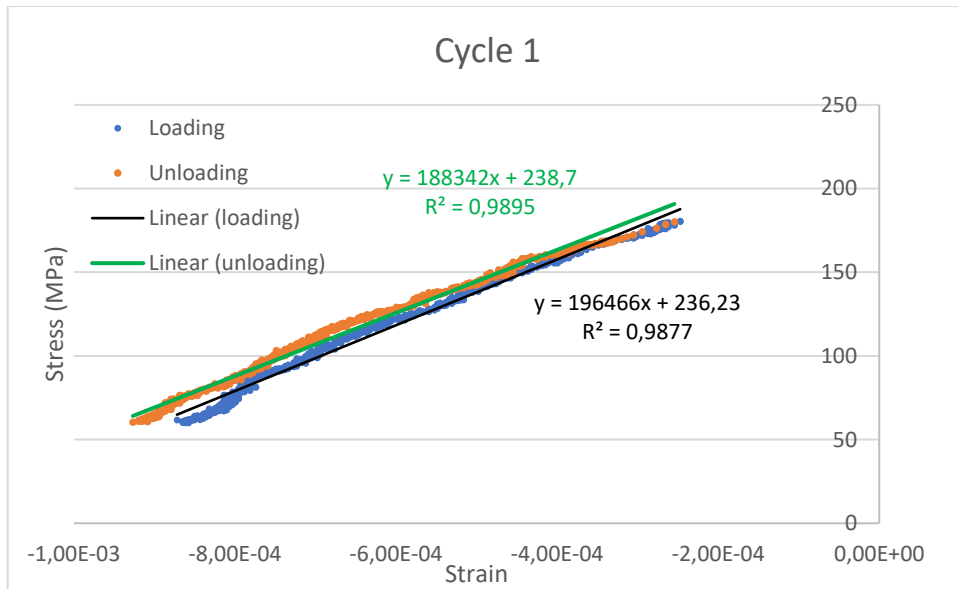


Figure 58: Cycle 1 for specimen A at 400 °C

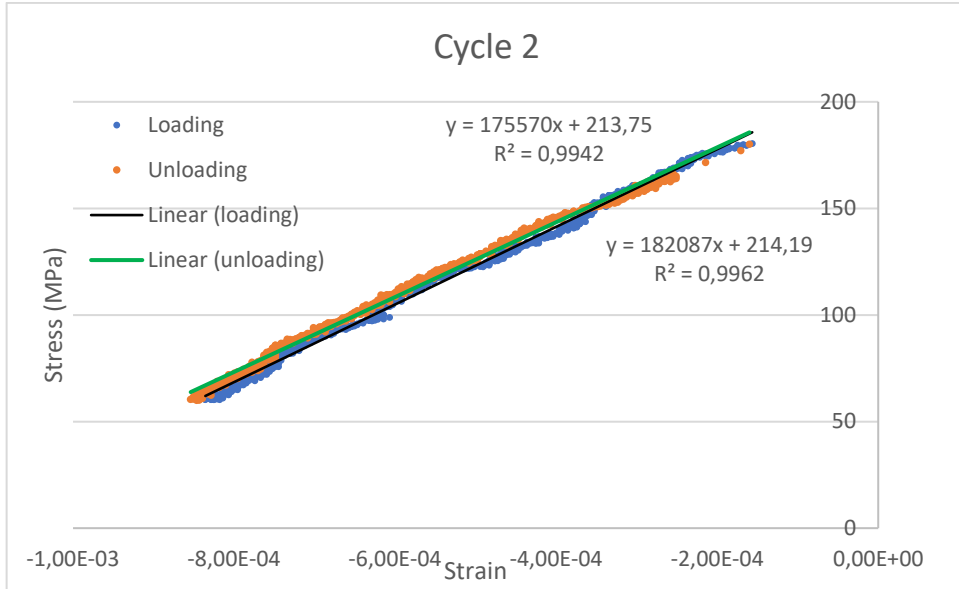


Figure 59: Cycle 2 for specimen A at 400 °C

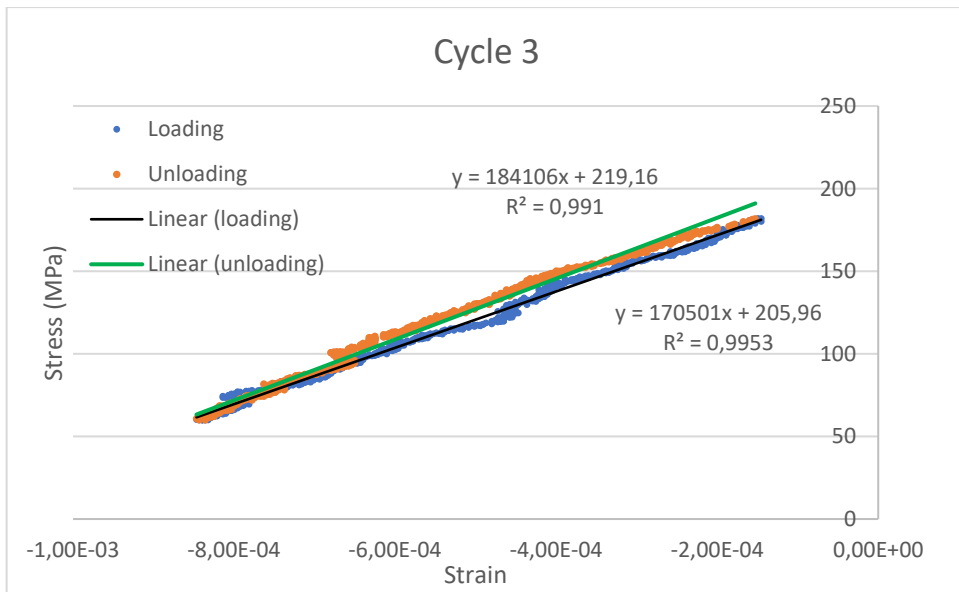


Figure 603: Cycle 3 for specimen A at 400 °C

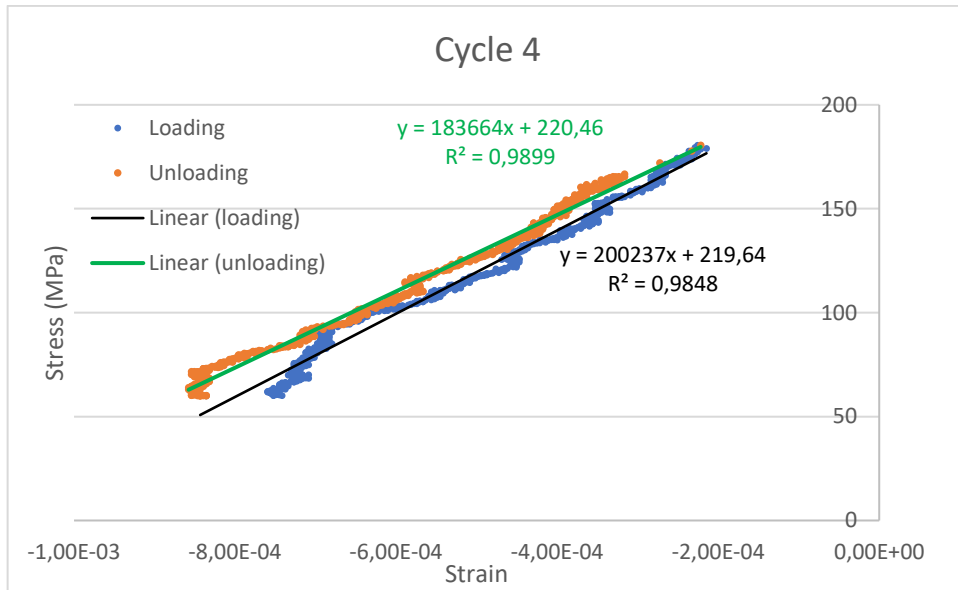


Figure 61: Cycle 4 for specimen A at 400 °C

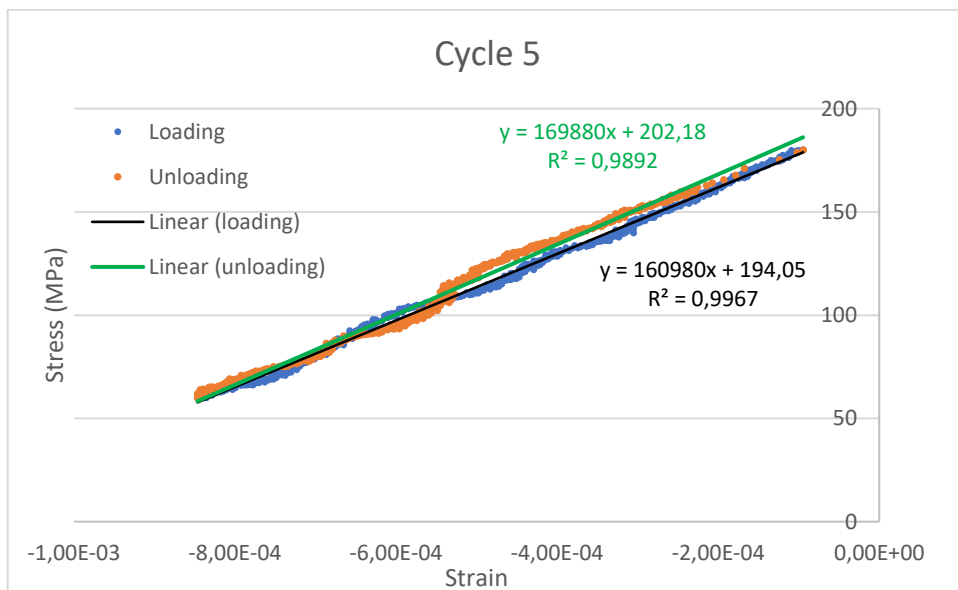


Figure 62: Cycle 5 for specimen A at 400 °C

- 6) The slopes of the trendlines of the stress-strain curve are used to calculate the average Young's modulus. A slope is taken in consideration for the calculation of the average Young's modulus if it respects these conditions:
- its value is close to the other slopes and to the value of Young's modulus of the steel found in literature;
 - R^2 is close to 1 (0,9 or higher).

E[MPa]	
Loading	Unloading
196465,8	188342,2
182087,4	175570,2
170501	184106,5
200236,6	183664,4
160980	169880,5
Average	181183 MPa
Std dev	12224 MPa

Table 17: Slopes for the specimen A at 400 °C

All the slopes of table 17 are used to calculate the average Young's modulus. By way of example, it is shown a situation in which some slopes are not considered for the calculation of the average. The slopes of trendlines which refers to steel 1 at 600 °C are listed in the table 18:

E [MPa]	
Growth	Decline
123394,6	126848,5
143064,1	147211,4
152360,6	153438,9
108380,1	130964,1
124351,4	142131,5
Average	147641 MPa
Std dev	5181 MPa

Table 18: Slopes for the specimen A at 600 °C

In this case the 5 values highlighted in red are excluded from the calculation of the average because too low in comparison to the results obtained by the company Comtes in previous tests. (The Young's modulus obtained previously by 3 tensile tests on 3 different specimens was 146 GPa).

- 7) The average static Young's modulus is plotted as a function of the temperature:

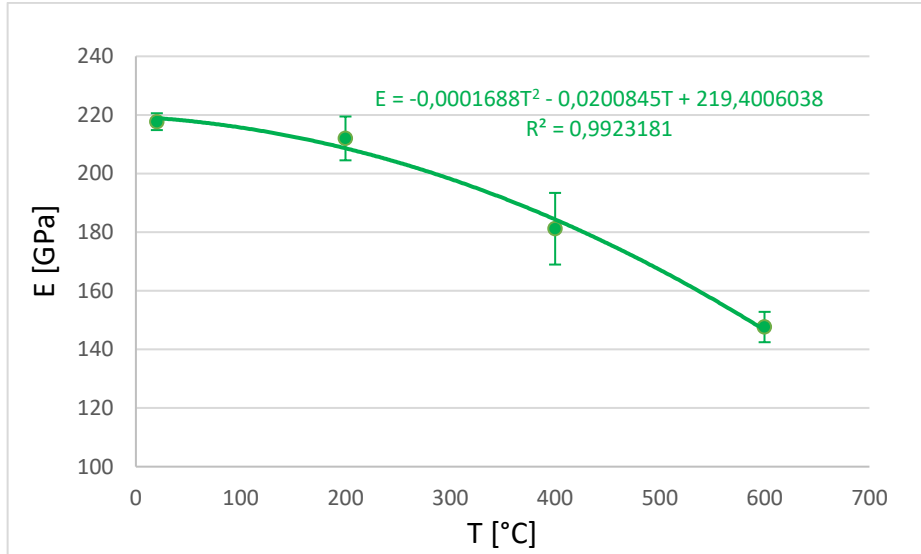


Figure 63: Static Young's modulus of steel 1 as a function of the temperature

The points represent the average static Young's modulus at different temperature and the dashes are the standard deviations. The behavior of the elastic modulus of the steel 1 up to 600°C can be well represented by a quadratic curve ($R^2 > 0,99$).

The literature suggests also different alternatives at the quadratic curve; it is possible to choose an exponential trendline: $E = E_0 - BT e^{-\left(\frac{T_0}{T}\right)}$, where E_0 , B and T_0 are empirical constants; this is valid when the variation of the Poisson ratio with temperature is small. [21] Another alternative is $E = [k - (k_1 T)^2]^6$, where k and k_1 are constants. [21]

For other kind of steels (e.g. steel 2,25Cr-1Mo virgin and aged) Young's modulus can be described by linear fits in the range from room temperature up to 600 °C. [22]

In this work the quadratic curve is used to fit the data because it is visually the best and provides a higher coefficient of determination R^2 in comparison with exponential and linear trendline. (see figures 63, 64 and 65).

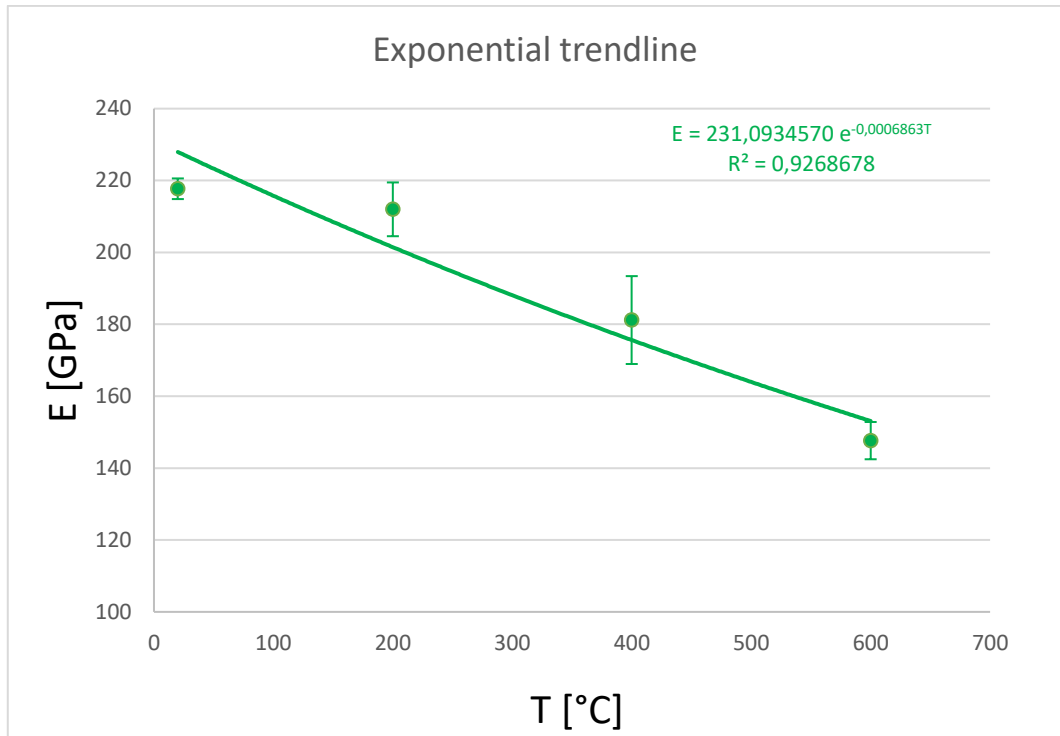


Figure 64: Exponential trendline

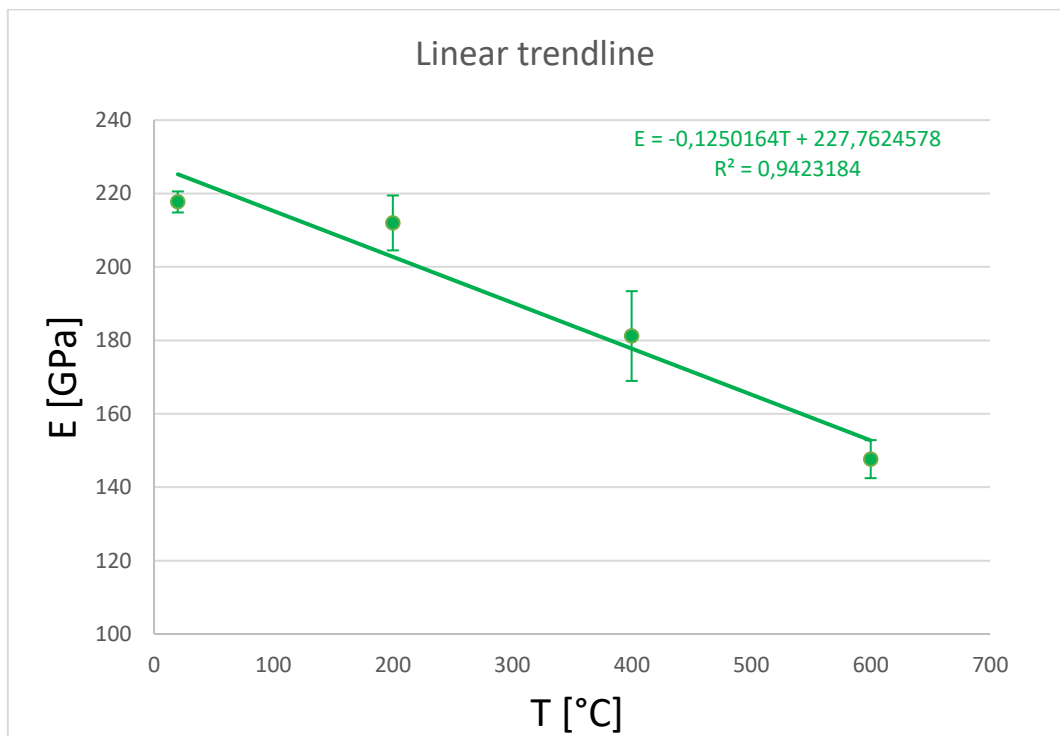


Figure 65: Linear trendline

2.6.2 Analysis of the data of impulse excitation tests

For the impulse excitation method at room temperature, the average of 5 measurements of dynamic Young's modulus, shear modulus and Poisson's ratio are reported.

Regarding the impulse excitation method at high temperature, the software of the equipment RFDA HT1050 calculates Young's modulus after the specimen is hit by the projectile. In general, this operation happens every two minutes therefore it has a value of dynamic Young's modulus every 6 °C. The trend of dynamic Young's modulus as a function of the temperature is plotted and a quadratic curve is used to fit the data.

Finally, the trends of static and dynamic Young's modulus as a function of the temperature are compared and an equation which links these two magnitudes is found.

2.6.3 Procedure to find the relationship between static and dynamic Young's modulus

To have a relationship between the static and dynamic Young's modulus the trendlines equations of the static and dynamic Young's modulus as a function of the temperature (paragraph 10.6) are used. For the steel 1, they are used:

- $E_{\text{static}} = -0,0001688T^2 - 0,0200845T + 219,4006038$
- $E_{\text{dynamic small}} = -0,0000489T^2 - 0,0452328T + 212,9551352$
- $E_{\text{dynamic full}} = -0,0000458T^2 - 0,0460605T + 209,2757279$

Young's modulus every 10°C from room temperature up to 600 °C are reported as in the table 19;

T [°C]	$E_{\text{dynamic small}}$ [GPa]	$E_{\text{dynamic full}}$ [GPa]	E_{stat} [GPa]
30	211,5541412	207,8526929	218,6461
40	211,0675832	207,3600279	218,3271
50	210,5712452	206,8582029	217,9744
60	210,0651272	206,3472179	217,5879
...
600	168,2114552	165,1514279	146,5819

Table 19: Dynamic and static Young's modulus as a function of the temperature every 10 °C

A second-degree equation is fit between dynamic Young's modulus of the small specimen and static Young's modulus and between dynamic Young's modulus of the full size specimen.

For the steel 1, they are (y is E_{dynamic} and x is E_{static}):

- $E_{\text{dynamic small specimens}} - E_{\text{static}}: y = 0,0029x^2 - 0,5058x + 179,99$
- $E_{\text{dynamic full size specimens}} - E_{\text{static}}: y = 0,003x^2 - 0,5483x + 181,27$

The same procedure is adopted for the steel 2 and 3.

Chapter 3

Results

3.1 Results of the static Young's modulus for steel 1

Stress-strain curves for specimen A at room temperature with extensometer MTS 634.12:

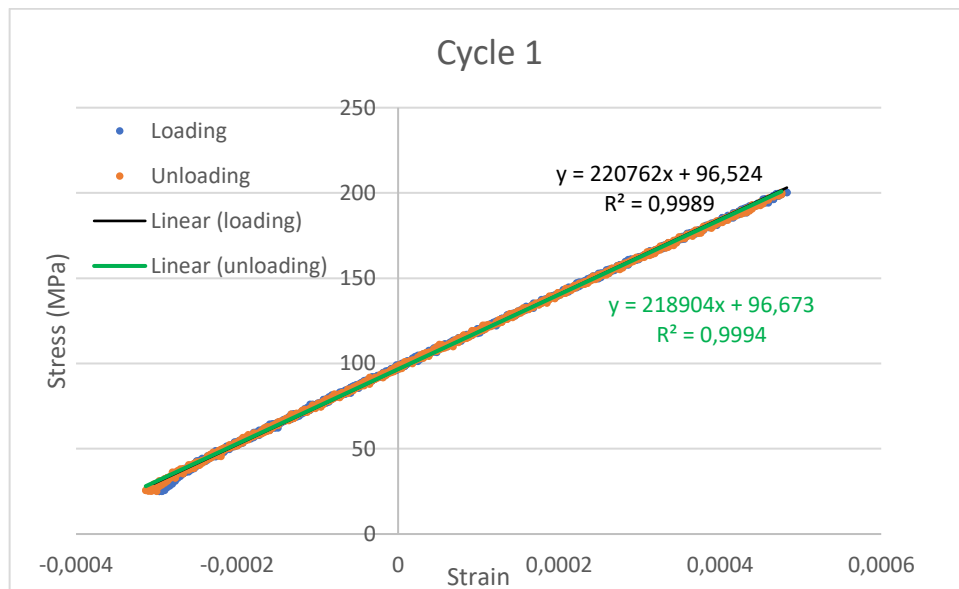


Figure 66: Cycle 1 for specimen A at room temperature (extensometer MTS)

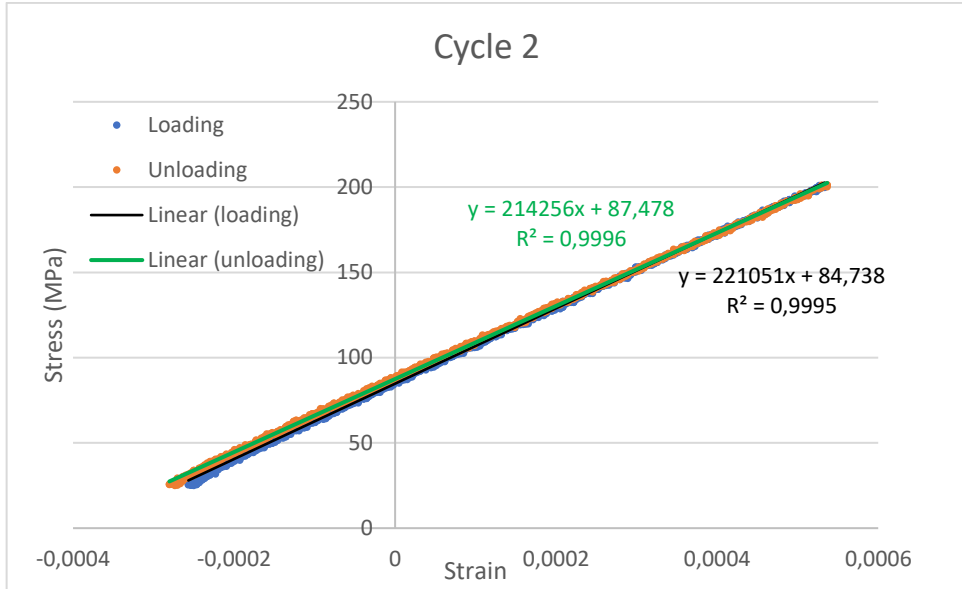


Figure 67: Cycle 2 for specimen A at room temperature (extensometer MTS)

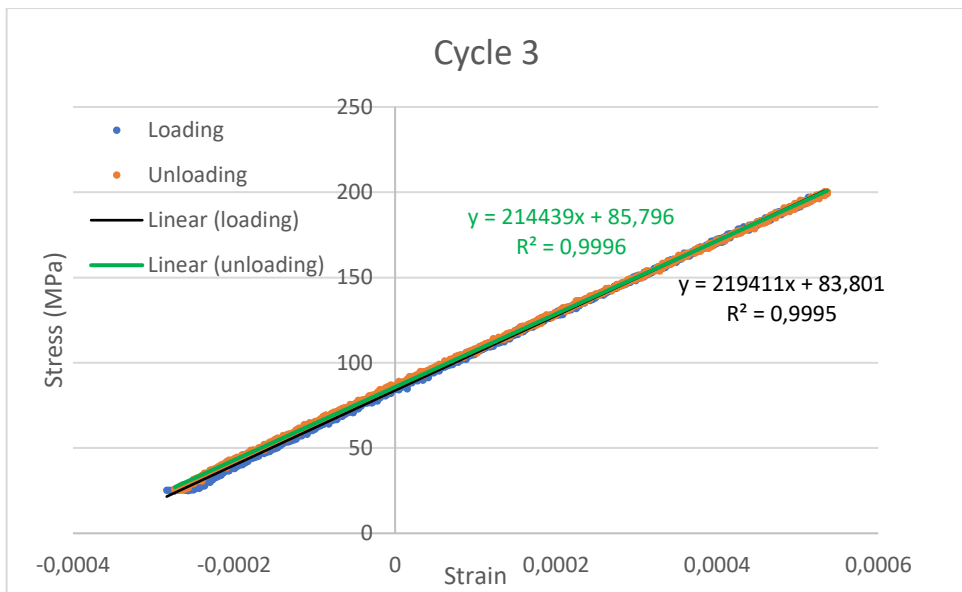


Figure 68: Cycle 3 for specimen A at room temperature (extensometer MTS)

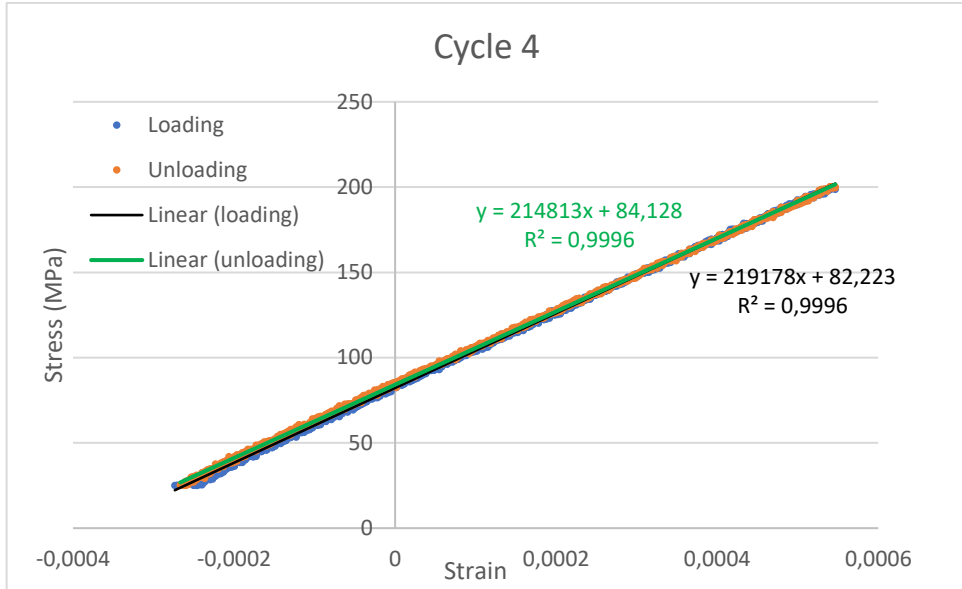


Figure 69: Cycle 4 for specimen A at room temperature (extensometer MTS)

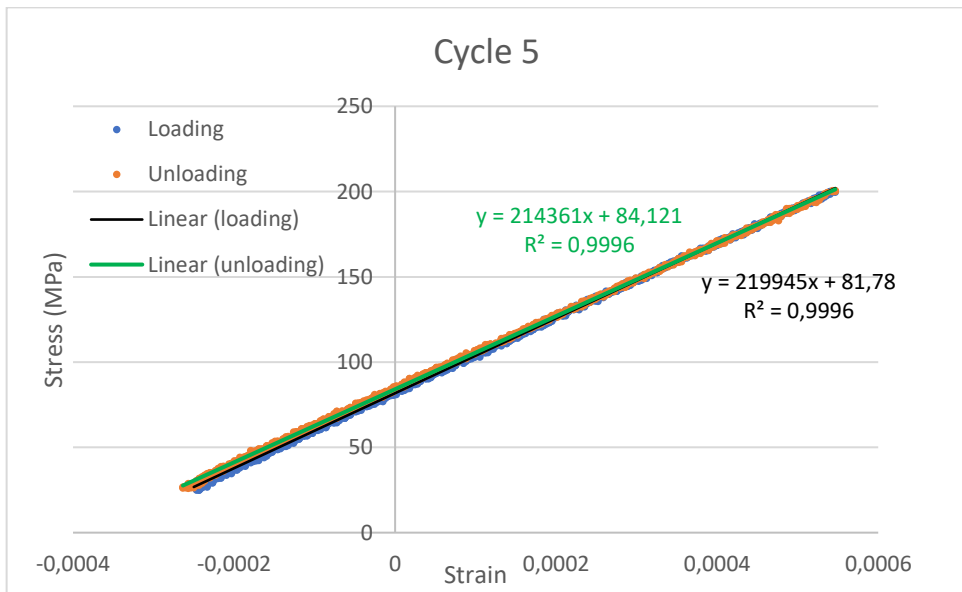


Figure 70: Cycle 5 for specimen A at room temperature (extensometer MTS)

The slopes for the specimen A at room temperature are listed in the table 20:

E [MPa]	
Loading	Unloading
220762,1	218903,7
221050,5	214255,7
219411,4	214438,6
219178,4	214813
219945,2	214360,9
Average	217712 Mpa
Std.dev.	2871 Mpa

Table 20: Slopes for the specimen A at room temperature (extensometer MTS)

All the slopes are used for the calculation of the average Young's modulus which results 217,7 GPa with a standard deviation of 2,71 GPa.

Stress-strain curves for specimen A at room temperature with extensometer Epsilon Model 3549 (ceramic extensometer):

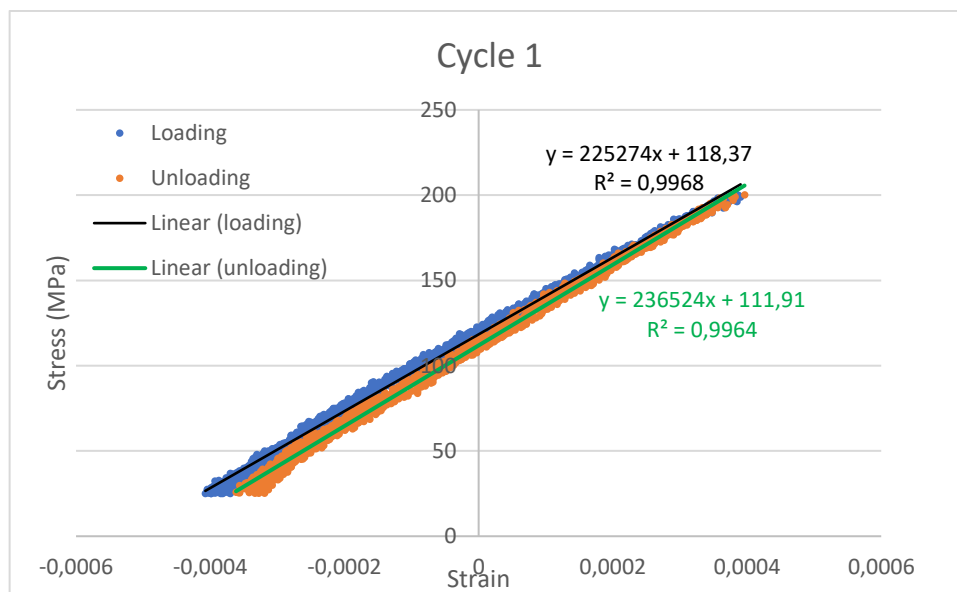


Figure 71: Cycle 1 for specimen A at room temperature (extensometer Epsilon Model 3549)

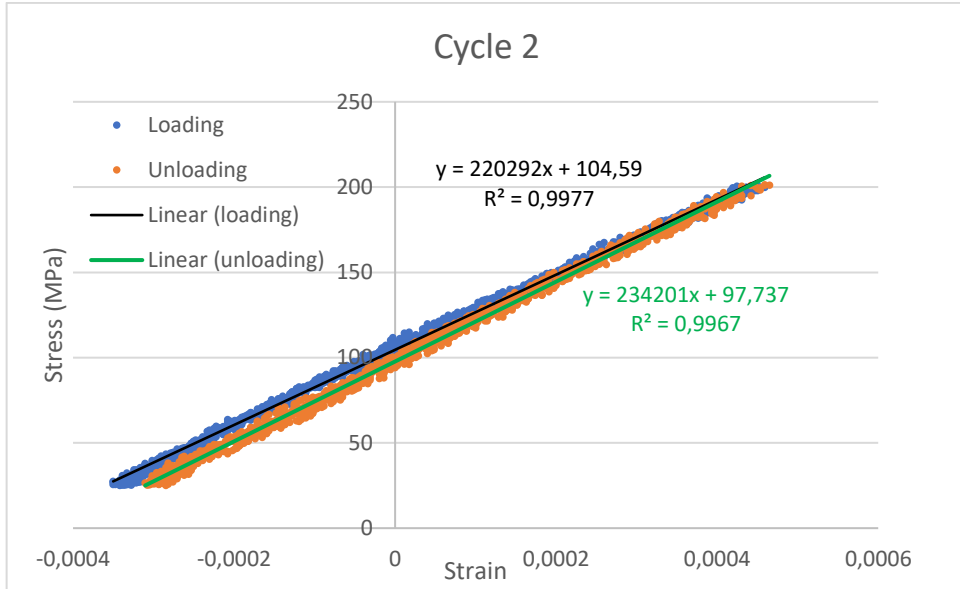


Figure 72: Cycle 2 for specimen A at room temperature (extensometer Epsilon Model 3549)

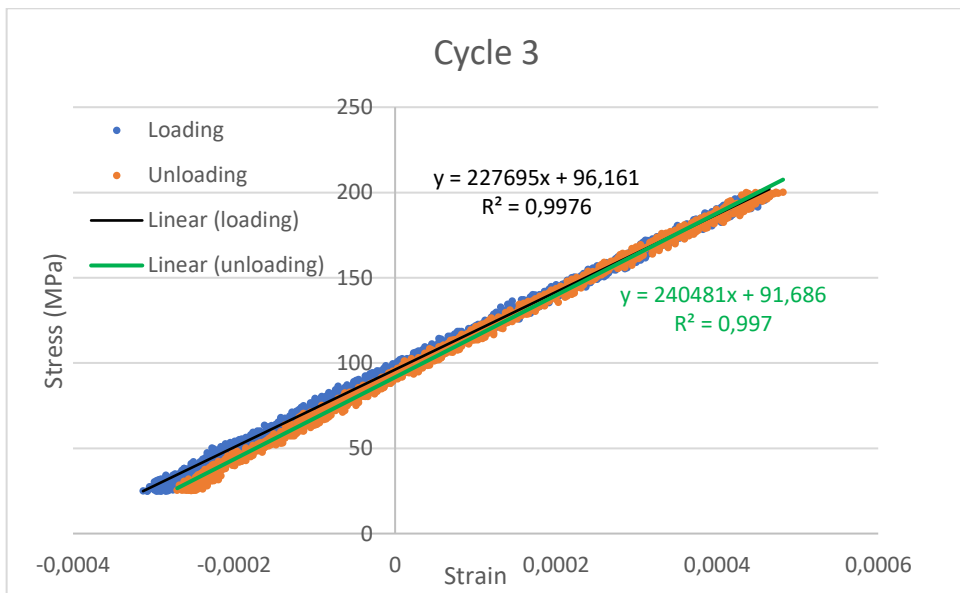


Figure 73: Cycle 3 for specimen A at room temperature (extensometer Epsilon Model 3549)

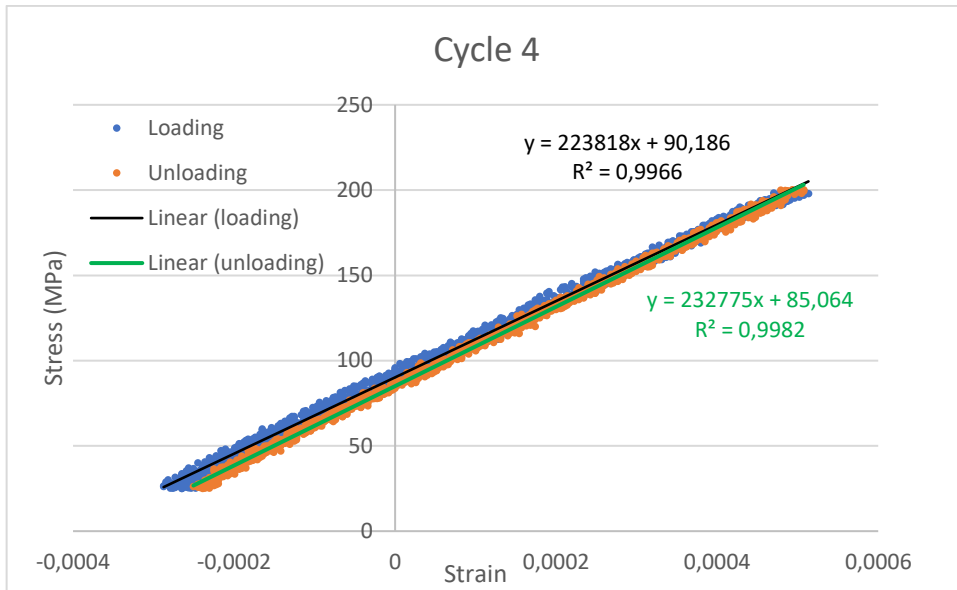


Figure 74: Cycle 4 for specimen A at room temperature (extensometer Epsilon Model 3549)

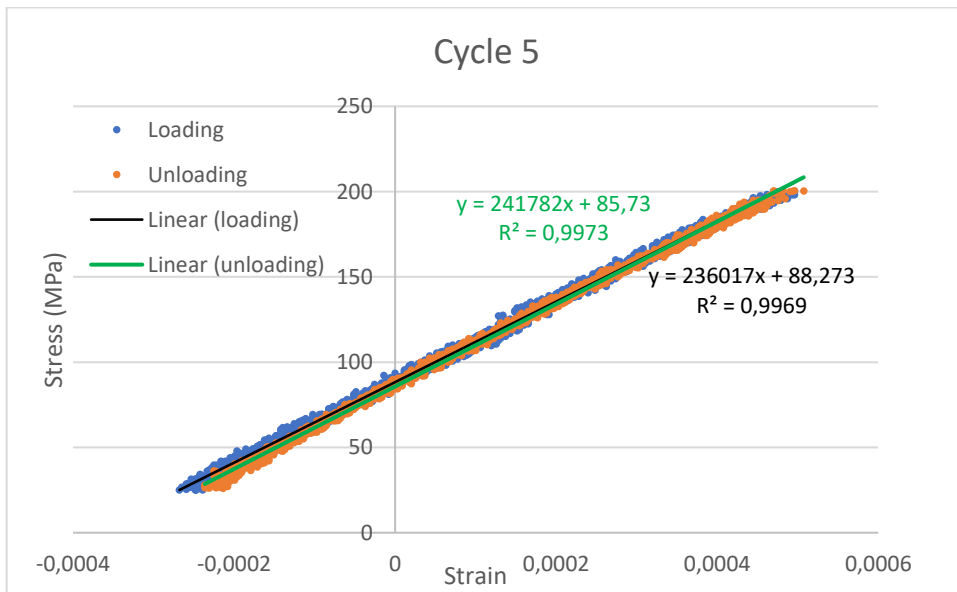


Figure 75: Cycle 5 for specimen A at room temperature (extensometer Epsilon Model 3549)

The slopes for the specimen A at room temperature using the ceramic extensometer are listed in the table 21:

E [MPa]	
Loading	Unloading
225273,9	236415,9
220291,7	234200,5
227695,4	240481,3
223818,3	232775,4
236017,3	241782,3
Average	224270 MPa
Std.dev.	3096 MPa

Table 21: Slopes for the specimen A at room temperature (extensometer Epsilon Model 3549)

The average Young's modulus results of 224,3 GPa with a standard deviation of 3,10 GPa.

Stress-strain curves for specimen A at 200 °C with extensometer Epsilon model 3549:

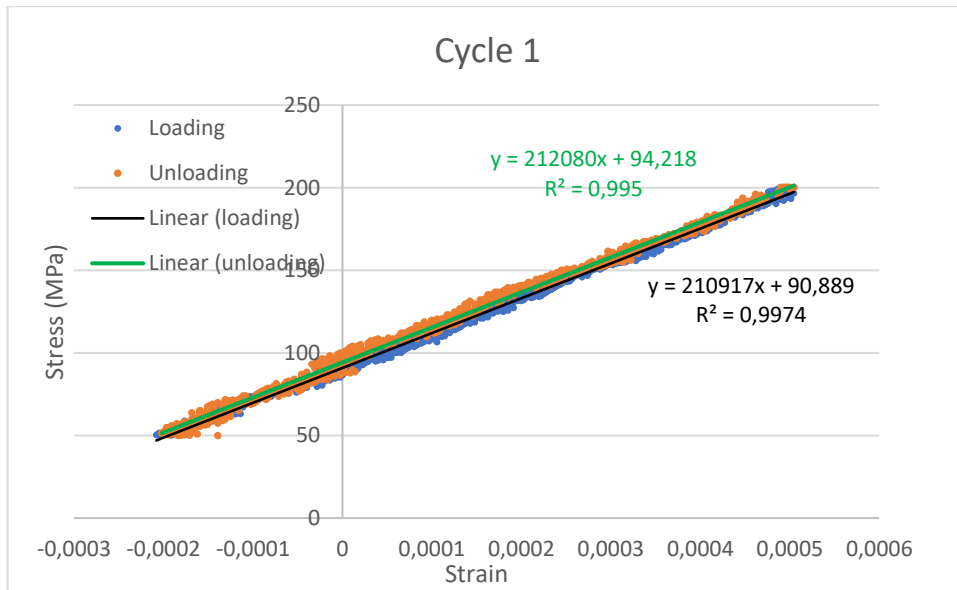


Figure 76: Cycle 1 for specimen A at 200 °C (extensometer Epsilon Model 3549)

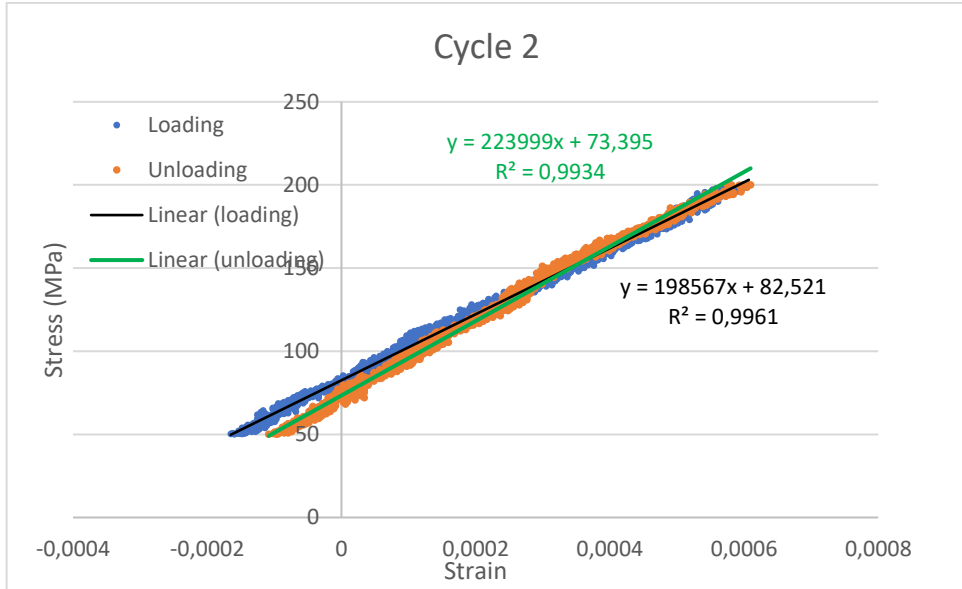


Figure 77: Cycle 2 for specimen A at 200 °C (extensometer Epsilon Model 3549)

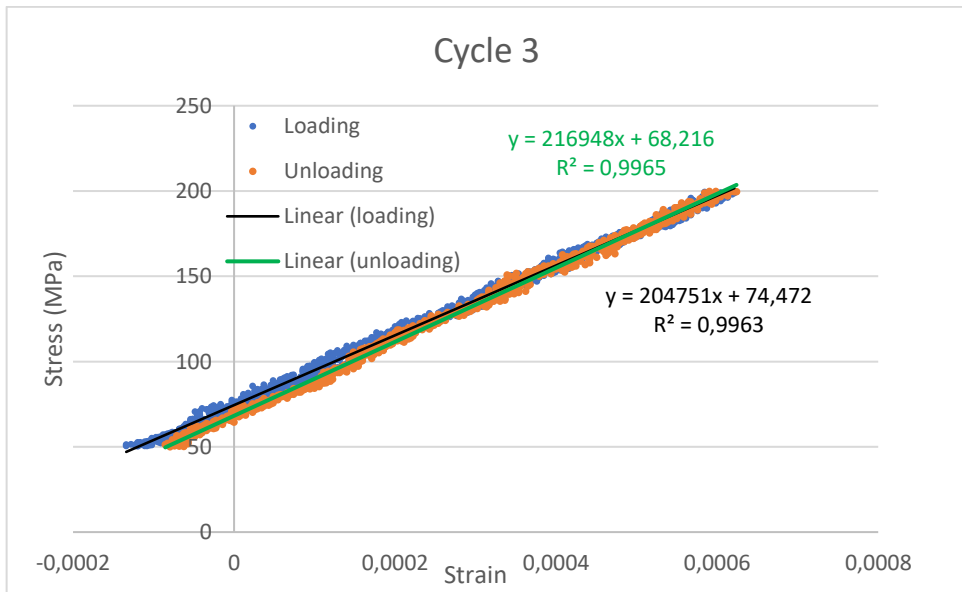


Figure 78: Cycle 3 for specimen A at 200 °C (extensometer Epsilon Model 3549)

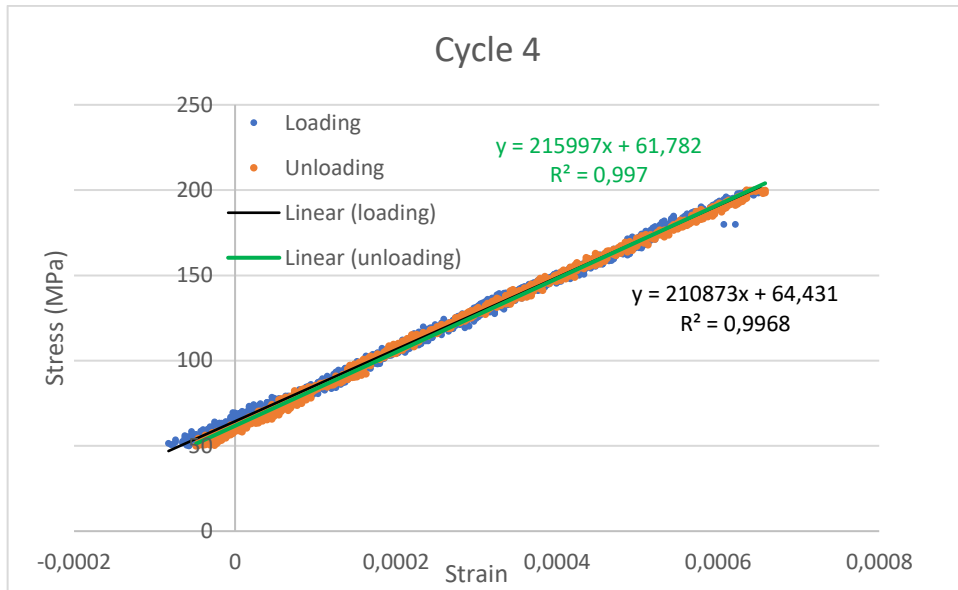


Figure 79: Cycle 4 for specimen A at 200 °C (extensometer Epsilon Model 3549)

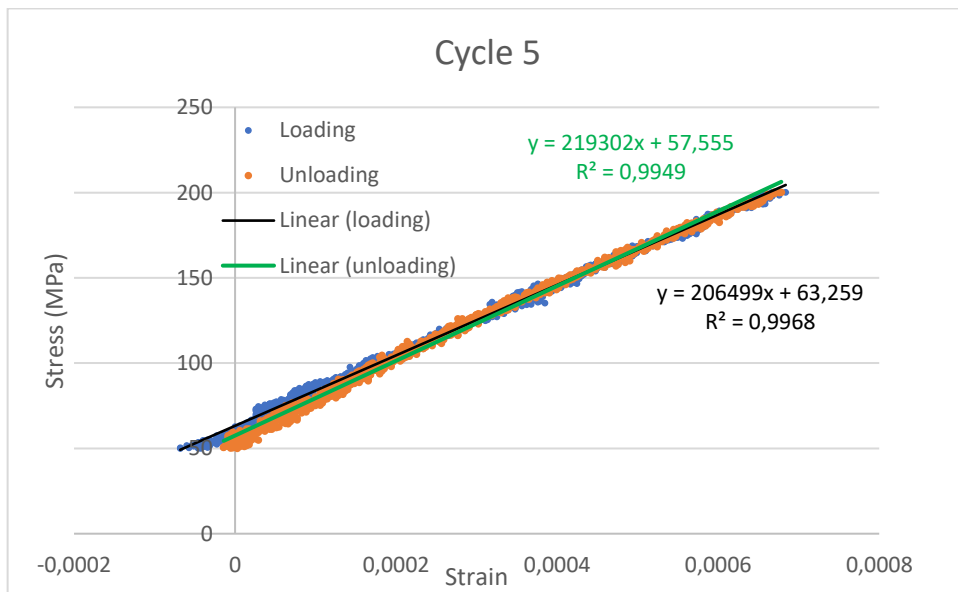


Figure 80: Cycle 5 for specimen A at 200 °C (extensometer Epsilon Model 3549)

The slopes for the specimen A at 200 °C using the ceramic extensometer are listed in the table 22:

E[MPa]	
Loading	Unloading
210917,1	212079,8
198566,9	223998,5
204750,6	216948,2
210873,3	215997
206498,6	219301,6
Average	211993 MPa
Std dev	7479 MPa

Table 22: Slopes for the specimen A at 200 °C (extensometer Epsilon Model 3549)

All the slopes are used for the calculation of the average Young's modulus; it is 212,0 GPa with a standard deviation of 7,48 GPa.

Stress-strain curves for specimen A at 400 °C with extensometer Epsilon model 3549:

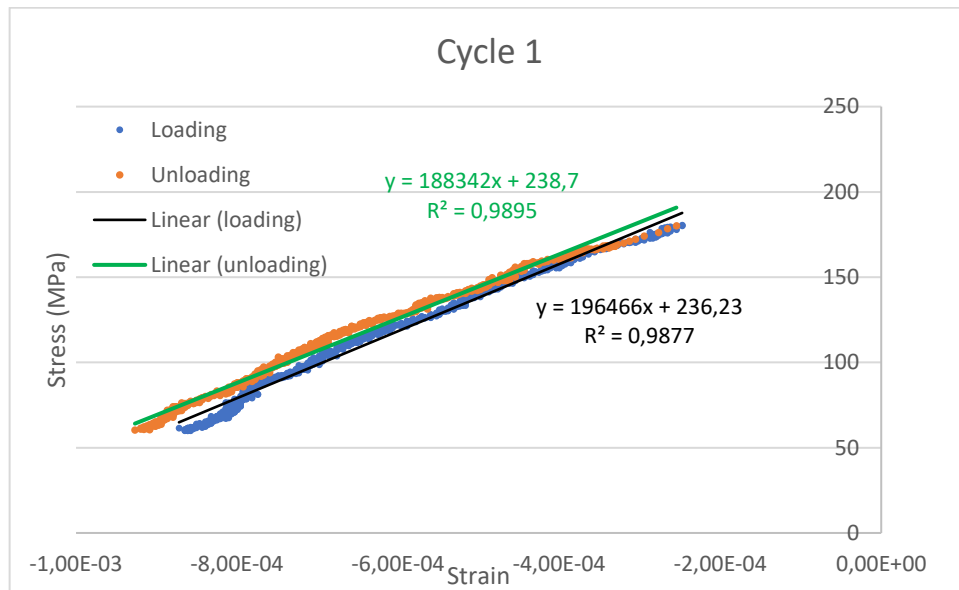


Figure 81: Cycle 1 for specimen A at 400 °C (extensometer Epsilon Model 3549)

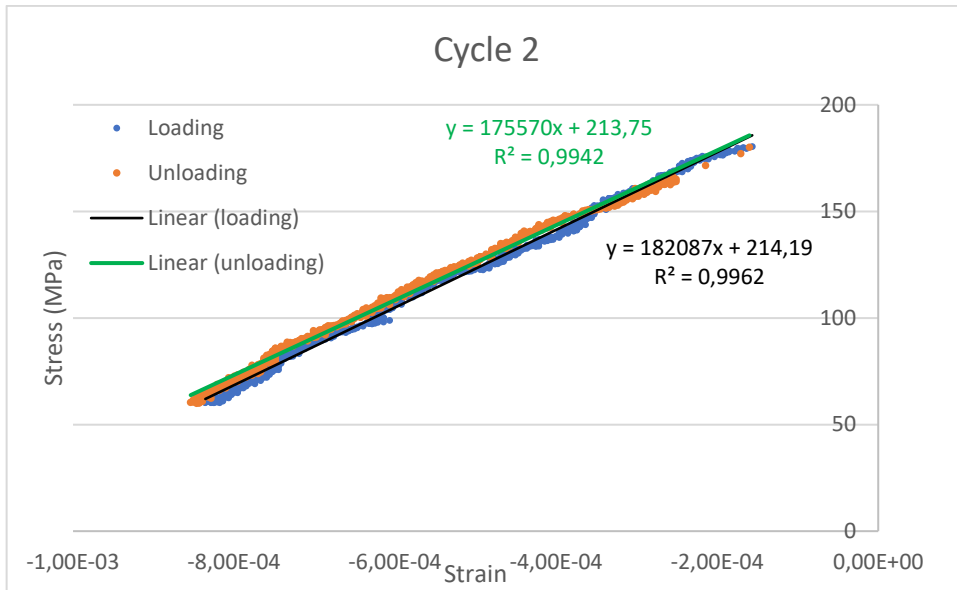


Figure 82: Cycle 2 for specimen A at 400 °C (extensometer Epsilon Model 3549)

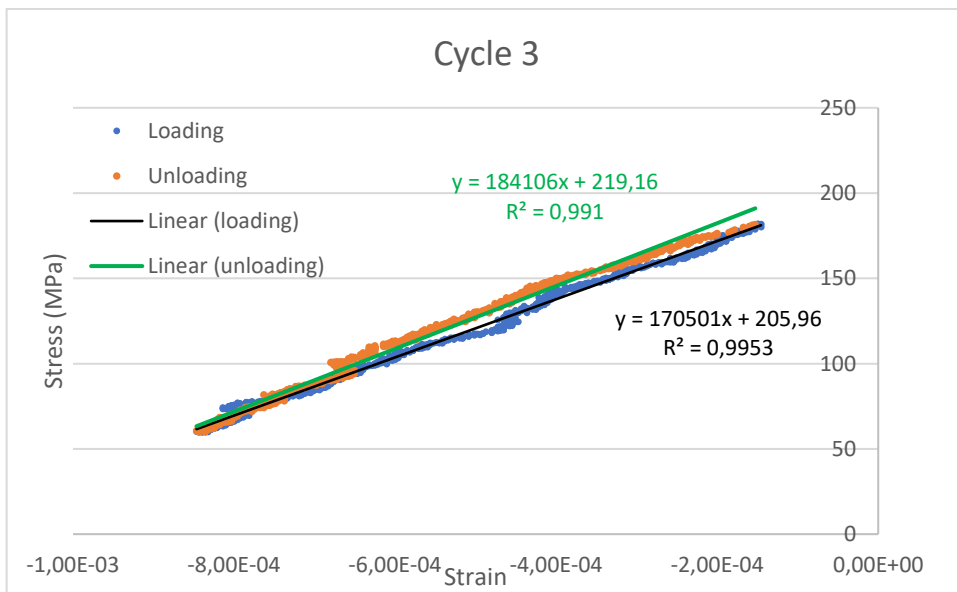


Figure 83: Cycle 3 for specimen A at 400 °C (extensometer Epsilon Model 3549)

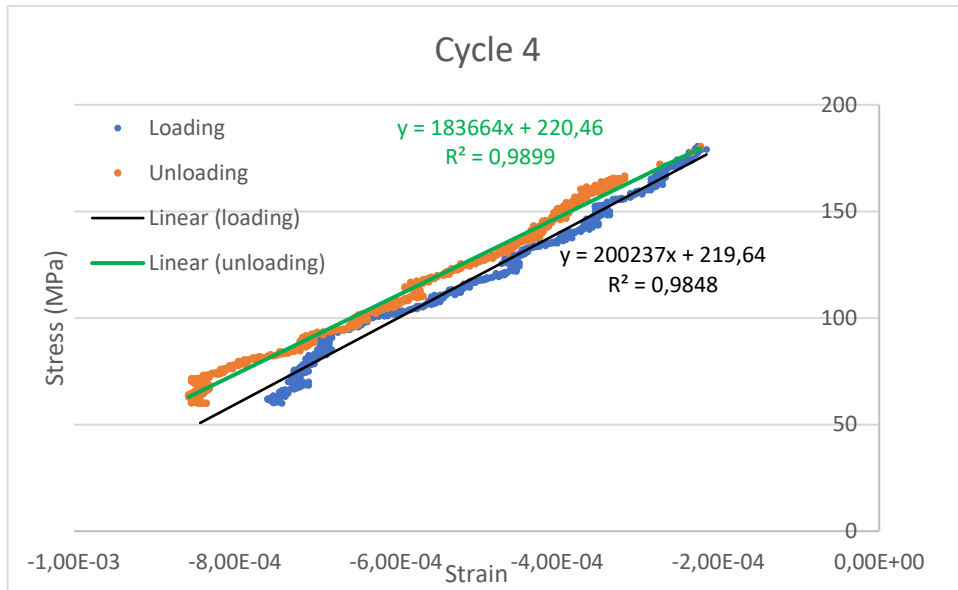


Figure 84: Cycle 4 for specimen A at 400 °C (extensometer Epsilon Model 3549)

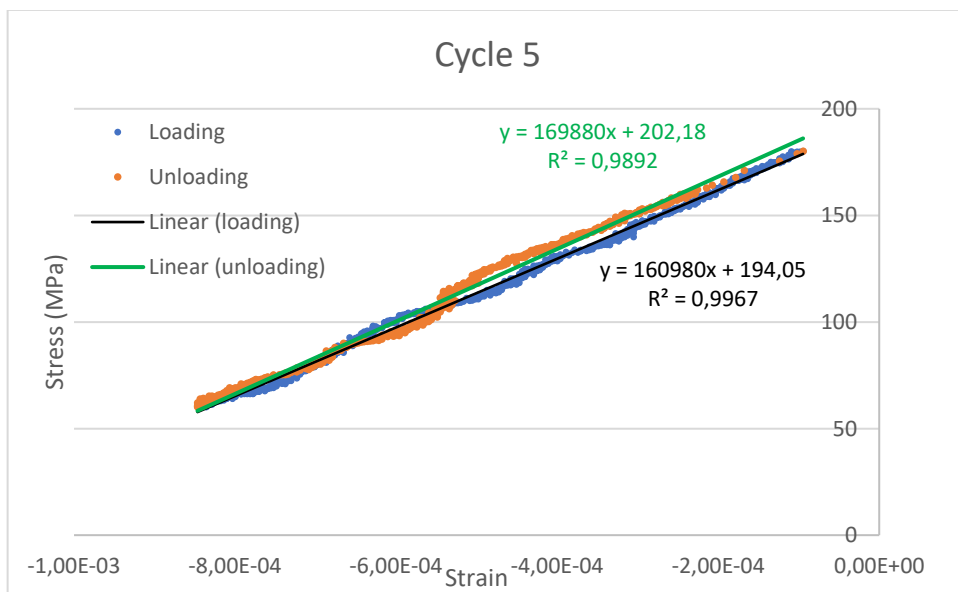


Figure 85: Cycle 5 for specimen A at 400 °C (extensometer Epsilon Model 3549)

The slopes for the specimen A at 400 °C using the ceramic extensometer are listed in the table 23:

E[MPa]	
Loading	Unloading
196465,8	188342,2
182087,4	175570,2
170501	184106,5
200236,6	183664,4
160980	169880,5
Average	181183 MPa
Std dev	12224 MPa

Table 23: Slopes for the specimen A at 400 °C (extensometer Epsilon Model 3549)

All the slopes are used for the calculation of the average Young's modulus; it results of 181,2 GPa with a standard deviation of 12,2 GPa.

Stress-strain curves for specimen A at 600 °C with extensometer Epsilon model 3549:

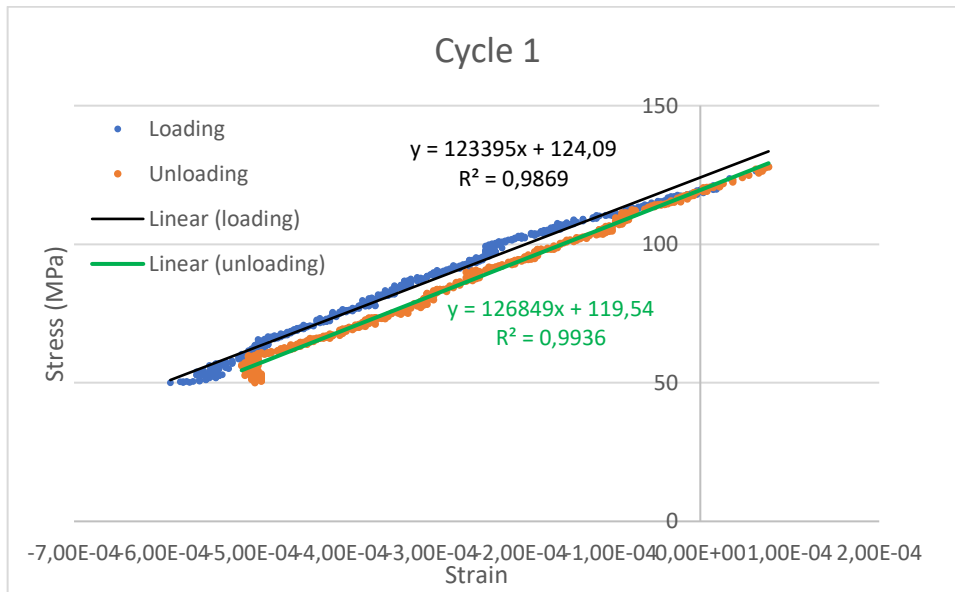


Figure 86: Cycle 1 for specimen A at 600 °C (extensometer Epsilon Model 3549)

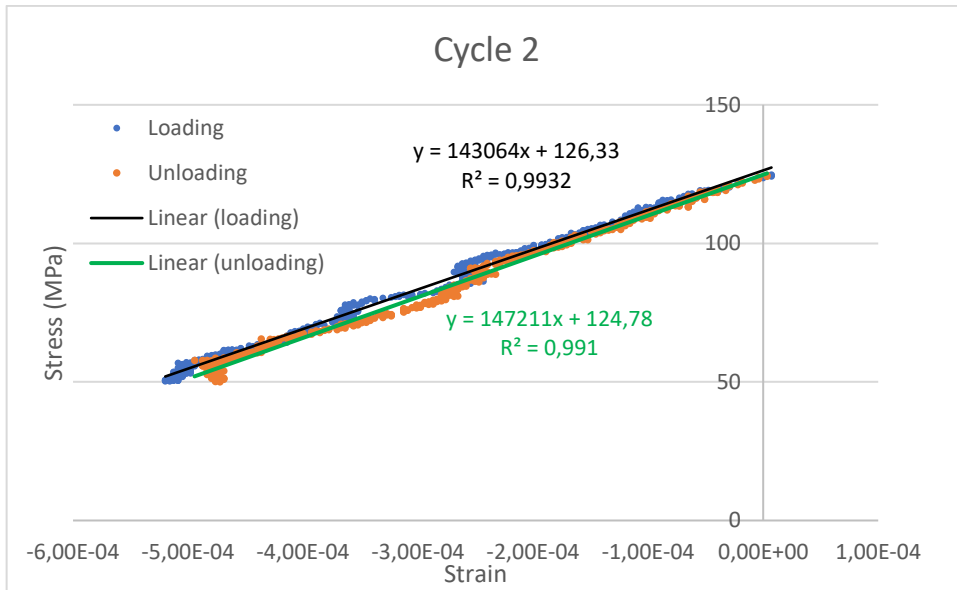


Figure 87: Cycle 2 for specimen A at 600 °C (extensometer Epsilon Model 3549)

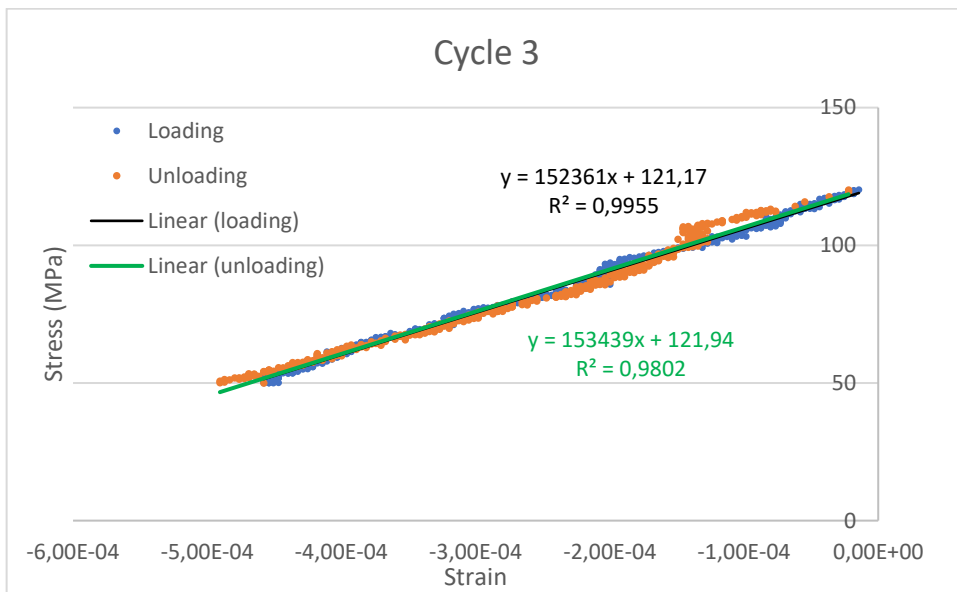


Figure 88: Cycle 3 for specimen A at 600 °C (extensometer Epsilon Model 3549)

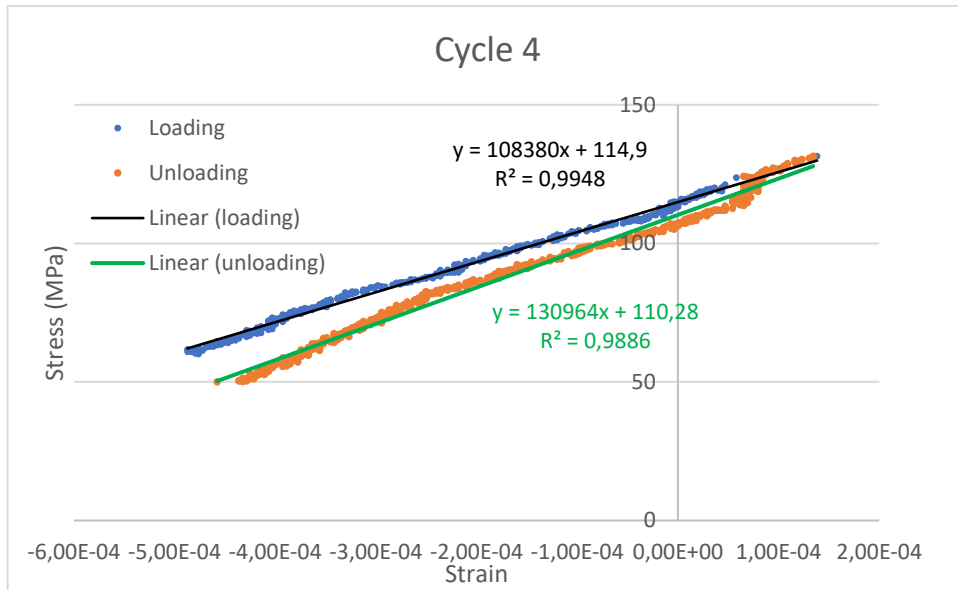


Figure 89: Cycle 4 for specimen A at 600 °C (extensometer Epsilon Model 3549)

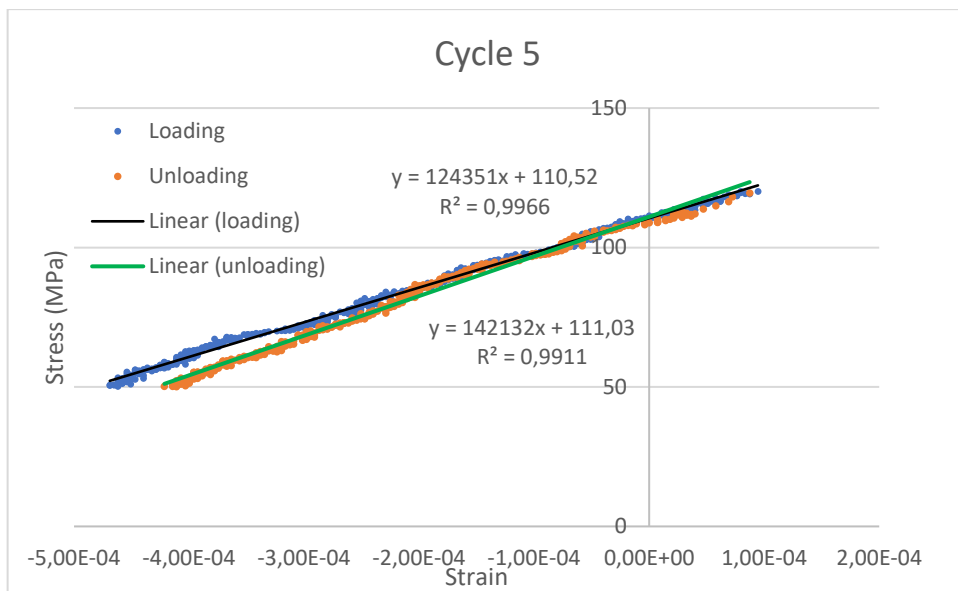


Figure 90: Cycle 5 for specimen A at 600 °C (extensometer Epsilon Model 3549)

The slopes for the specimen A at 600 °C using the ceramic extensometer are listed in the table 24:

E [MPa]	
Growth	Decline
123394,6	126848,5
143064,1	147211,4
152360,6	153438,9
108380,1	130964,1
124351,4	142131,5
Average	147641 MPa
Std dev	5181 MPa

Table 24: Slopes for the specimen A at 600 °C (extensometer Epsilon Model 3549)

For the calculation of the average Young's modulus at 600 °C the second, the third and half of fifth cycle have been considered. The average is 147,6 GPa and the standard deviation is 5,18 GPa.

In the table 25, the result obtained using extensometer MTS is highlighted in yellow while the results from the ceramic extensometer are in grey.

T [°C]	E stat [GPa]	Std. Dev. [GPa]	E stat [GPa]	Std. Dev. [GPa]
RT	217,7	2,87	224,3	3,10
200	212,0	7,48	212,0	7,48
400	181,2	12,22	181,2	12,22
600	147,6	5,18	147,6	5,18

Table 25: Static Young's modulus for steel 1

The trendline which describes the behavior of Young's modulus of the steel 1 as a function of the temperature is: $E = -0,0001688T^2 - 0,0200845T + 219,4006038$ and it is shown in the figure 91.

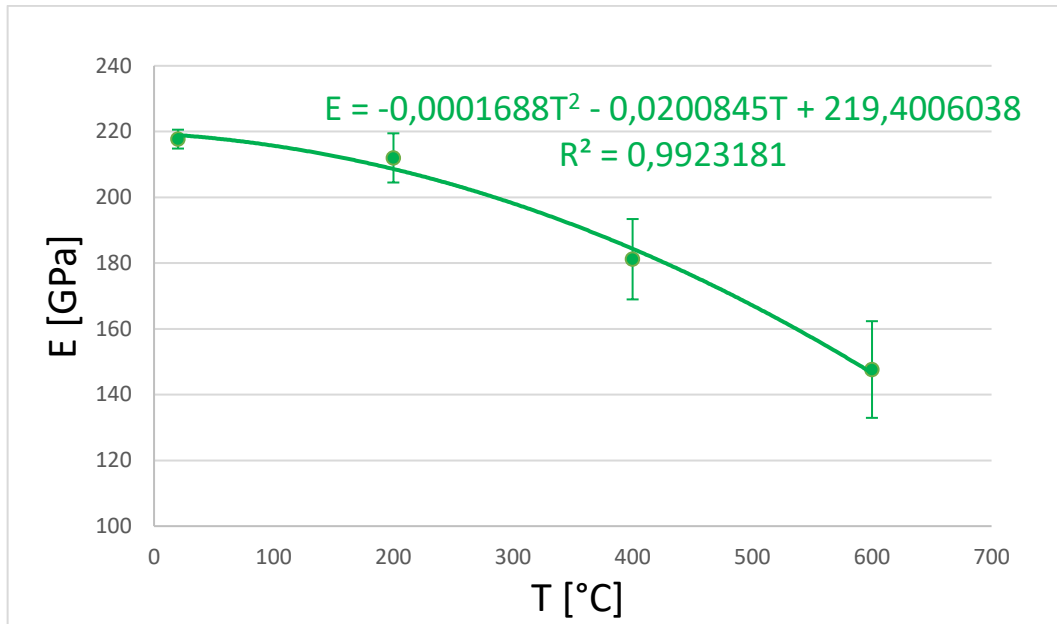


Figure 91: Trendline of static Young's modulus using extensometer MTS at room temperature and ceramic extensometer at high temperatures (steel 1).

3.2 Results of the static Young's modulus for steel 2

Stress-strain curves for specimen B at room temperature with extensometer MTS 634.12:

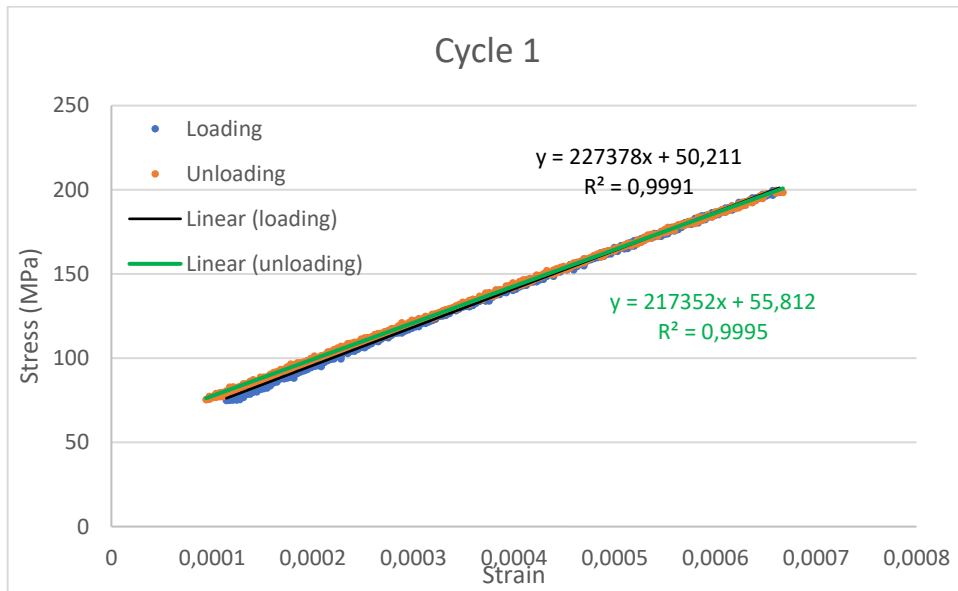


Figure 92: Cycle 1 for specimen B at room temperature (extensometer MTS)

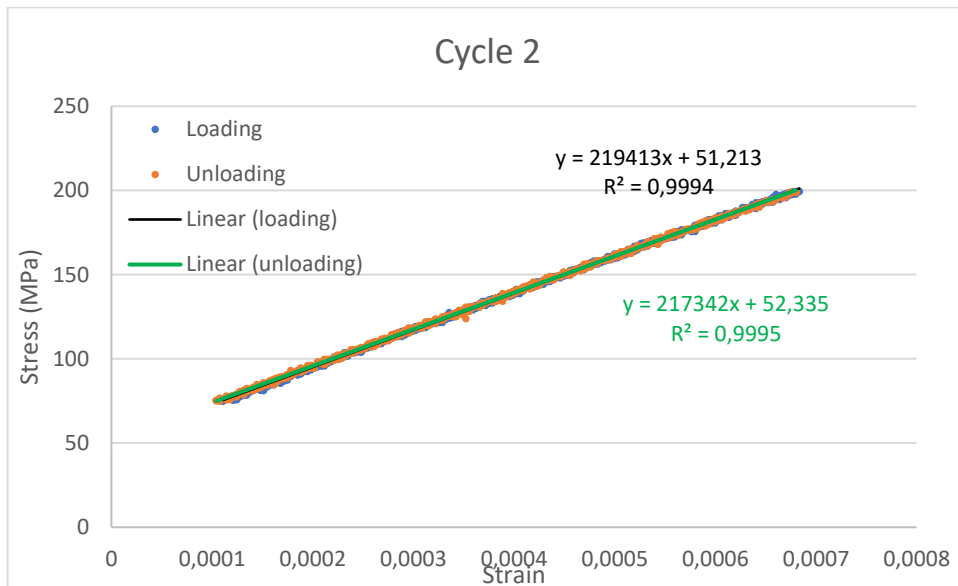


Figure 93: Cycle 2 for specimen B at room temperature (extensometer MTS)

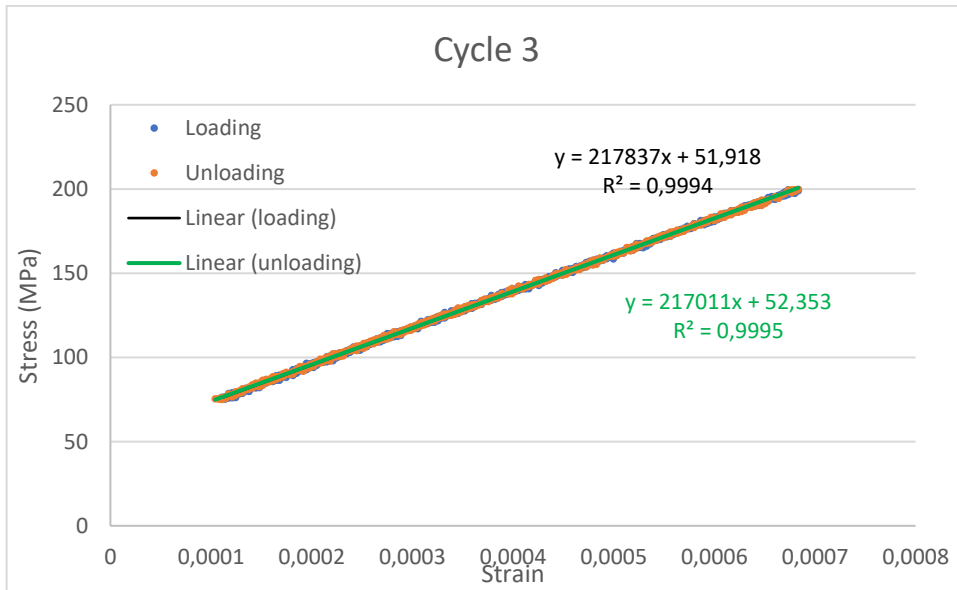


Figure 94: Cycle 3 for specimen B at room temperature (extensometer MTS)

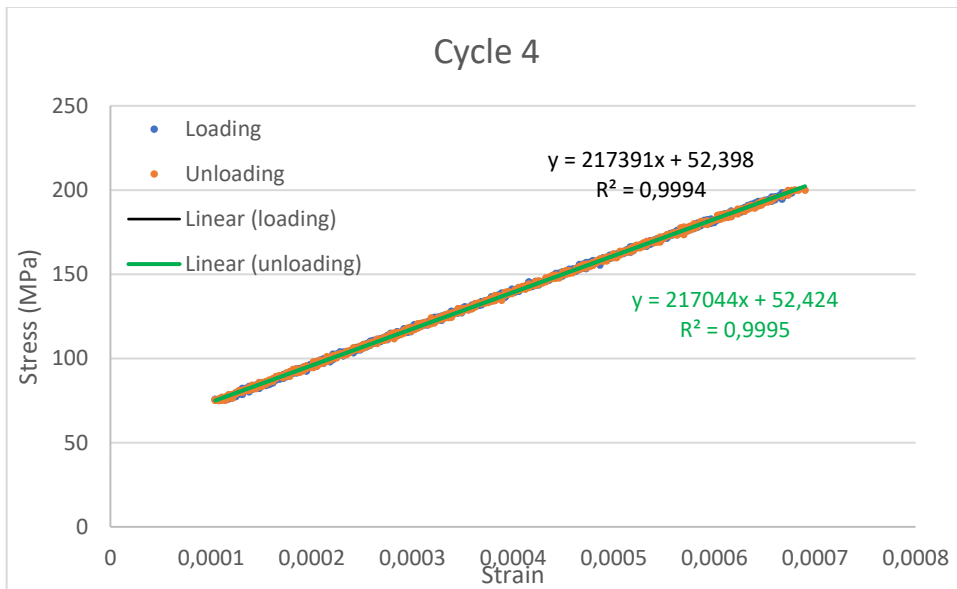


Figure 95: Cycle 4 for specimen B at room temperature (extensometer MTS)

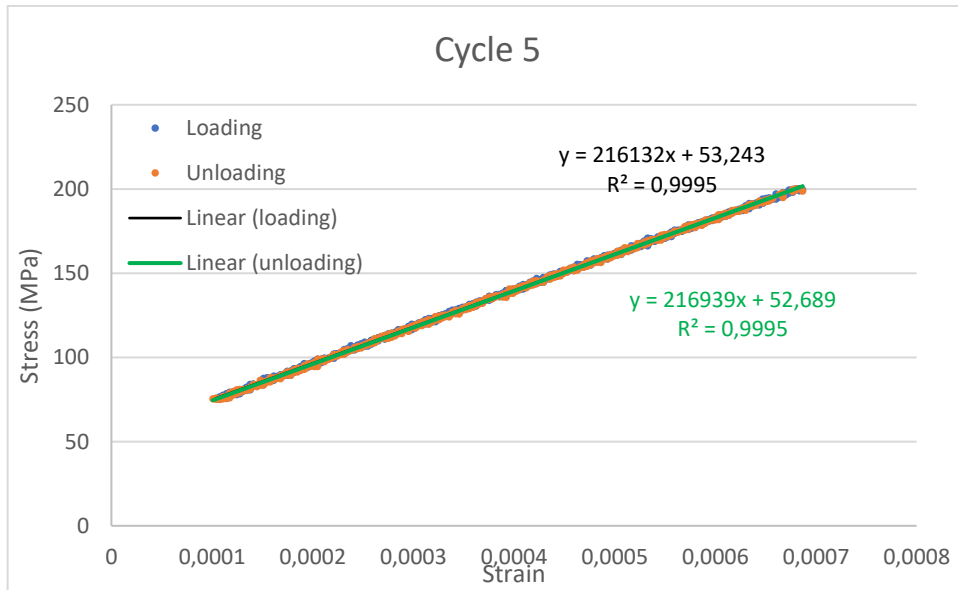


Figure 96: Cycle 5 for specimen B at room temperature (extensometer MTS)

The slopes for the specimen B at room temperature are listed in the table 26.

E [MPa]	
Loading	Unloading
227378,2	217351,5
219412,7	217342,1
217837,1	217011
217388,8	217037,5
216132,4	216939,2
Average	218383 MPa
Std.dev.	3270 MPa

Table 26: Slopes for the specimen B at room temperature (extensometer MTS)

All the slopes are used for the calculation of the average Young's modulus which results of 218,4 GPa with a standard deviation of 3,27 GPa.

Stess-strain curves for specimen B at room temperature with extensometer Epsilon Model 3549 (ceramic extensometer):

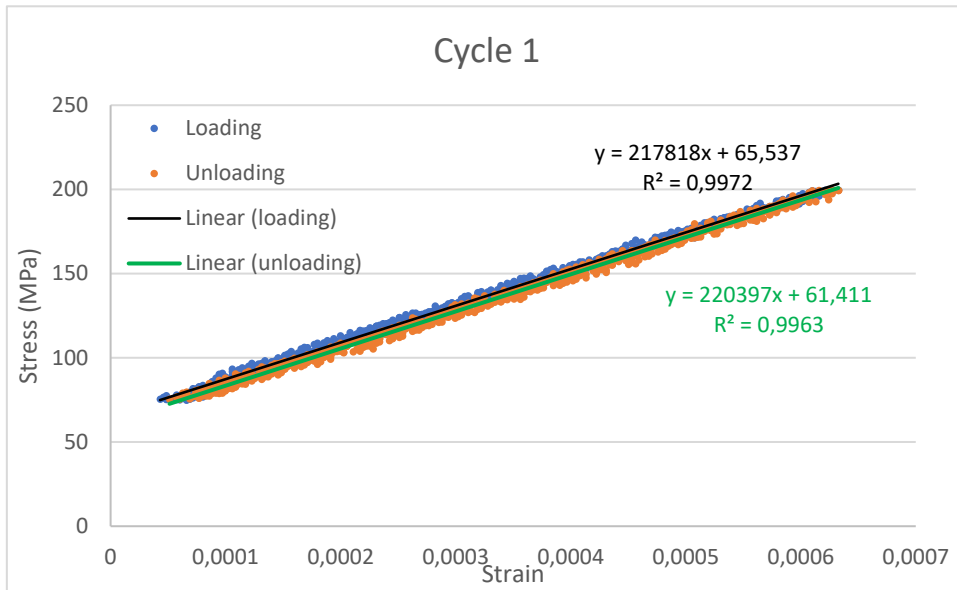


Figure 97: Cycle 1 for specimen B at room temperature (extensometer Epsilon Model 3549)

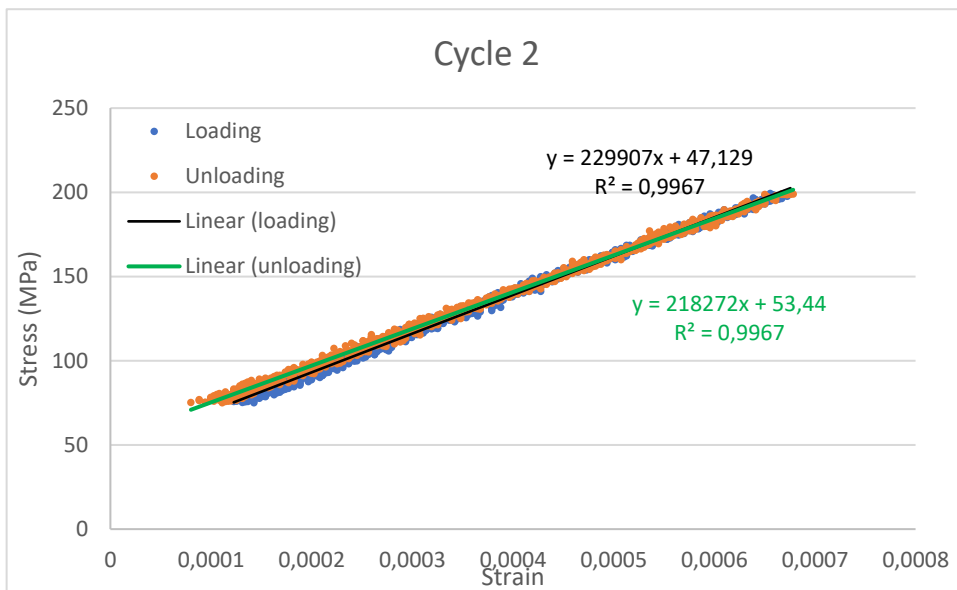


Figure 98: Cycle 2 for specimen B at room temperature (extensometer Epsilon Model 3549)

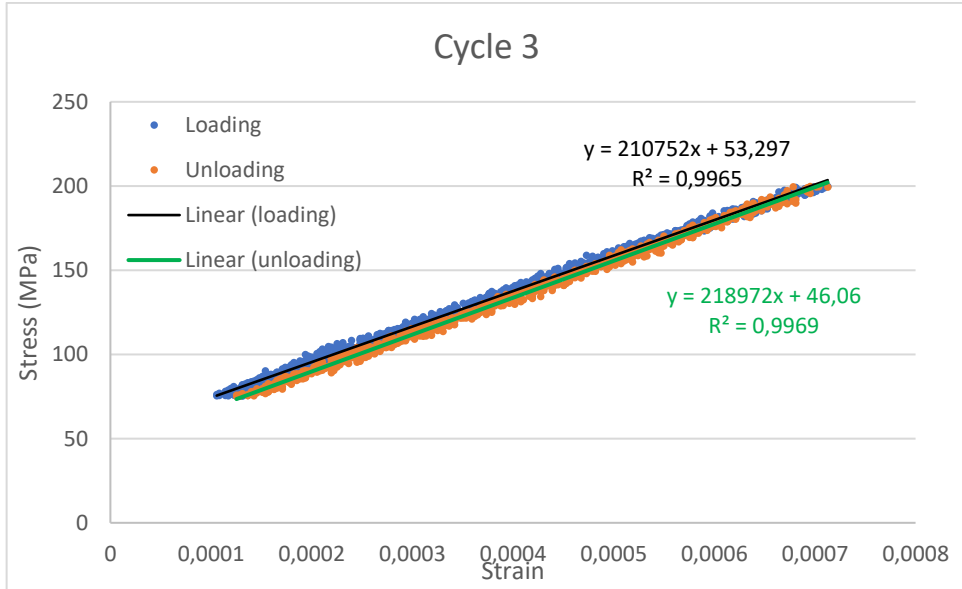


Figure 99: Cycle 3 for specimen B at room temperature (extensometer Epsilon Model 3549)

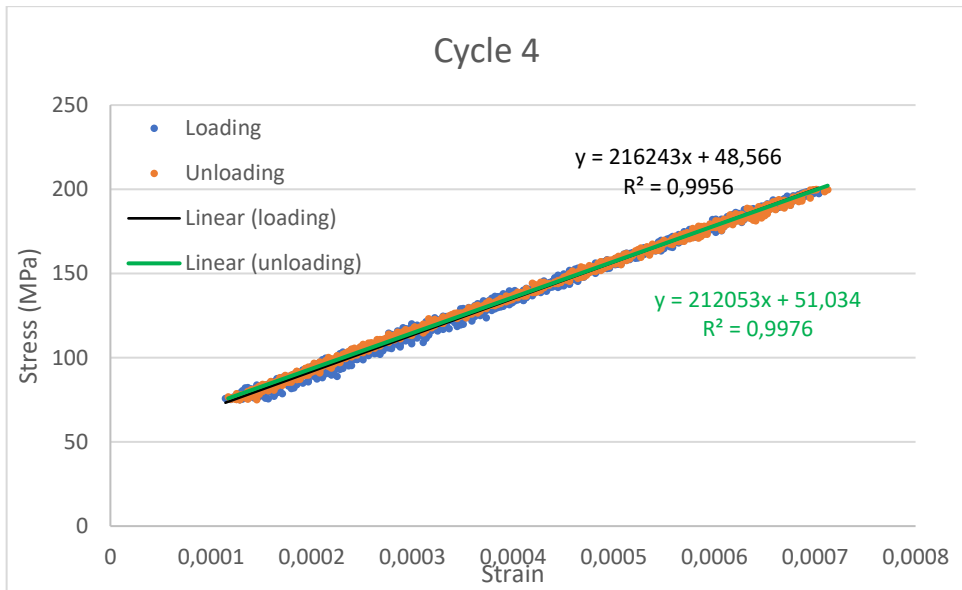


Figure 100: Cycle 4 for specimen B at room temperature (extensometer Epsilon Model 3549)

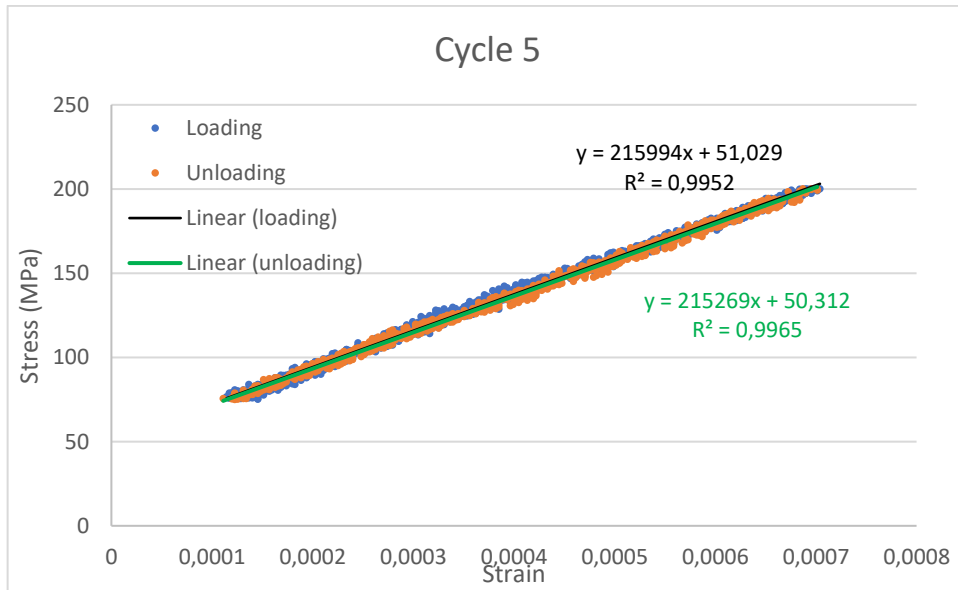


Figure 101: Cycle 5 for specimen B at room temperature (extensometer Epsilon Model 3549)

The slopes for the specimen B at room temperature using the ceramic extensometer are listed in the table 27:

E [MPa]	
Loading	Unloading
217817,9	220397,3
229907,3	218271,9
210751,6	218972,4
216227,8	211981,7
215994	215268,6
Average	217559 MPa
Std.dev.	5270 MPa

Table 27: Slopes for the specimen B at room temperature (extensometer Epsilon Model 3549)

All the slopes are used for the calculation of the average Young's modulus; it is 217,6 GPa with a standard deviation of 5,27 GPa.

Stress-strain curves for specimen B at 200 °C with extensometer Epsilon model 3549:

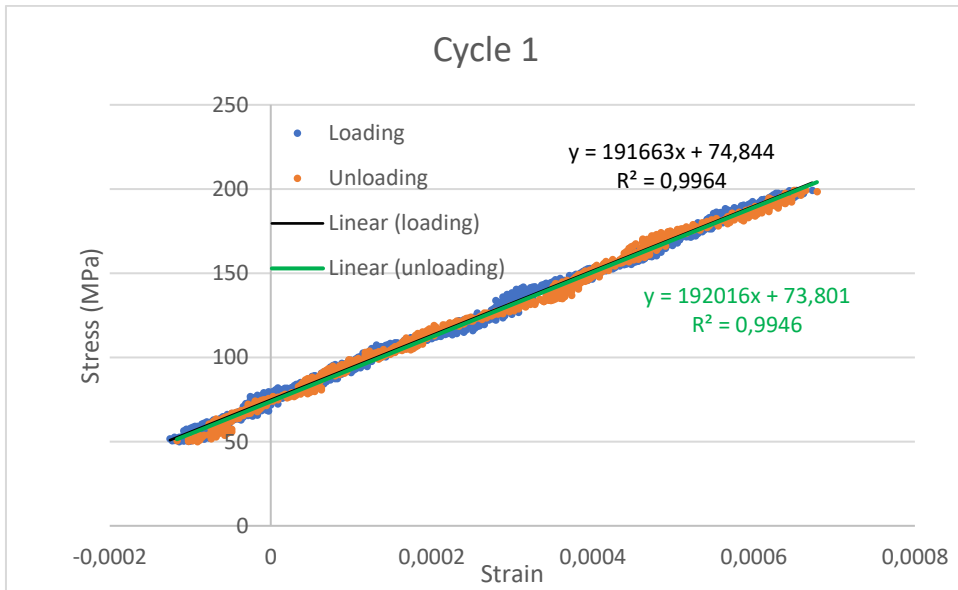


Figure 102: Cycle 1 for specimen B at 200 °C (extensometer Epsilon Model 3549)

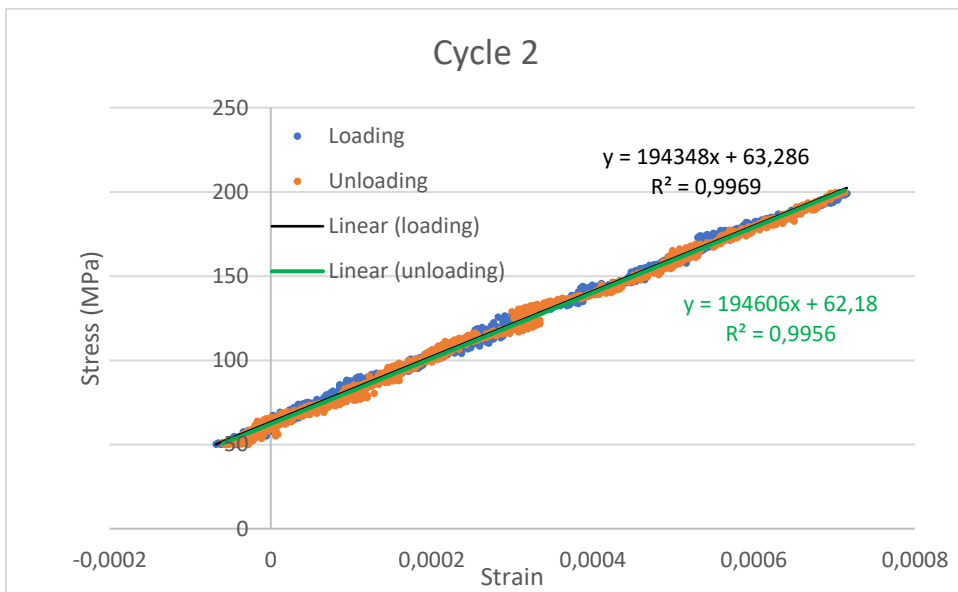


Figure 103: Cycle 2 for specimen B at 200 °C (extensometer Epsilon Model 3549)

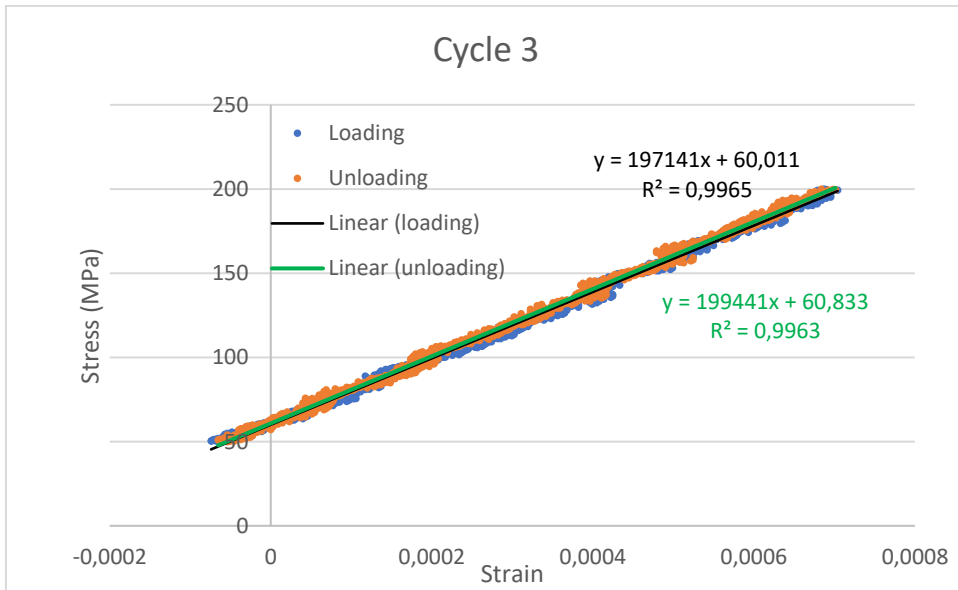


Figure 104: Cycle 3 for specimen B at 200 °C (extensometer Epsilon Model 3549)

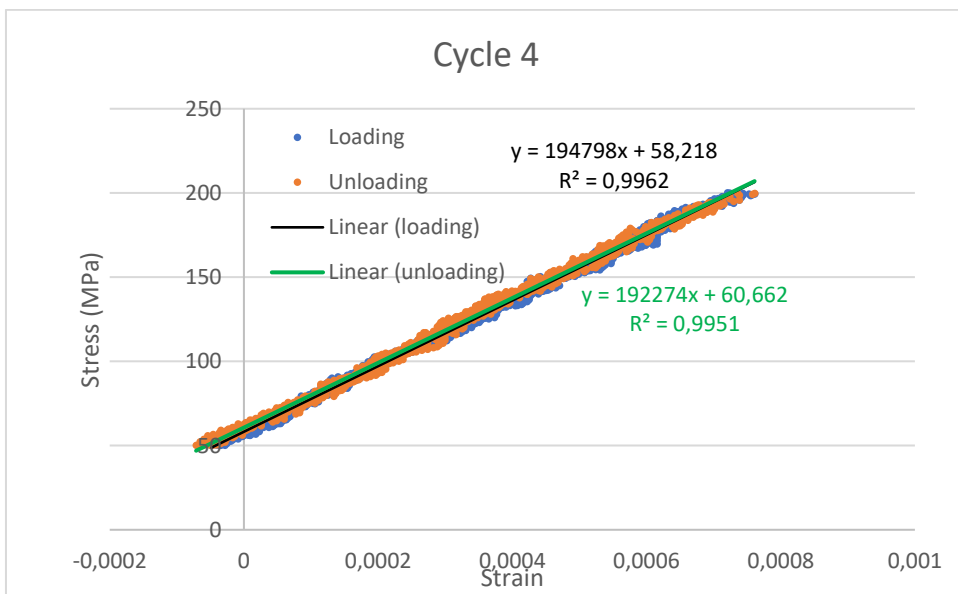


Figure 105: Cycle 4 for specimen B at 200 °C (extensometer Epsilon Model 3549)

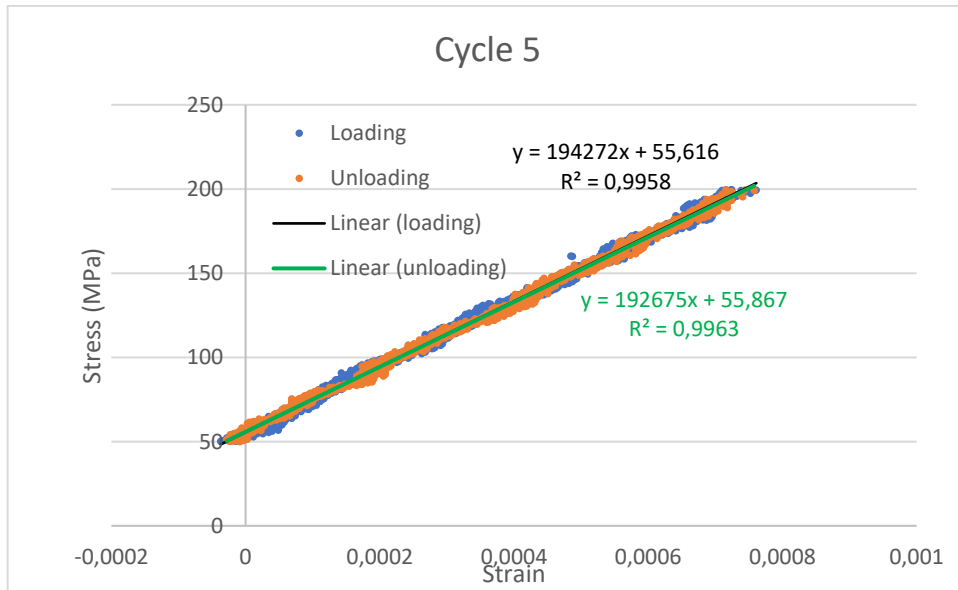


Figure 106: Cycle 5 for specimen B at 200 °C (extensometer Epsilon Model 3549)

The slopes for the specimen B at 200 °C using the ceramic extensometer are listed in the table 28:

E[MPa]	
Loading	Unloading
191662,7	192015,5
194347,6	194605,5
197141,5	199441,2
194798,3	192274
194271,6	192674,7
Average	194323 MPa
Std dev	2444 MPa

Table 28: Slopes for the specimen B at 200 °C (extensometer Epsilon Model 3549)

All the slopes are used for the calculation of the average Young's modulus; it is 194,3 GPa with a standard deviation of 2,44 GPa.

Stress-strain curves for specimen B at 400 °C with extensometer Epsilon model 3549:

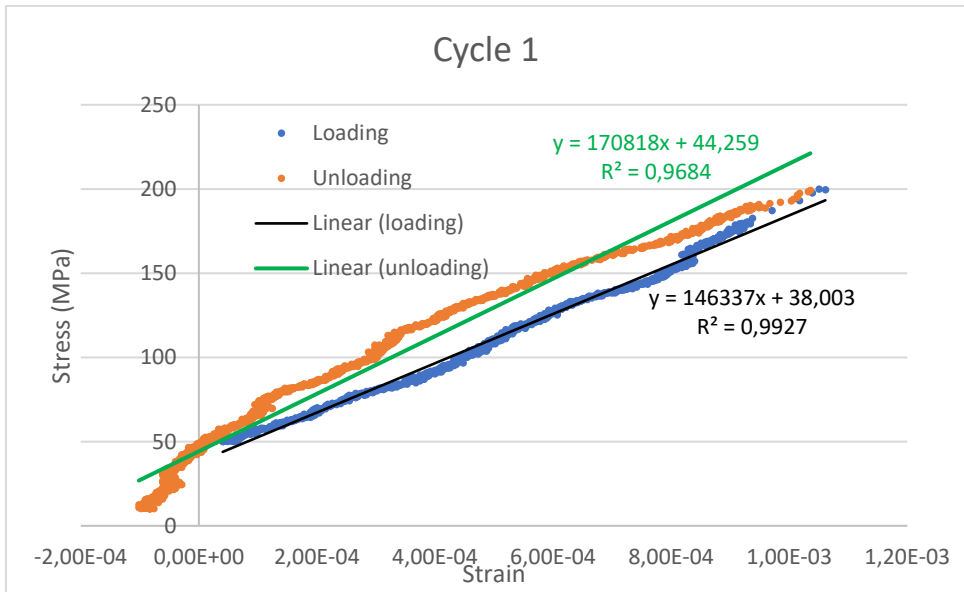


Figure 107: Cycle 1 for specimen B at 400 °C (extensometer Epsilon Model 3549)

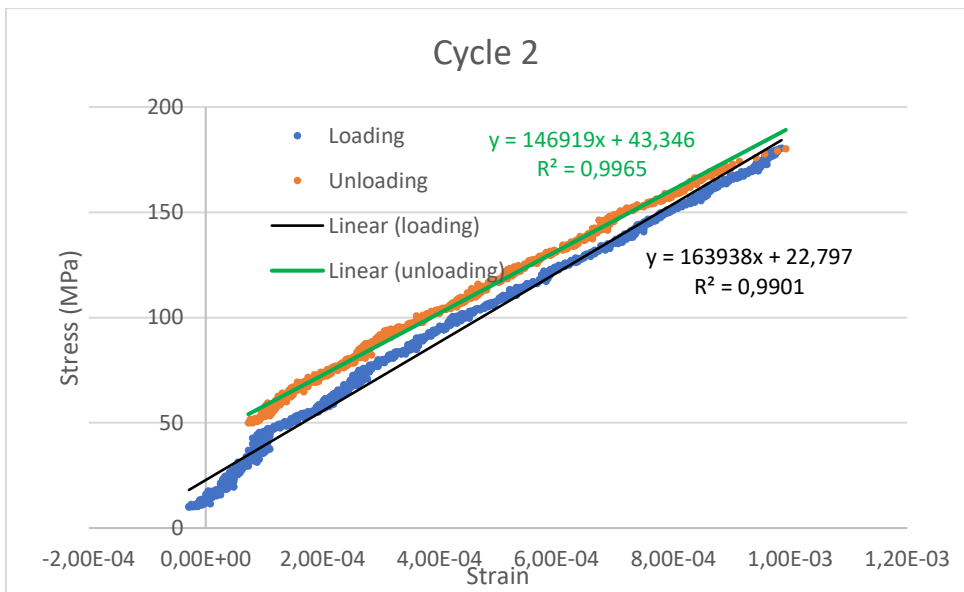


Figure 108: Cycle 2 for specimen B at 400 °C (extensometer Epsilon Model 3549)

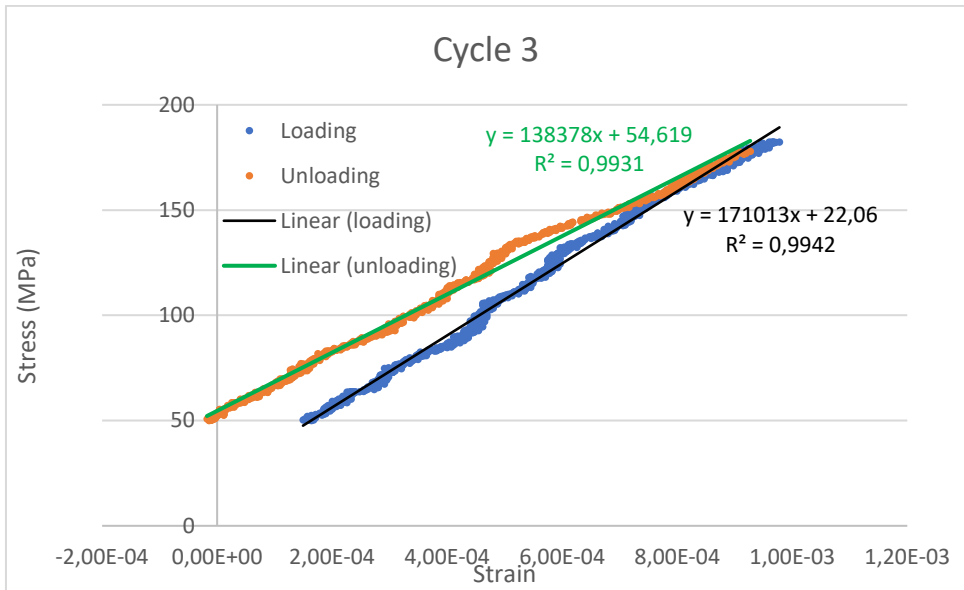


Figure 109: Cycle 3 for specimen B at 400 °C (extensometer Epsilon Model 3549)

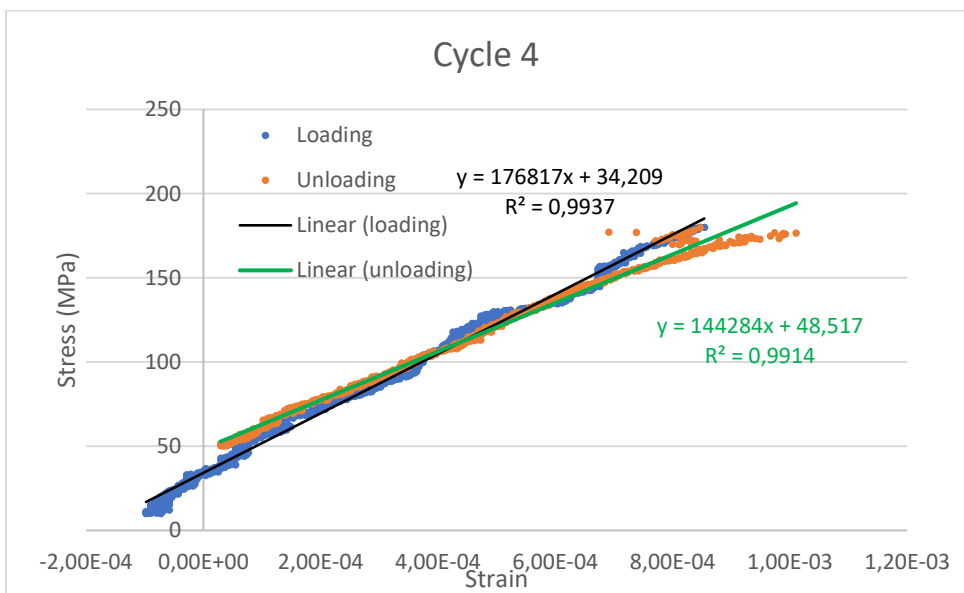


Figure 110: Cycle 4 for specimen B at 400 °C (extensometer Epsilon Model 3549)

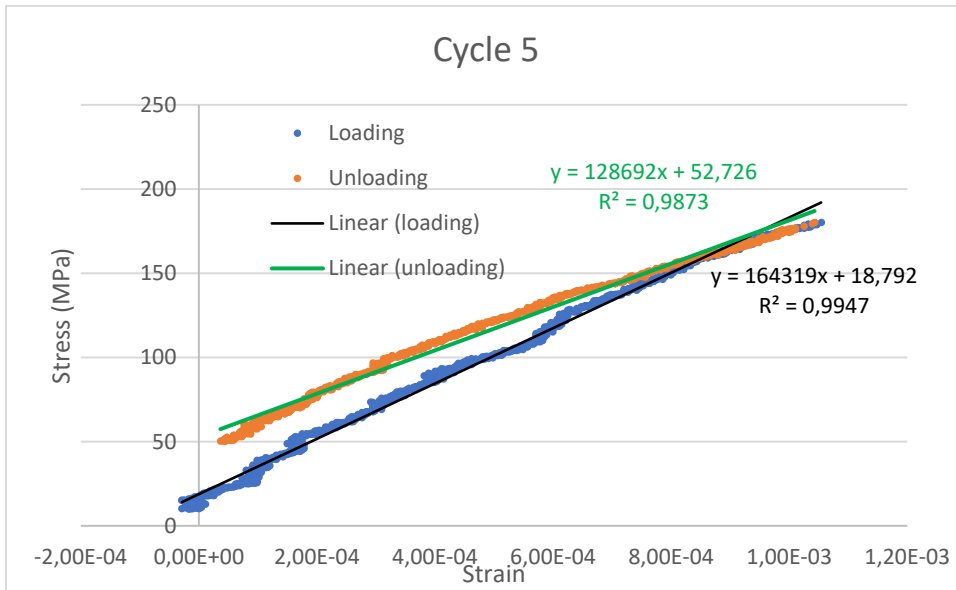


Figure 111: Cycle 5 for specimen B at 400 °C (extensometer Epsilon Model 3549)

The slopes for the specimen B at 400 °C using the ceramic extensometer are listed in the table 29:

	E[MPa]	
	Loading	Unloading
	146337,5	170817,51
	163937,5	146918,59
	171013	138378,5
	176817,3	144283,88
	164318,8	128691,95
Average	169381 MPa	
Std dev	5368 MPa	

Table 29: Slopes for the specimen B at 400 °C (extensometer Epsilon Model 3549)

The average Young's modulus results of 169,4 GPa with a standard deviation of 5,36 GPa.

Stress-strain curves for specimen B at 600 °C with extensometer Epsilon model 3549:

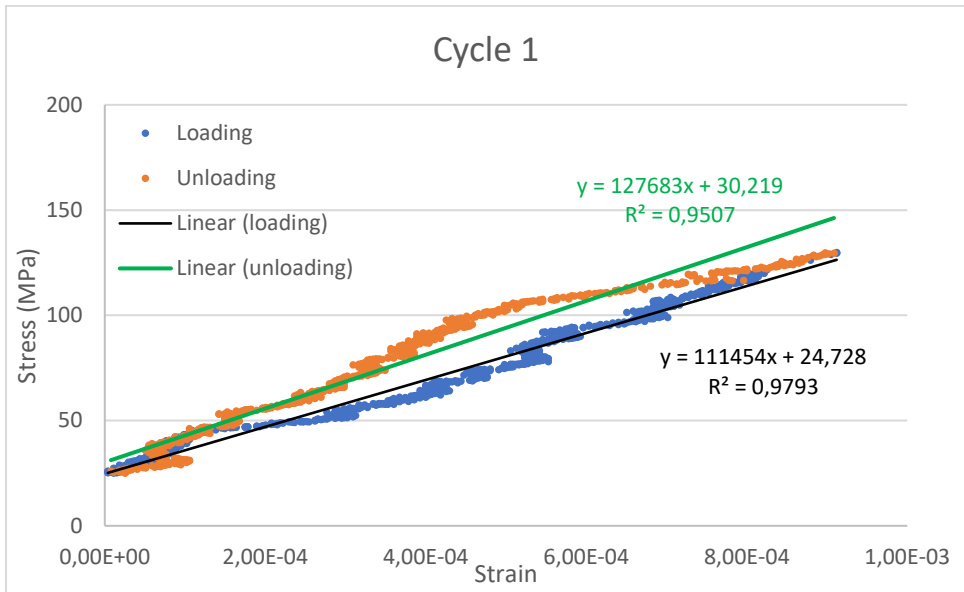


Figure 112: Cycle 1 for specimen B at 600 °C (extensometer Epsilon Model 3549)

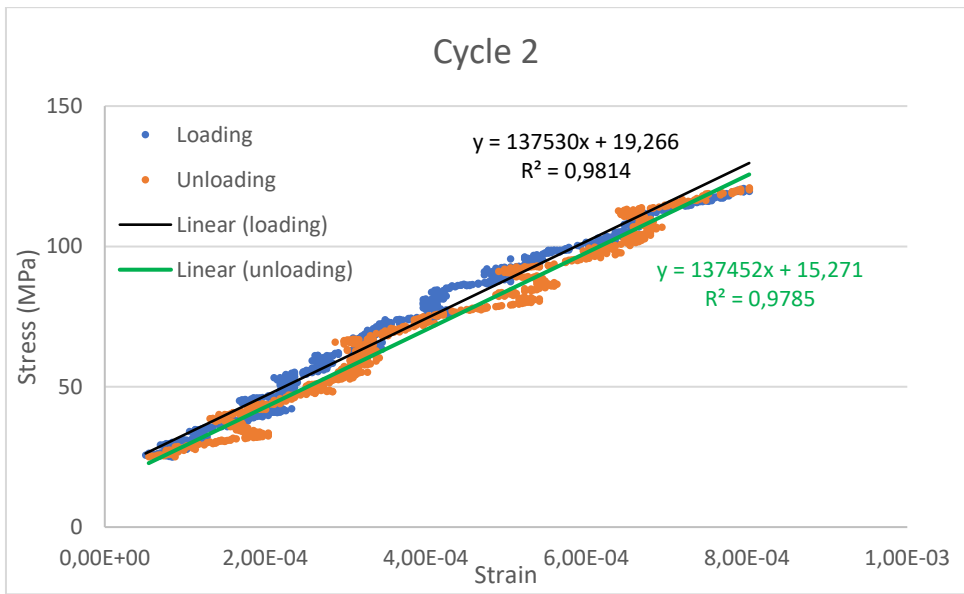
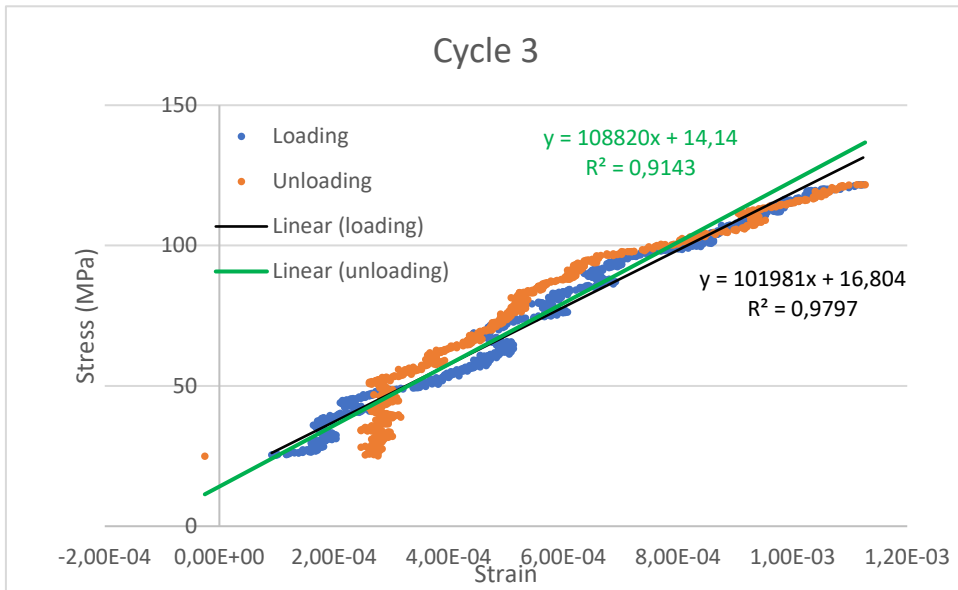


Figure 113: Cycle 2 for specimen B at 600 °C (extensometer Epsilon Model 3549)



Figur3 114: Cycle 3 for specimen B at 600 °C (extensometer Epsilon Model 3549)

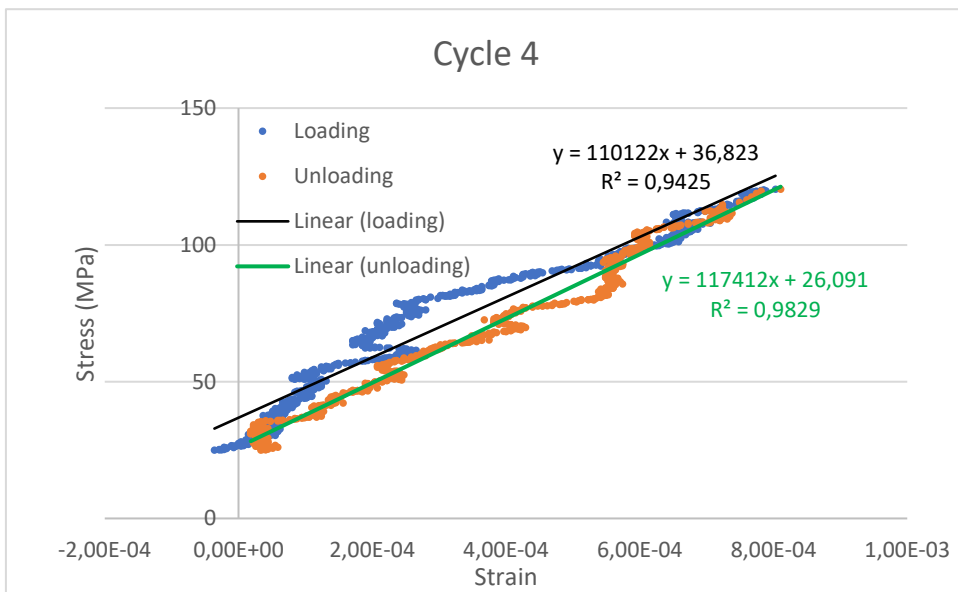


Figure 115: Cycle 4 for specimen B at 600 °C (extensometer Epsilon Model 3549)

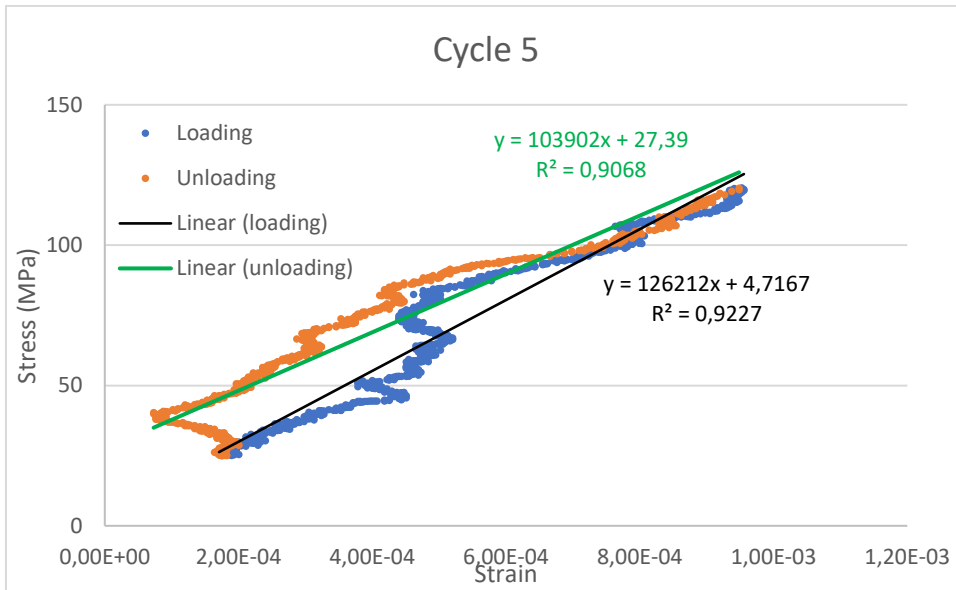


Figure 116: Cycle 5 for specimen B at 600 °C (extensometer Epsilon Model 3549)

The slopes for the specimen B at 600 °C using the ceramic extensometer are listed in the table 30:

		E [MPa]	
		Growth	Decline
		111454,2	127683,09
		137530,2	137451,98
		101980,6	108820,12
		110121,6	117412,04
		126212,4	103901,91
Average		137491 MPa	
Std dev		55 MPa	

Table 30: Slopes for the specimen B at 600 °C (extensometer Epsilon Model 3549)

The average Young's modulus is 137,5 GPa and the standard deviation is 0,055 GPa.

In the table 31, the result obtained using extensometer MTS is highlighted in yellow while the results from the ceramic extensometer are in grey.

T [°C]	E stat [GPa]	Std. Dev. [GPa]	E stat [GPa]	Std. Dev. [GPa]
RT	218,4	3,27	217,6	5,27
200	194,3	2,44	194,3	2,44
400	169,4	5,37	169,4	20,01
600	137,5	0,055	137,5	0,055

Table 31: Static Young's modulus for steel 2

The trendline which describes the behavior of Young's modulus of the steel 2 as a function of the temperature is $E = -0,0000352T^2 - 0,1161618T + 220,2522841$ and it is shown in the figure 117.

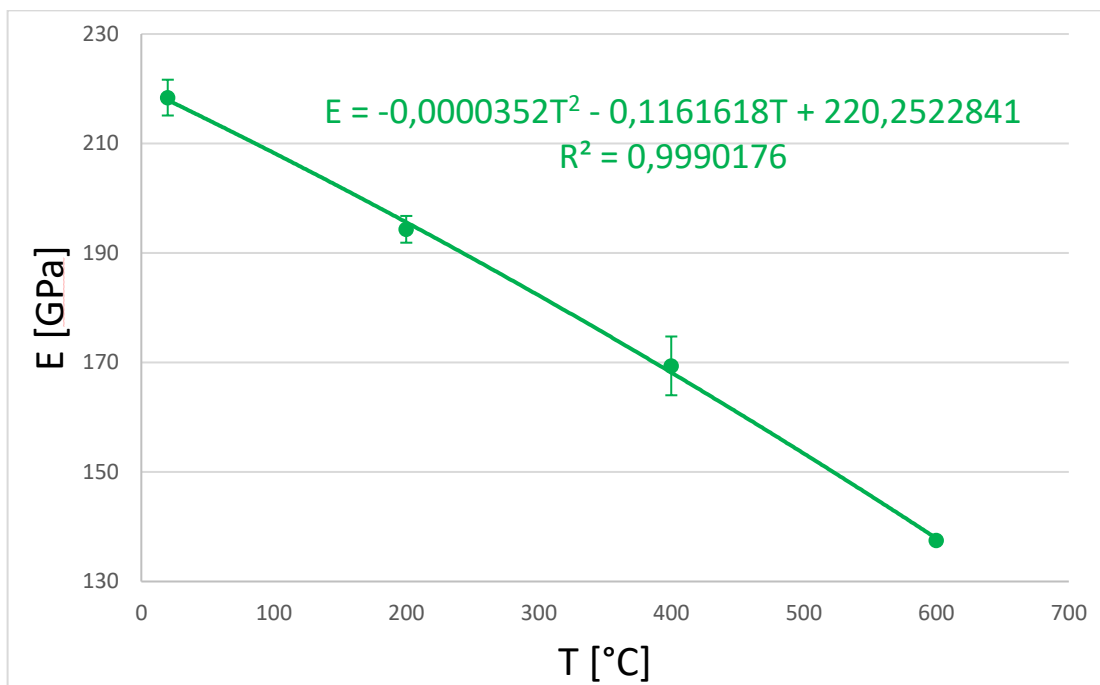


Figure 117: Trendline of static Young's modulus using extensometer MTS at room temperature and ceramic extensometer at high temperatures (steel 2).

3.3 Results of the static Young's modulus for steel 3

Stress-strain curves for specimen C at room temperature with extensometer MTS 634.12:

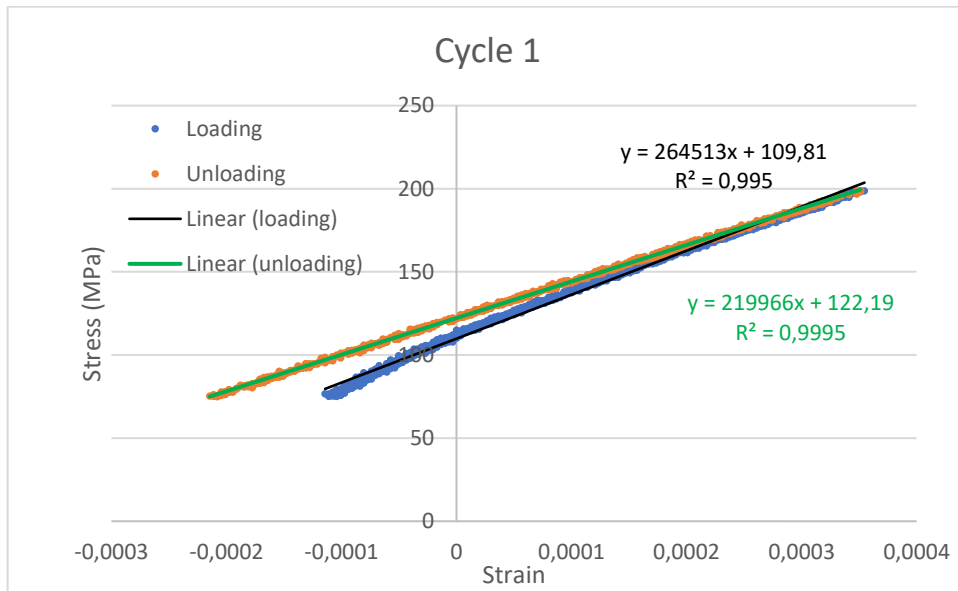


Figure 118: Cycle 1 for specimen C at room temperature (extensometer MTS)

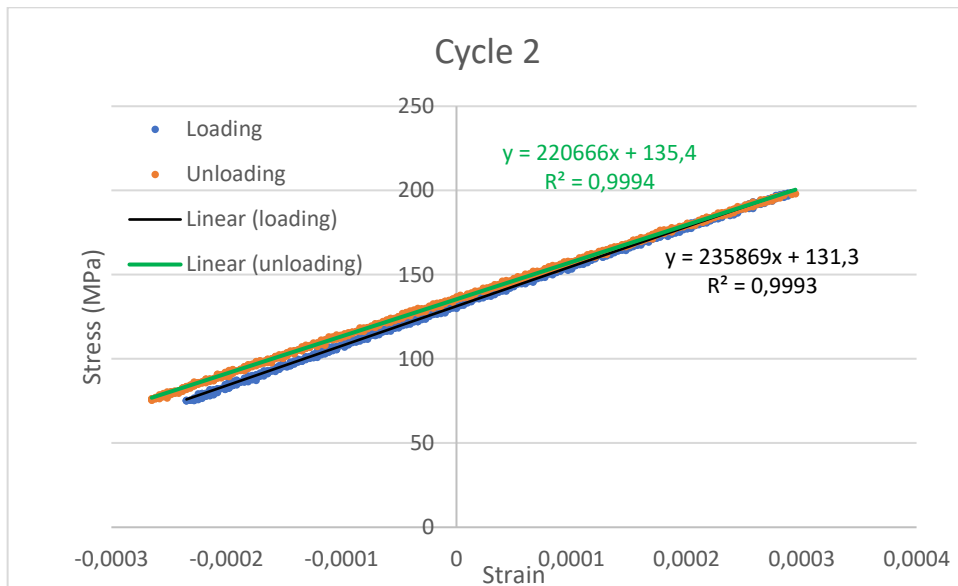


Figure 119: Cycle 2 for specimen C at room temperature (extensometer MTS)

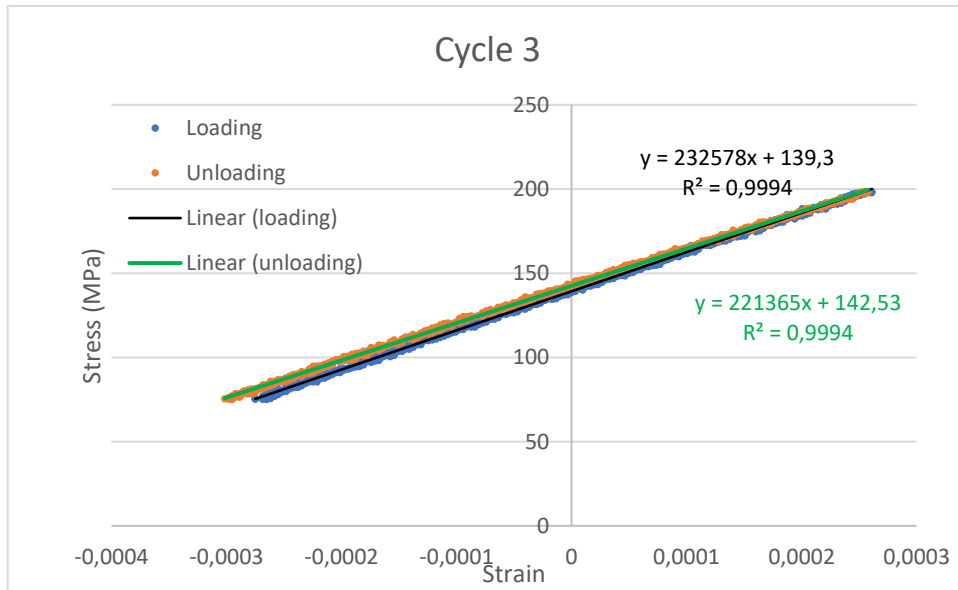


Figure 120: Cycle 3 for specimen C at room temperature (extensometer MTS)

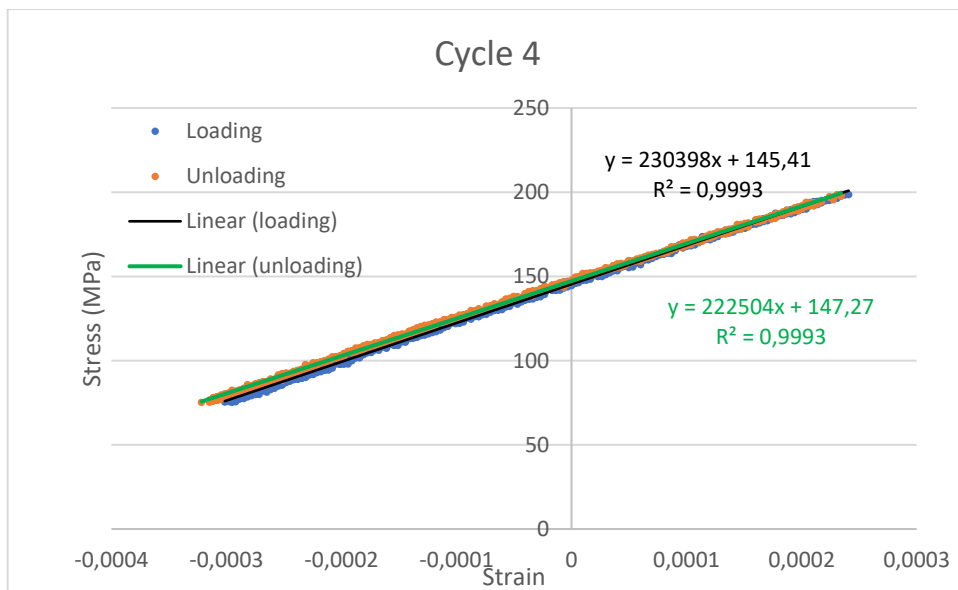


Figure 121: Cycle 4 for specimen C at room temperature (extensometer MTS)

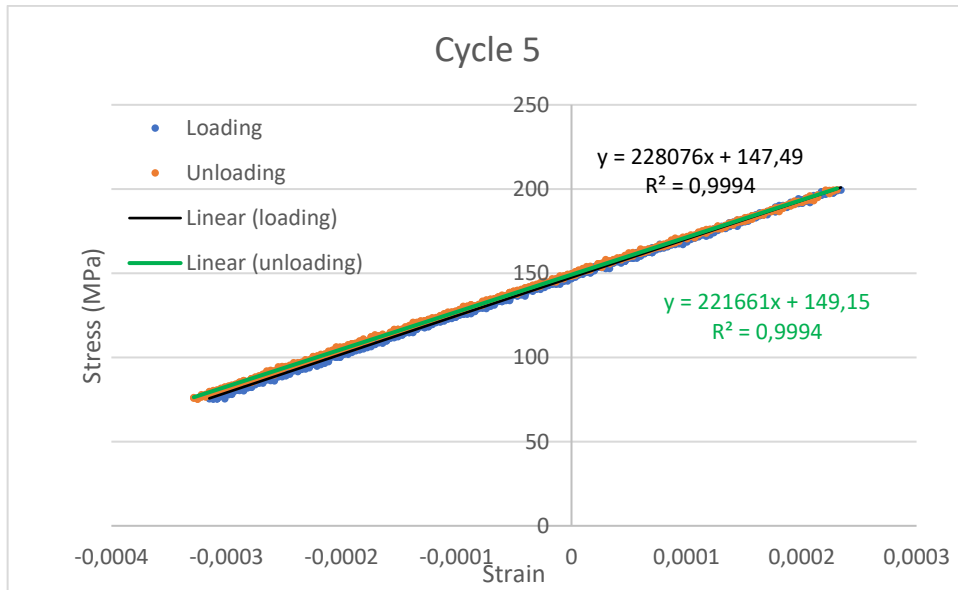


Figure 122: Cycle 5 for specimen C at room temperature (extensometer MTS)

The slopes for the specimen C at room temperature are listed in the table 32:

E [MPa]	
Loading	Unloading
264512,7	219965,9
235868,8	220666,3
232577,5	221365,4
230398,3	222504
228076,3	221661
Average	225898 MPa
Std.dev.	5933 MPa

Table 32: Slopes for the specimen C at room temperature (extensometer MTS)

The average Young's modulus which results of 225,9 GPa with a standard deviation of 5,93 GPa.

Stress-strain curves for specimen C at room temperature with extensometer Epsilon Model 3549 (ceramic extensometer):

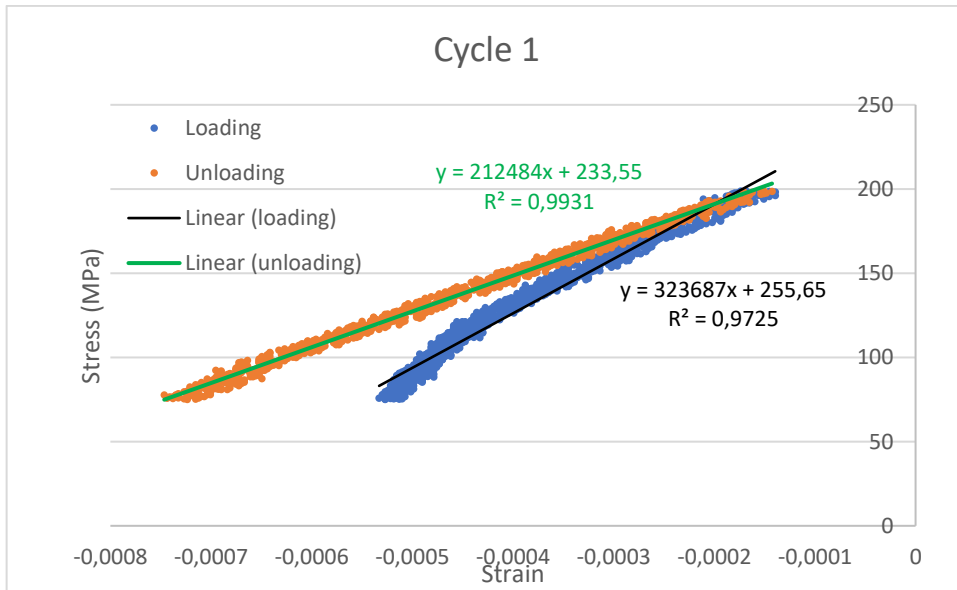


Figure 123: Cycle 1 for specimen C at room temperature (extensometer Epsilon Model 3549)

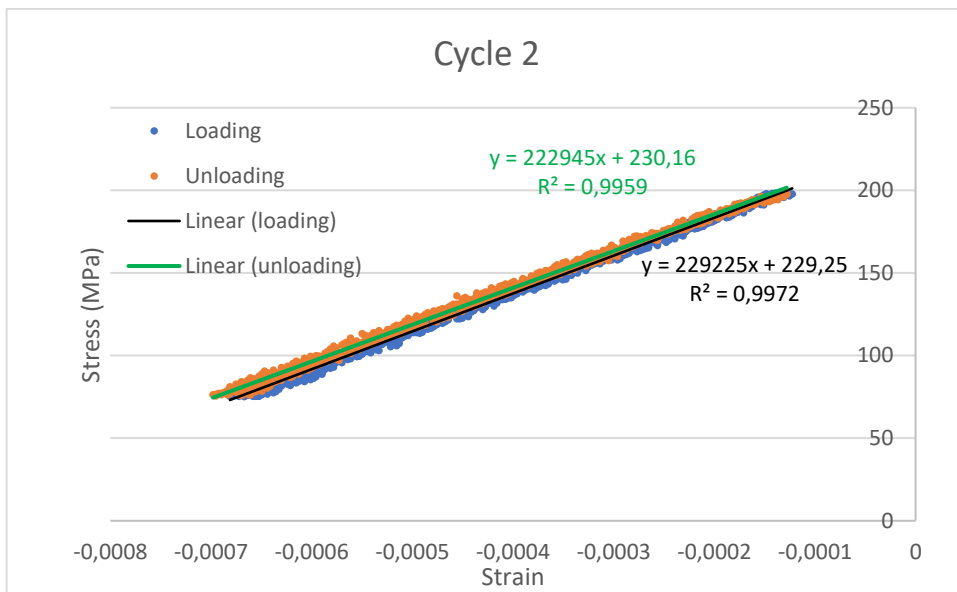


Figure 124: Cycle 2 for specimen C at room temperature (extensometer Epsilon Model 3549)

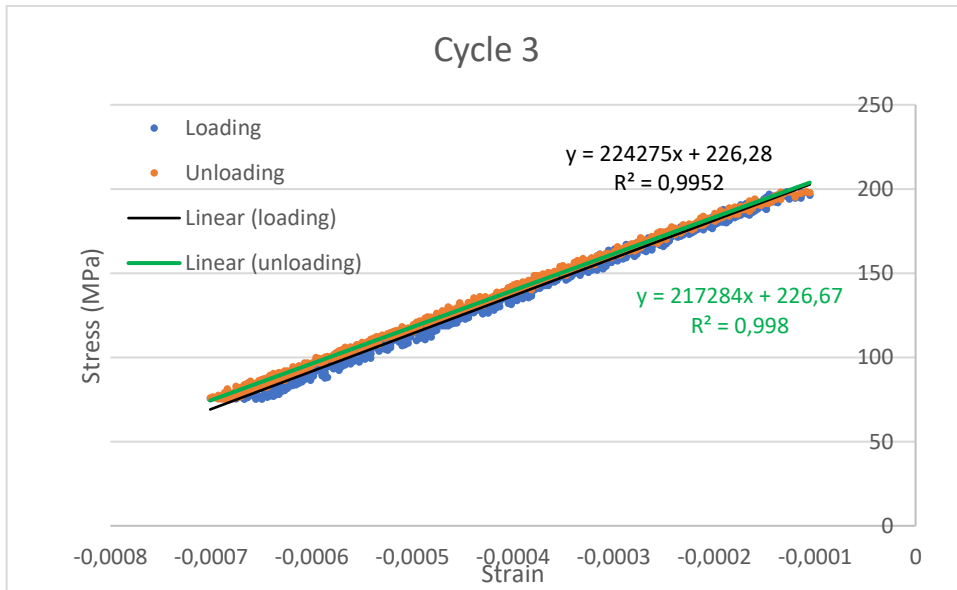


Figure 125: Cycle 3 for specimen C at room temperature (extensometer Epsilon Model 3549)

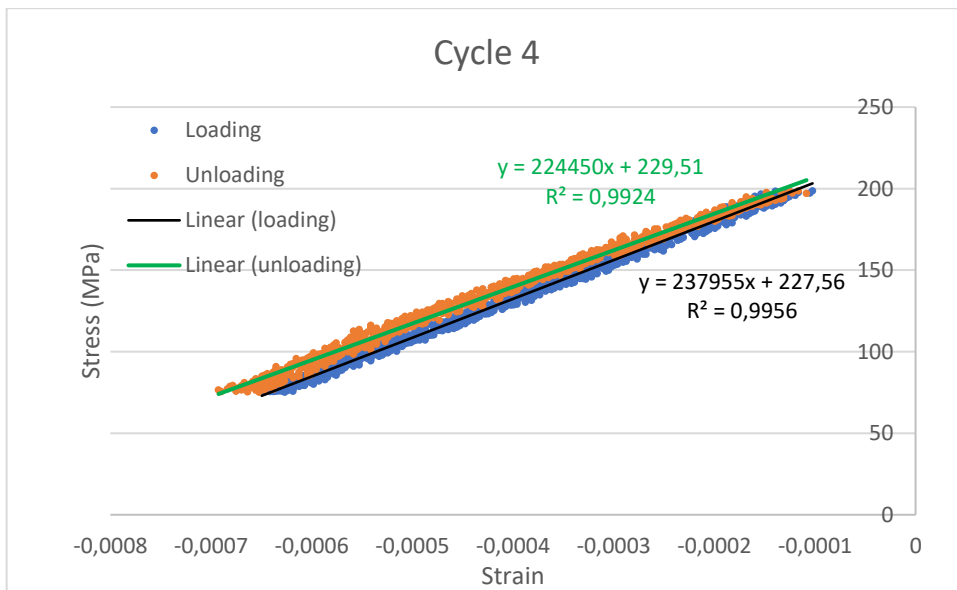


Figure 126: Cycle 4 for specimen C at room temperature (extensometer Epsilon Model 3549)

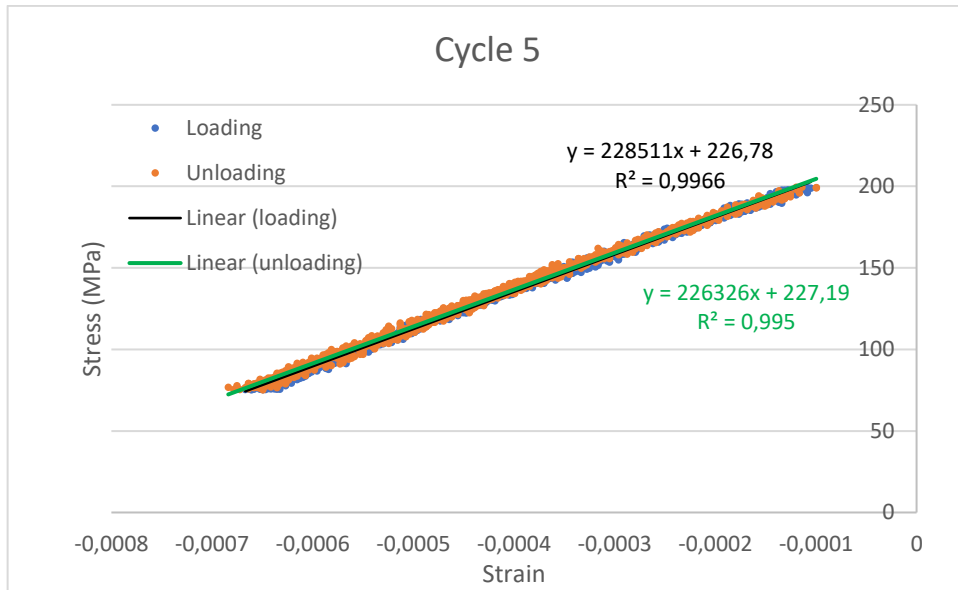


Figure 127: Cycle 5 for specimen C at room temperature (extensometer Epsilon Model 3549)

The slopes for the specimen C at room temperature using the ceramic extensometer are listed in the table 33:

E [MPa]	
Loading	Unloading
323687,1	212483,9
229225,5	222944,6
224275,5	217284,2
237955,1	224449,9
228511,5	226326,2
Average	224828 MPa
Std.dev.	7252 MPa

Table 33: Slopes for the specimen C at room temperature (extensometer Epsilon Model 3549)

The average Young's modulus is 224,8 GPa with a standard deviation of 7,25 GPa.

Stress-strain curves for specimen C at 200 °C with extensometer Epsilon model 3549:

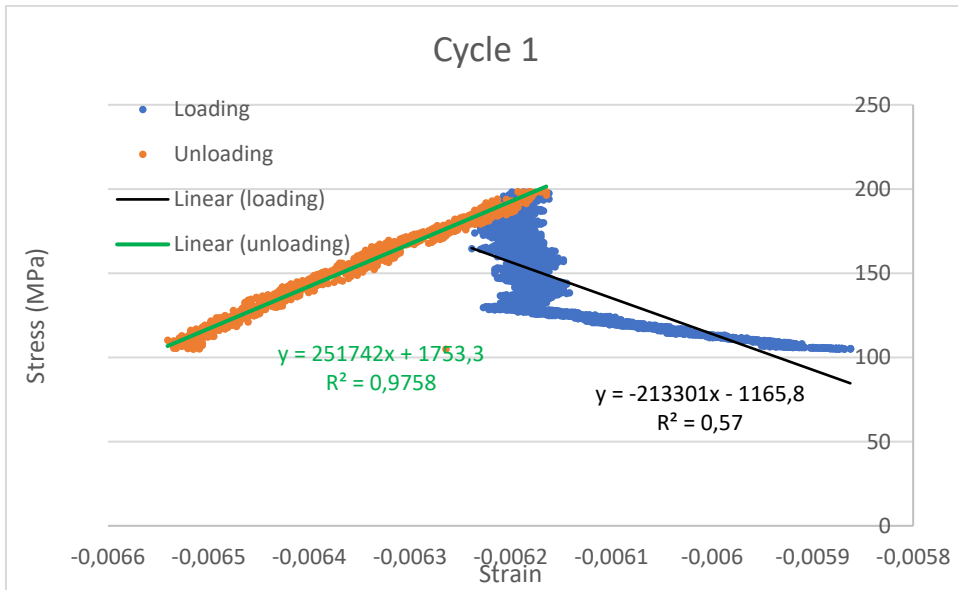


Figure 128: Cycle 1 for specimen C at 200 °C (extensometer Epsilon Model 3549)

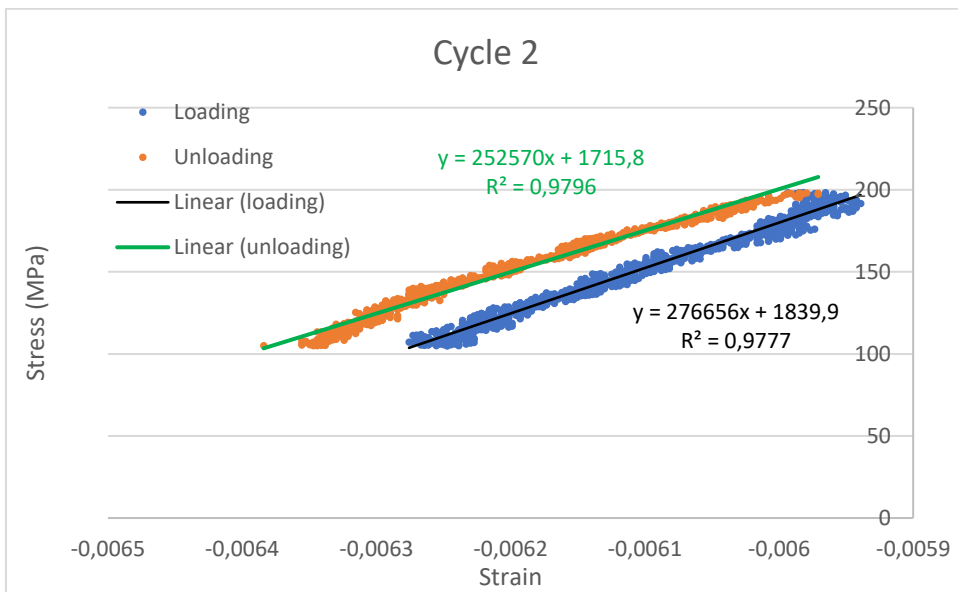


Figure 129: Cycle 2 for specimen C at 200 °C (extensometer Epsilon Model 3549)

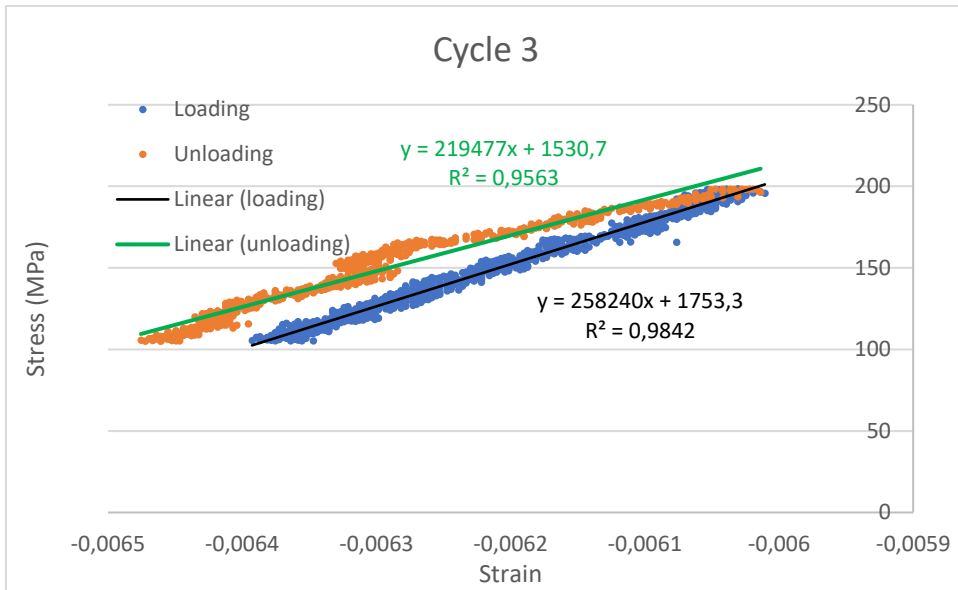


Figure 130: Cycle 3 for specimen C at 200 °C (extensometer Epsilon Model 3549)

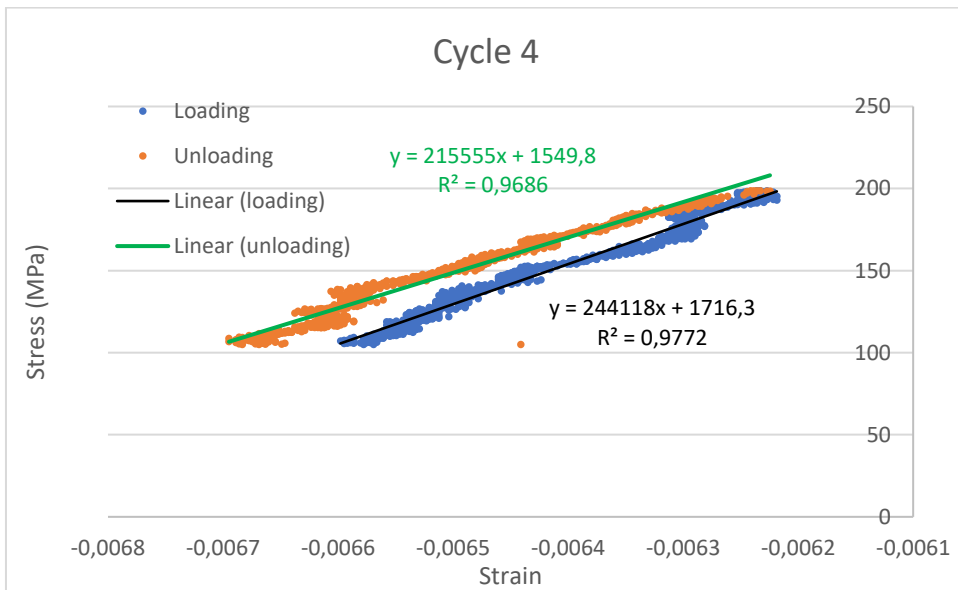


Figure 131: Cycle 4 for specimen C at 200 °C (extensometer Epsilon Model 3549)

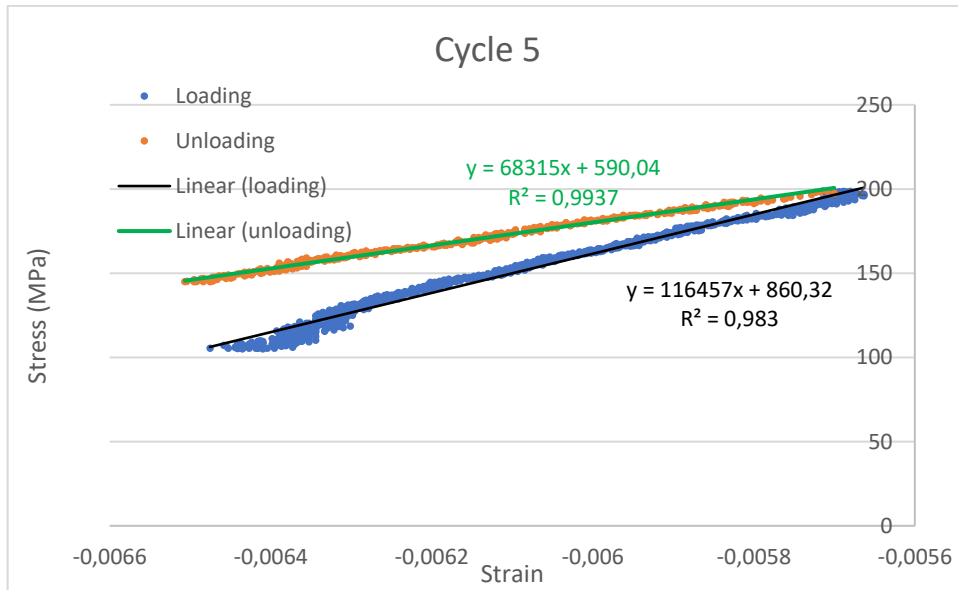


Figure 132: Cycle 5 for specimen C at 200 °C (extensometer Epsilon Model 3549)

The slopes for the specimen C at 200 °C using the ceramic extensometer are listed in the table 34:

E[MPa]	
Loading	Unloading
-213301	251741,8
276656,1	252570
258239,7	219477
244117,5	215555,3
116456,7	68314,65
Average	217516 MPa
Std dev	2773 MPa

Table 34: Slopes for the specimen C at 200 °C (extensometer Epsilon Model 3549)

The average Young's modulus is 217,5 GPa with a standard deviation of 2,77 GPa.

Stress-strain curves for specimen C at 400 °C with extensometer Epsilon model 3549:

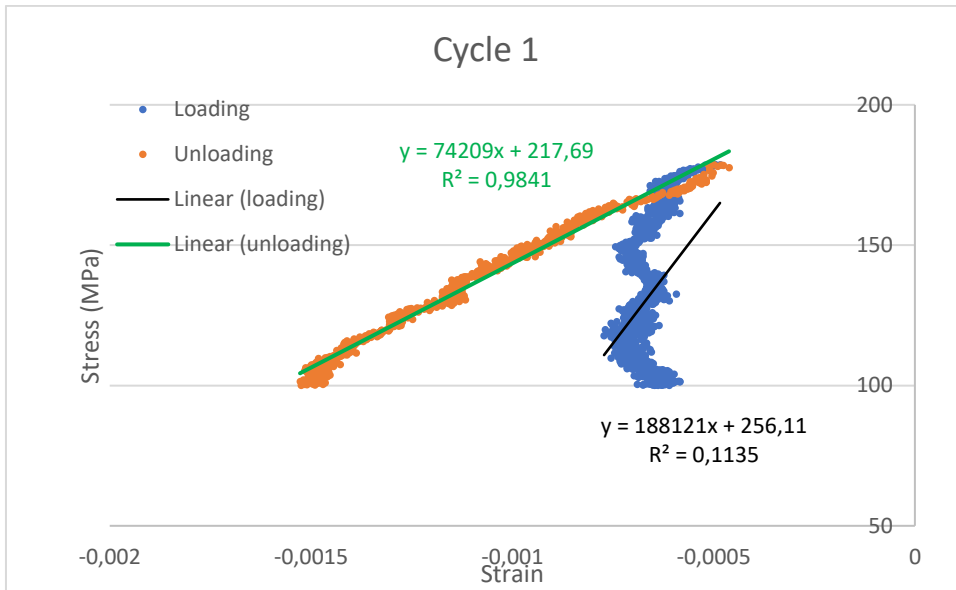


Figure 133: Cycle 1 for specimen C at 400 °C (extensometer Epsilon Model 3549)

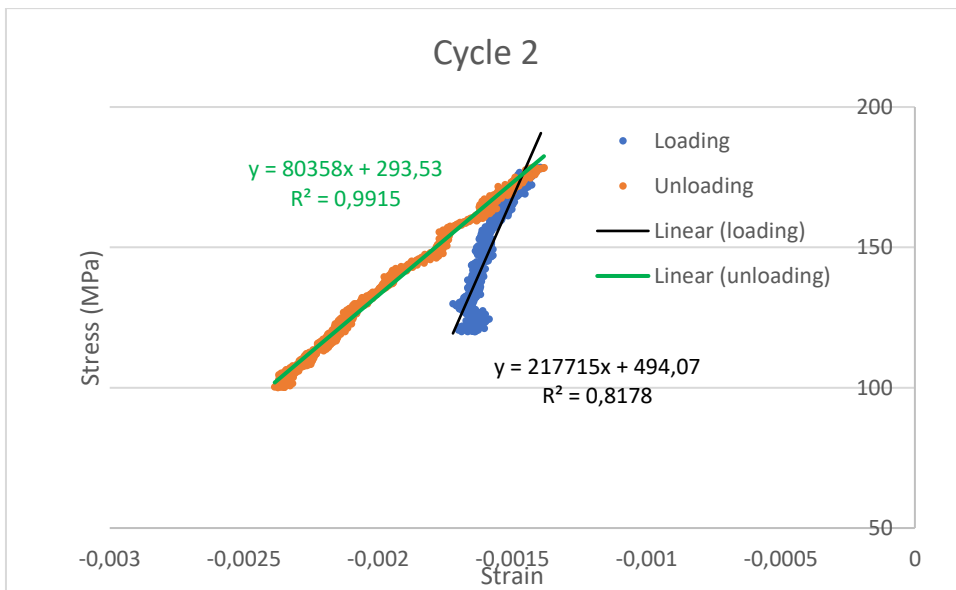


Figure 134: Cycle 2 for specimen C at 400 °C (extensometer Epsilon Model 3549)

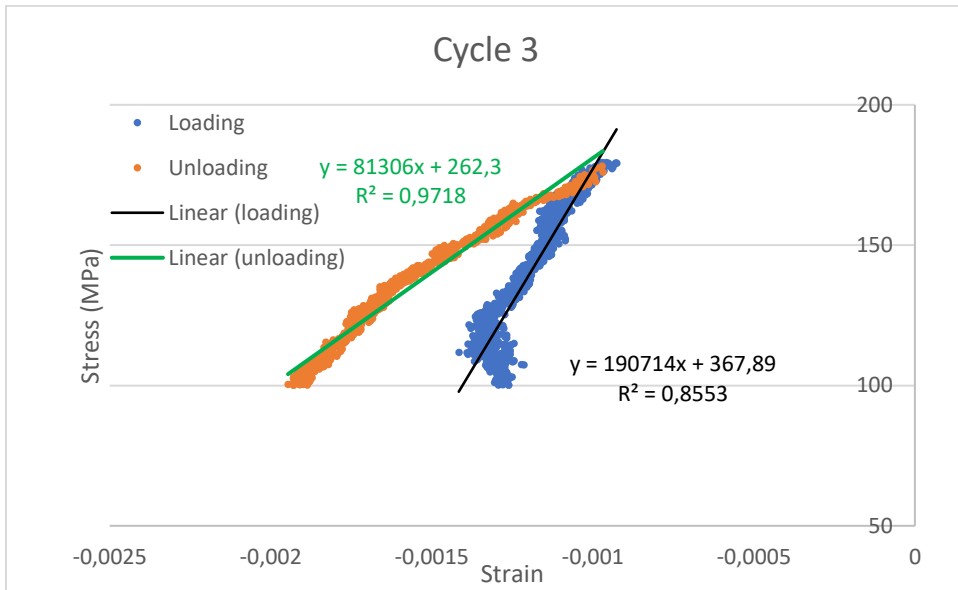


Figure 135: Cycle 3 for specimen C at 400 °C (extensometer Epsilon Model 3549)

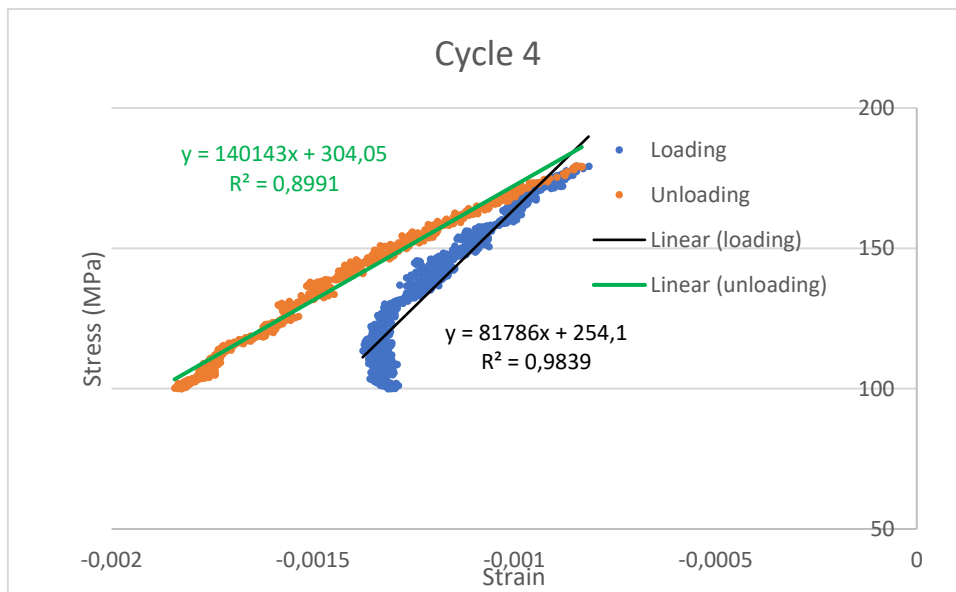


Figure 136: Cycle 4 for specimen C at 400 °C (extensometer Epsilon Model 3549)

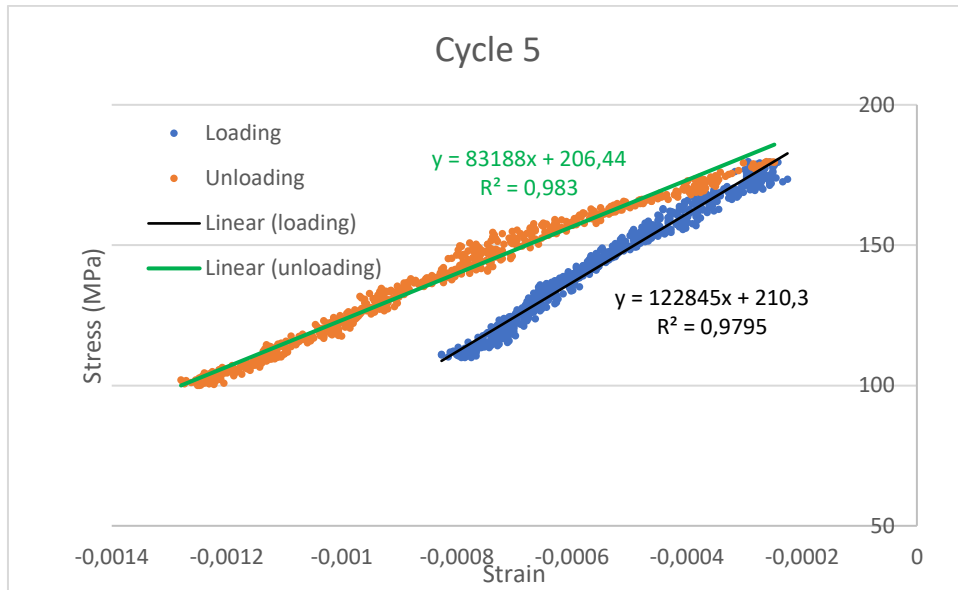


Figure 137: Cycle 5 for specimen C at 400 °C (extensometer Epsilon Model 3549)

The slopes for the specimen C at 400 °C using the ceramic extensometer are listed in the table 35:

E[MPa]	
Loading	Unloading
188121,5	74208,74
217715,1	80358,37
190713,7	81306,15
140142,5	81785,97
122845,3	83187,76
Average	184173 MPa
Std dev	32259 MPa

Table 35: Slopes for the specimen C at 400 °C (extensometer Epsilon Model 3549)

The average Young's modulus results of 184,2 GPa with a standard deviation of 32,26 GPa.

Stress-strain curves for specimen B at 600 °C with extensometer Epsilon model 3549:

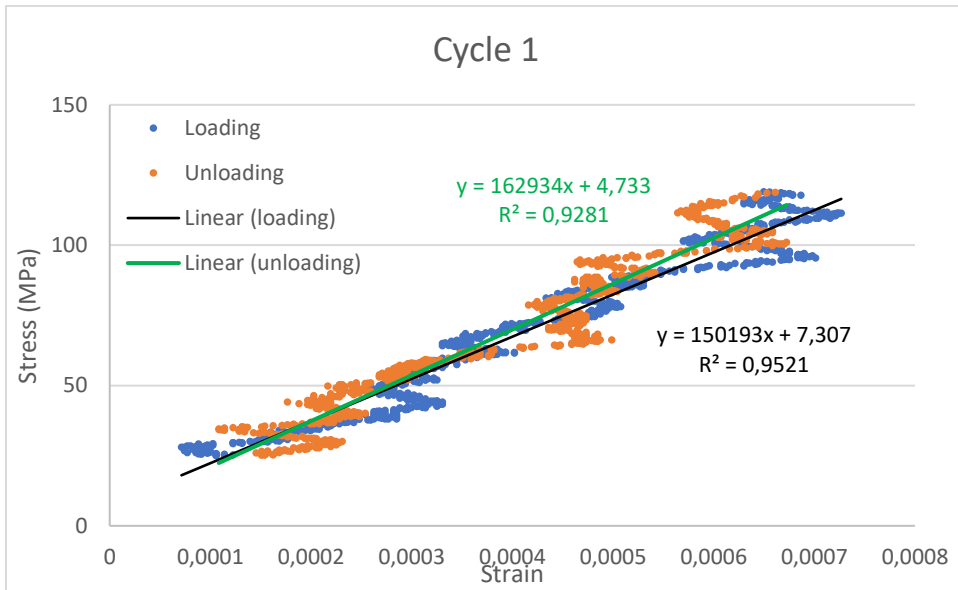


Figure 138: Cycle 1 for specimen C at 600 °C (extensometer Epsilon Model 3549)

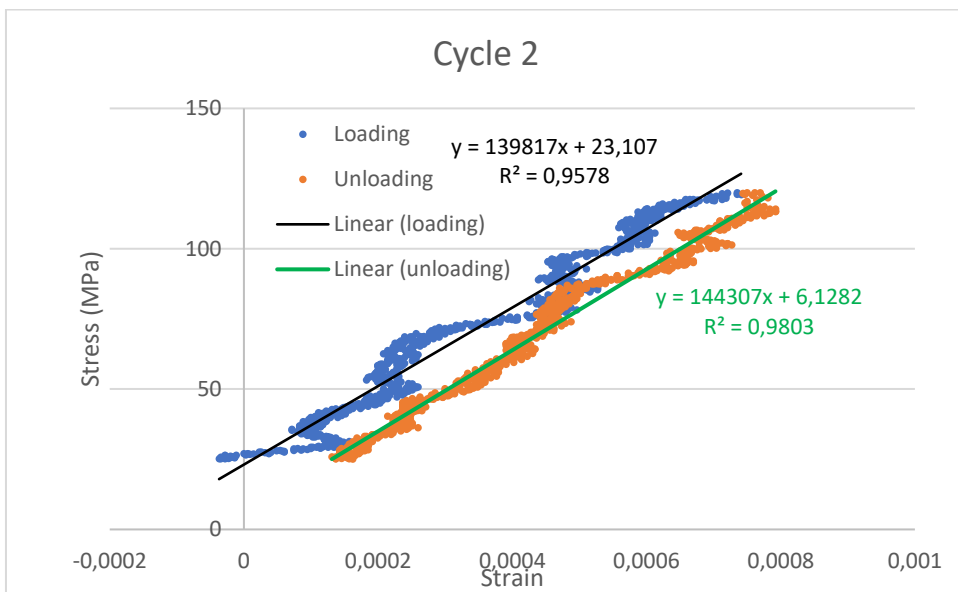


Figure 139: Cycle 2 for specimen C at 600 °C (extensometer Epsilon Model 3549)

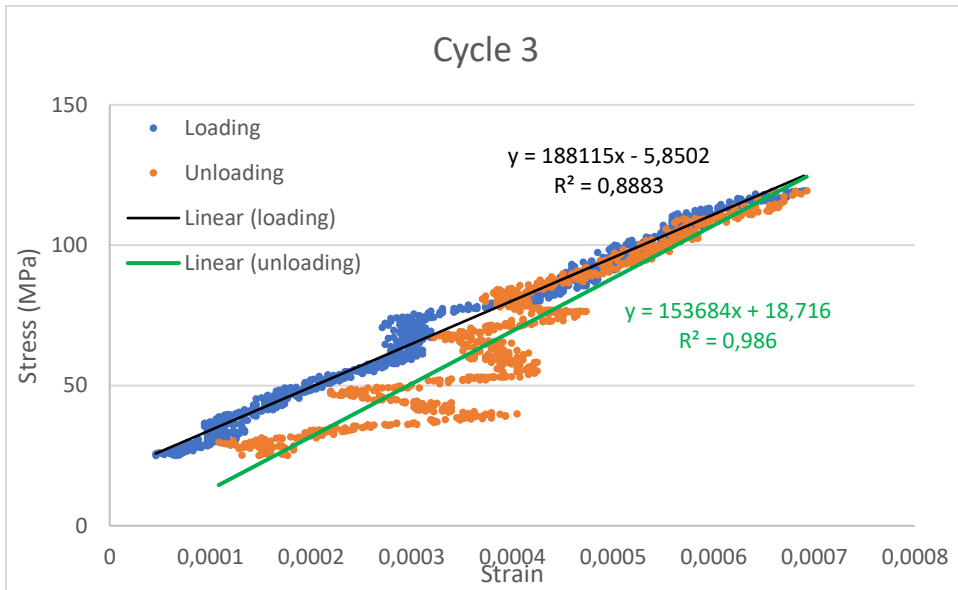


Figure 140: Cycle 3 for specimen C at 600 °C (extensometer Epsilon Model 3549)

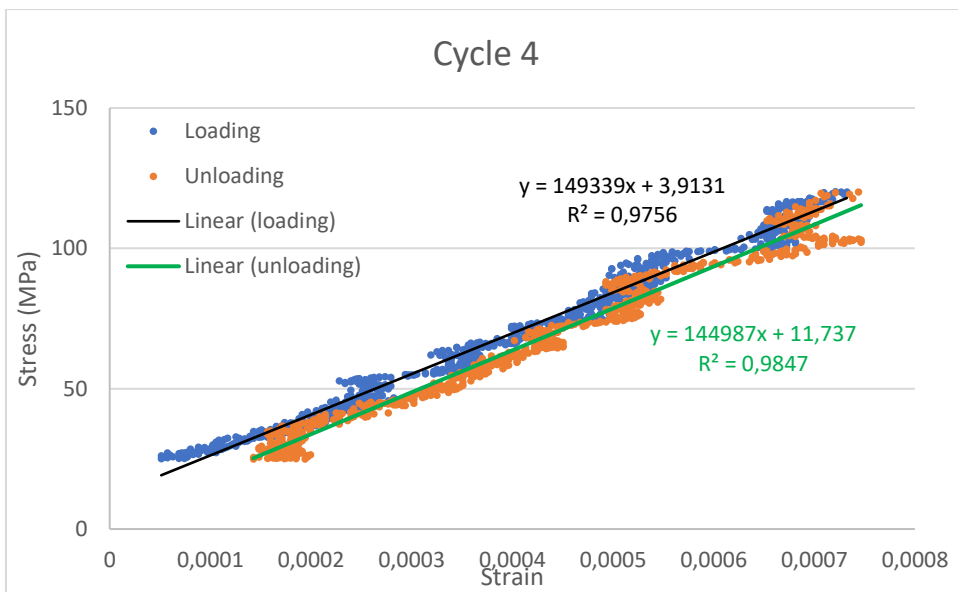


Figure 141: Cycle 4 for specimen C at 600 °C (extensometer Epsilon Model 3549)

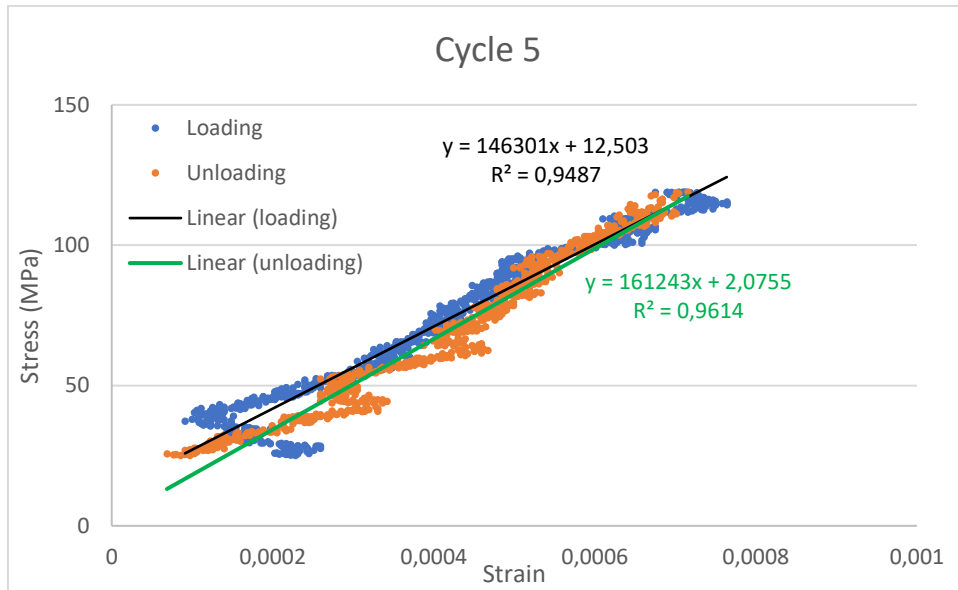


Figure 142: Cycle 5 for specimen C at 600 °C (extensometer Epsilon Model 3549)

The slopes for the specimen C at 600 °C using the ceramic extensometer are listed in the table 36:

		E [MPa]	
		Growth	Decline
		111454,2	127683,09
		137530,2	137451,98
		101980,6	108820,12
		110121,6	117412,04
		126212,4	103901,91
Average		154092 MPa	
Std dev		14015 MPa	

Table 36: Slopes for the specimen C at 600 °C (extensometer Epsilon Model 3549)

The average Young's modulus is 154,1 GPa and the standard deviation is 14,01 GPa.

In the table 37, the result obtained using extensometer MTS is highlighted in yellow while the results from the ceramic extensometer are in grey.

T [°C]	E stat [GPa]	Std. Dev. [GPa]	E stat [GPa]	Std. Dev. [GPa]
RT	225,9	5,93	225,0	7,25
200	217,5	2,77	217,5	2,77
400	184,2	32,26	184,2	32,26
600	154,1	14,02	154,1	14,02

Table 37: Static Young's modulus for steel 3

The trendline which describes the behavior of Young's modulus of the steel 3 as a function of the temperature is $E = -0,0001263T^2 - 0,0503587T + 228,4692230$ and it is shown in the figure 143.

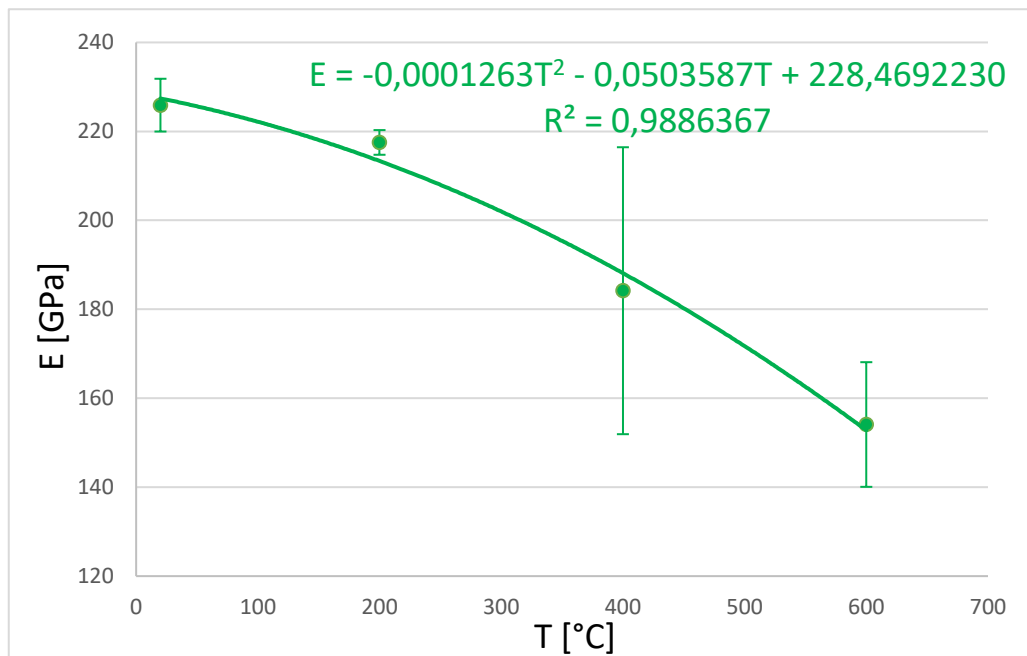


Figure 143: Trendline of static Young's modulus using extensometer MTS at room temperature and ceramic extensometer at high temperatures (steel 3).

It is important to underline that the two extensometers provide similar results for the three steels at room temperature.

3.4 Results of the dynamic Young's modulus at room temperature

In this paragraph, the dynamic Young's modulus, dynamic shear modulus and Poisson's ratio of the test specimens are shown.

- 5 measures of E , G and μ for sample D at room temperature:

M.	E [GPa]	Error E [GPa]	G [GPa]	Error G [GPa]	μ	f flexural [Hz]	f torsion [Hz]
1	213,26	1,04	80,85	0,15	0,319	37241,4	42055,7
2	213,26	1,04	80,85	0,15	0,319	37241,2	42055,6
3	213,27	1,04	80,86	0,15	0,319	37242,3	42057,3
4	213,25	1,04	80,86	0,15	0,319	37240,9	42056,7
5	213,14	1,04	80,78	0,15	0,319	37230,5	42037,5

Table 38: measures of E , G and μ of specimen D

- 5 measures of E , G and μ for sample E at room temperature:

M.	E [GPa]	Error E [GPa]	G [GPa]	Error G [GPa]	μ	f flexural [Hz]	f torsion [Hz]
1	206,41	0,53	78,91	0,11	0,308	36804,2	41677,3
2	206,86	0,53	78,91	0,11	0,311	36840,8	41677,4
3	206,86	0,53	78,92	0,11	0,311	36840,8	41680,0
4	207,54	0,53	78,93	0,11	0,315	36896,1	41681,1
5	206,86	0,53	78,92	0,11	0,311	36840,8	41680,1

Table 39: measures of E , G and μ of specimen E

- 5 measures of E , G and μ for sample F at room temperature:

M.	E [GPa]	Error E [GPa]	G [GPa]	Error G [GPa]	μ	f flexural [Hz]	f torsion [Hz]
1	212,23	1,11	80,24	0,18	0,323	37131,2	41863,1
2	212,23	1,11	80,23	0,18	0,323	37131,5	41862,3
3	212,24	1,11	80,23	0,18	0,323	37131,7	41862,7
4	212,24	1,11	80,24	0,18	0,323	37132,0	41863,1
5	212,24	1,11	80,24	0,18	0,323	37132,4	41863,5

Table 40: measures of E , G and μ of specimen F

- 5 measures of E , G and μ for sample G at room temperature:

M.	E [GPa]	Error E [GPa]	G [GPa]	Error G [GPa]	μ	f flexural [Hz]	f torsion [Hz]
1	211,77	1,53	81,78	0,22	0,295	17323,8	28249,4
2	211,79	1,53	81,80	0,22	0,295	17324,4	28251,9
3	211,82	1,53	81,81	0,22	0,295	17326,0	28254,6
4	211,81	1,53	81,83	0,22	0,294	17325,6	28257,3
5	211,81	1,53	81,81	0,22	0,295	17325,5	28252,9

Table 41: measures of E , G and μ of specimen G

- 5 measures of E , G and μ for sample H at room temperature:

M.	E [GPa]	Error E [GPa]	G [GPa]	Error G [GPa]	μ	f flexural [Hz]	f torsion [Hz]
1	206,33	2,11	79,48	0,29	0,298	17108,5	27871,2
2	206,34	2,11	79,46	0,29	0,298	17108,6	27867,7
3	206,34	2,11	79,44	0,29	0,299	17108,7	27864,6
4	206,33	2,11	79,50	0,29	0,298	17108,7	27873,7
5	206,34	2,11	79,50	0,29	0,298	17109,0	27873,5

Table 42: measures of E , G and μ of specimen H

- 5 measures of E , G and μ for sample I at room temperature:

M.	E [GPa]	Error E [GPa]	G [GPa]	Error G [GPa]	μ	f flexural [Hz]	f torsion [Hz]
1	211,96	3,12	81,79	0,42	0,296	17336,5	28228,9
2	211,96	3,12	81,80	0,42	0,296	17336,5	28230,8
3	211,96	3,12	81,80	0,42	0,296	17336,6	28230,0
4	211,97	3,12	81,82	0,42	0,295	17336,9	28234,3
5	211,97	3,12	81,79	0,42	0,296	17336,9	28228,1

Table 43: measures of E , G and μ of specimen I

- 5 measures of E , G and μ for sample J at room temperature:

M.	E [GPa]	Error E [GPa]	G [GPa]	Error G [GPa]	μ	f flexural [Hz]	f torsion [Hz]
1	207,6	9,77	79,76	1,41	0,301	7221,07	9333,68
2	207,6	9,77	79,76	1,41	0,301	7221,08	9333,72
3	207,6	9,77	79,76	1,41	0,301	7221,1	9333,74
4	207,58	9,77	79,76	1,41	0,301	7220,7	9333,74
5	207,6	9,77	79,76	1,41	0,301	7221,11	9333,77

Table 44: measures of E , G and μ of specimen J

- 5 measures of E , G and μ for sample K at room temperature:

M.	E [GPa]	Error E [GPa]	G [GPa]	Error G [GPa]	μ	f flexural [Hz]	f torsion [Hz]
1	205,89	5,07	79,15	0,79	0,301	7144,98	9234,65
2	205,89	5,07	79,15	0,79	0,301	7144,98	9234,64
3	205,89	5,07	79,15	0,79	0,301	7144,98	9234,83
4	205,89	5,07	79,15	0,79	0,301	7145	9234,71
5	205,89	5,07	79,15	0,79	0,301	7145,01	9234,72

Table 45: measures of E, G and μ of specimen K

- 5 measures of E, G and μ for sample L at room temperature:

M.	E [GPa]	Error E [GPa]	G [GPa]	Error G [GPa]	μ	f flexural [Hz]	f torsion [Hz]
1	211,79	8,37	80,96	1,21	0,308	9487,36	10873,6
2	211,79	8,37	80,96	1,21	0,308	9487,38	10873,6
3	211,8	8,37	80,96	1,21	0,308	9487,4	10873,6
4	211,79	8,37	80,96	1,21	0,308	9487,39	10873,6
5	211,8	8,37	80,96	1,21	0,308	9487,42	10873,6

Table 46: measures of E, G and μ of specimen L

In the table 47 the averages and the standard deviations of dynamic Young's modulus, dynamic shear modulus and Poisson's ratio of specimens are summarized:

Specimen	E Average [GPa]	E Std. Dev. [GPa]	G Average [GPa]	G Std Dev [GPa]	μ Average	μ Std Dev
D	213,2	0,054	80,8	0,034	0,319	0
E	206,9	0,404	78,9	0,008	0,3112	0,00249
F	212,2	0,005	80,2	0,005	0,323	0
G	211,8	0,020	81,8	0,018	0,2948	0,00045
H	206,3	0,005	79,5	0,026	0,2982	0,00045
I	212,0	0,005	81,8	0,012	0,2958	0,00045
J	207,6	0,008	79,76	0	0,301	0
K	205,9	0	79,2	0	0,301	0
L	211,8	0,005	80,96	0	0,308	0

Table 47: Average E, G and μ and standard deviations

3.5 Results of the dynamic Young's modulus at high temperatures

In this paragraph, the trends of dynamic Young's modulus as a function of the temperature obtained by impulse excitation technique are shown.

The trend of dynamic Young's modulus in a range of RT - 600°C for specimen G (steel 1) is in figure 144. (In red the trendline during the heating phase and in blue during the cooling phase).

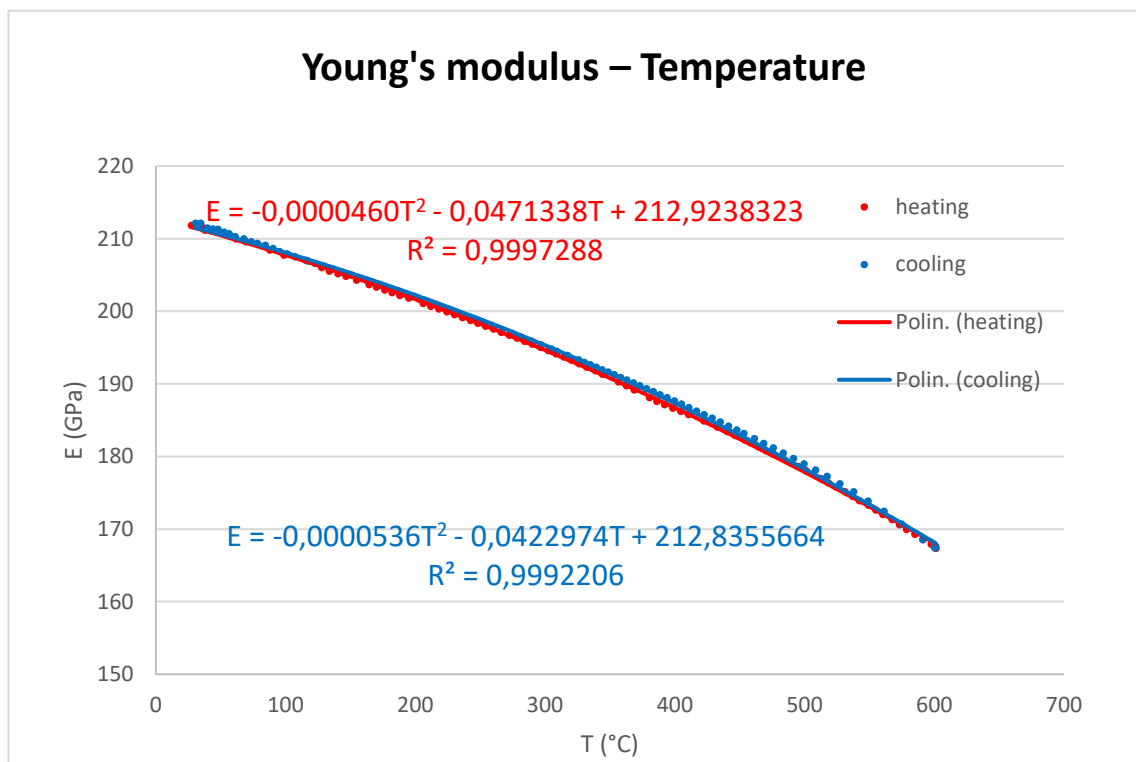


Figure 144: Young's modulus - T for sample G (RT - 600°C)

The trend of dynamic Young's modulus in a range of RT - 600°C for specimen H (steel 2) is in figure 145.

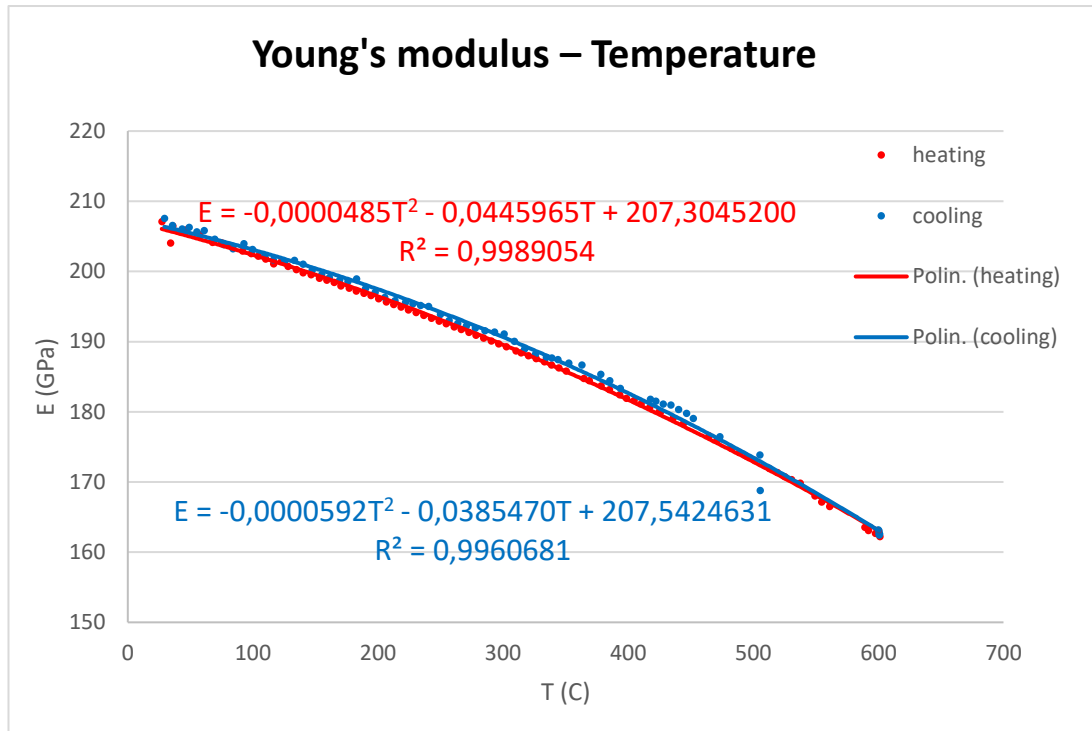


Figure 145: Young's modulus - T for sample H (RT - 600°C)

The trend of dynamic Young's modulus in a range of RT - 600°C for specimen I (steel 3) is in figure 146.

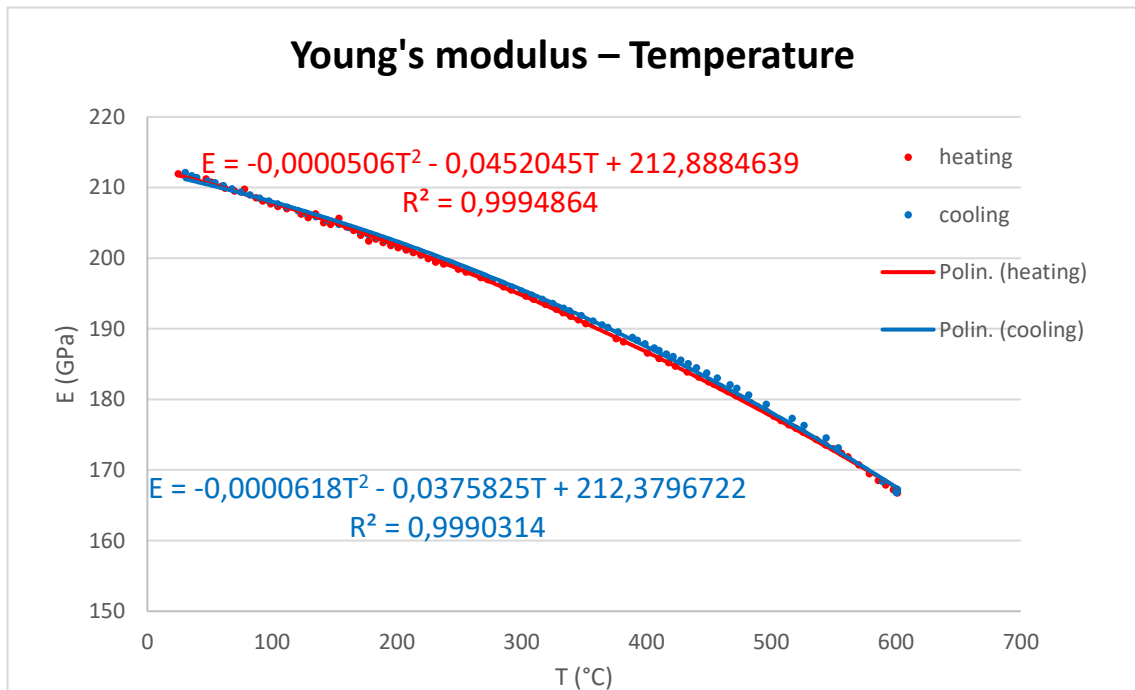


Figure 146: Young's modulus - T for sample I (RT - 600°C)

The trend of dynamic Young's modulus in a range of RT - 600°C for specimen J (steel 1) is in figure 147.

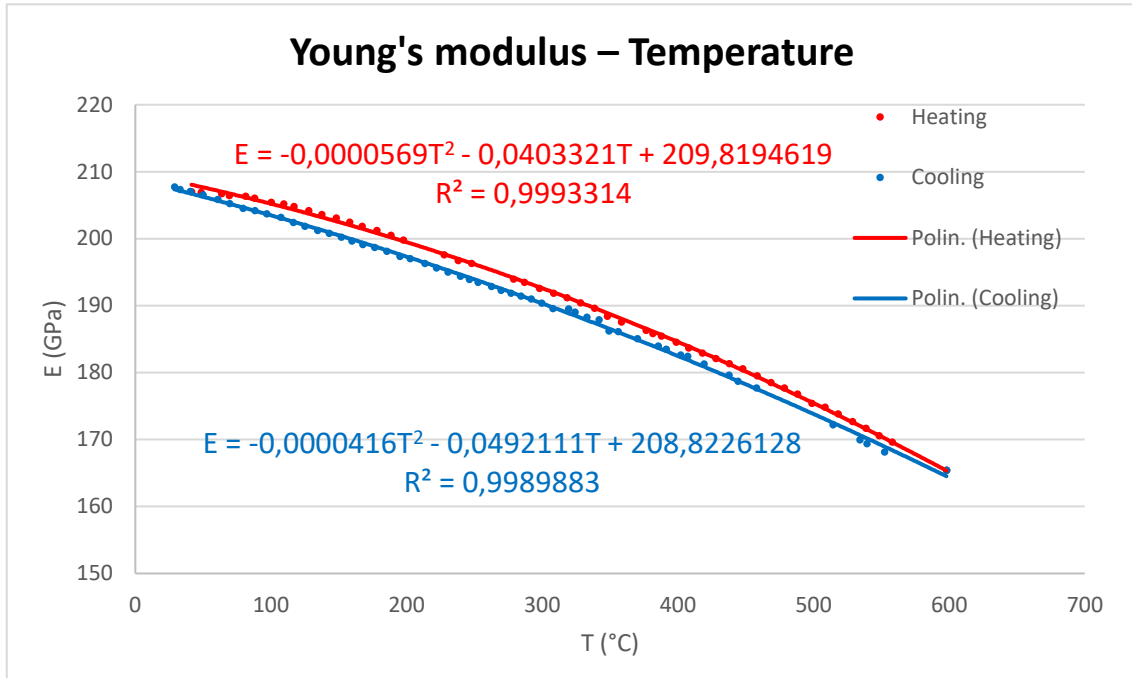


Figure 147: Young's modulus - T for sample J (RT - 600°C)

The trend of dynamic Young's modulus in a range of RT - 600°C for specimen K (steel 2) is in figure 148.

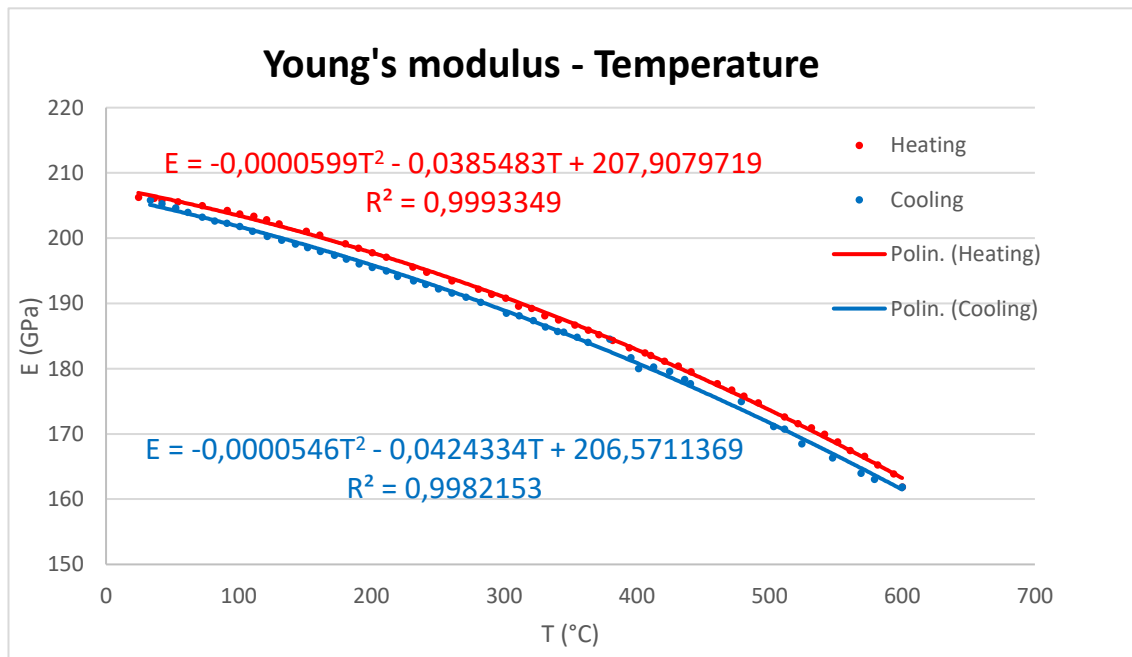


Figure 148: Young's modulus - T for sample K (RT - 600°C)

The trend of dynamic Young's modulus in a range of RT - 600°C for specimen L (steel 3) is in figure 149.

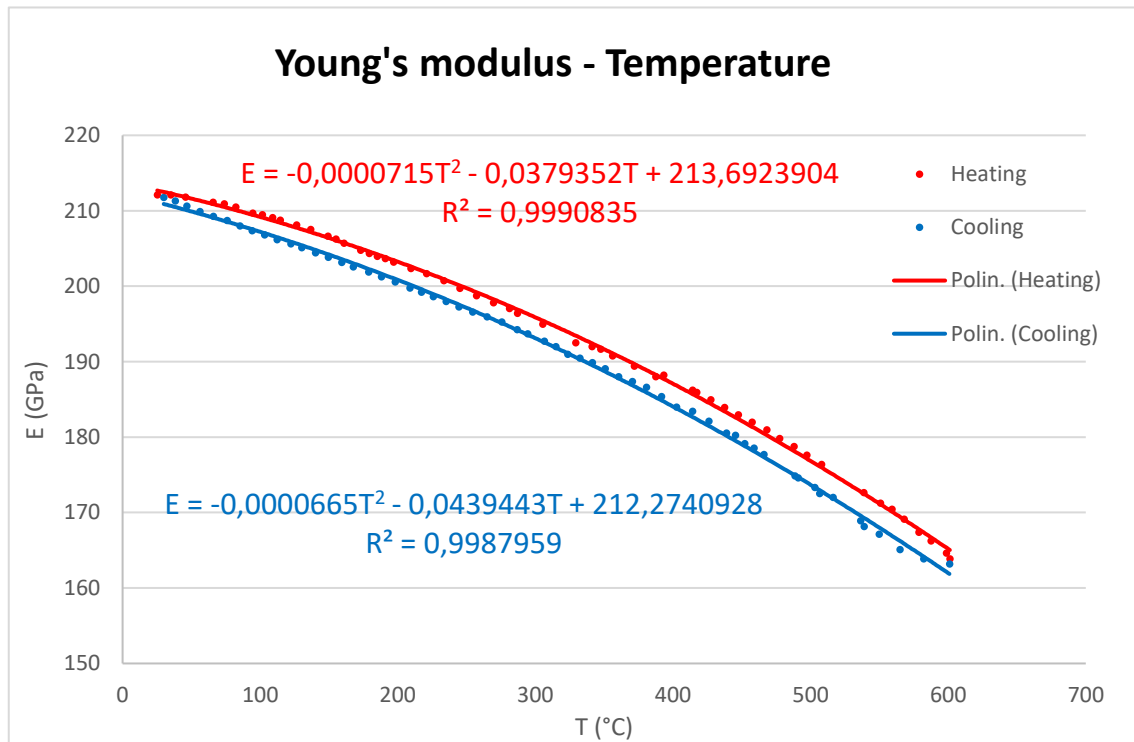


Figure 149: Young's modulus - T for sample L (RT - 600°C)

For the specimens D, E and F, the measurements of Young's modulus have not been possible because they are too small and light so the impulse moved them during the test.

The oxidation of a small surface layer does not affect Young's modulus which decreases with temperature according to the studies in literature. [21][23]

Regarding the trends of Young's modulus of the specimens J, K and L, the gap between heating and cooling phases probably derives from the different temperatures in the nucleus and on the surface.

3.6 Comparison between static and dynamic modulus and between dynamic Young's modulus of small and full size specimen

The figure 150 shows the behavior of static Young's modulus (in black), dynamic Young's modulus of small specimen (in red) and dynamic Young's modulus of full size specimen (in green) as a function of the temperature for the steel 1.

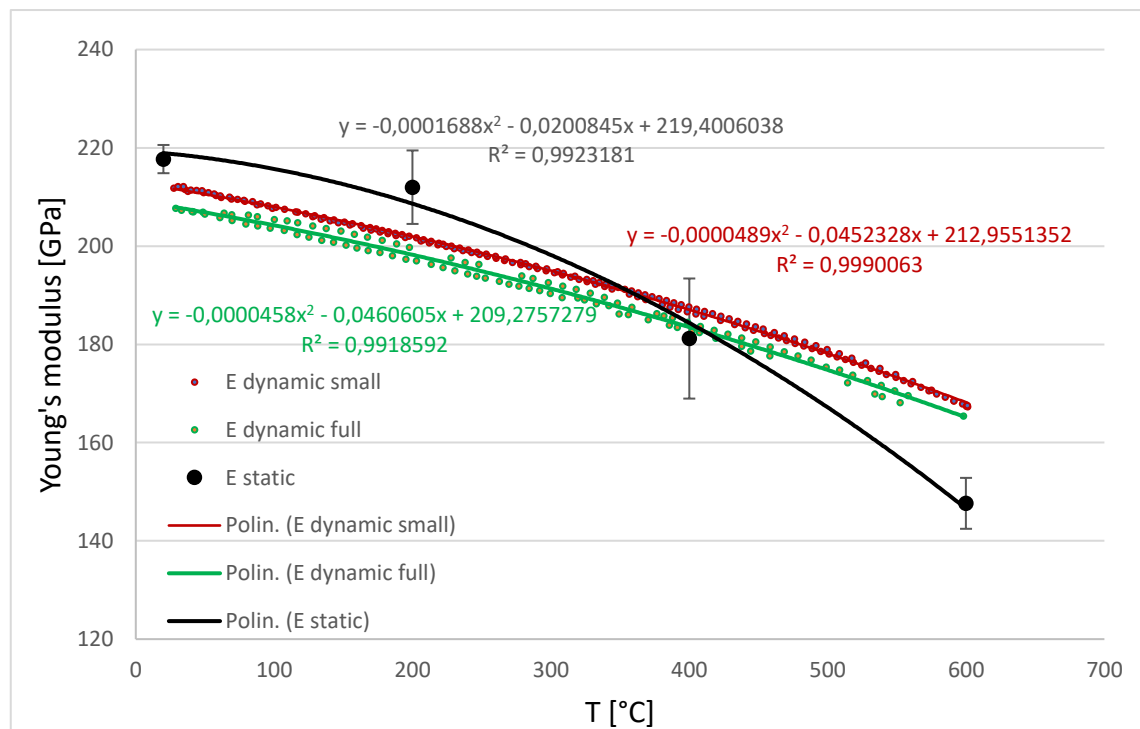


Figure 150: Static and dynamic Young's modulus as a function of the temperature for the steel 1

The trendlines are:

- $E_{\text{static}} = -0,0001688T^2 - 0,0200845T + 219,4006038$
- $E_{\text{dynamic small}} = -0,0000489T^2 - 0,0452328T + 212,9551352$
- $E_{\text{dynamic full}} = -0,0000458T^2 - 0,0460605T + 209,2757279$

The figure 151 shows the behavior of static Young's modulus (in black), dynamic Young's modulus of small specimen (in red) and dynamic Young's modulus of full size specimen (in green) as a function of the temperature for the steel 2.

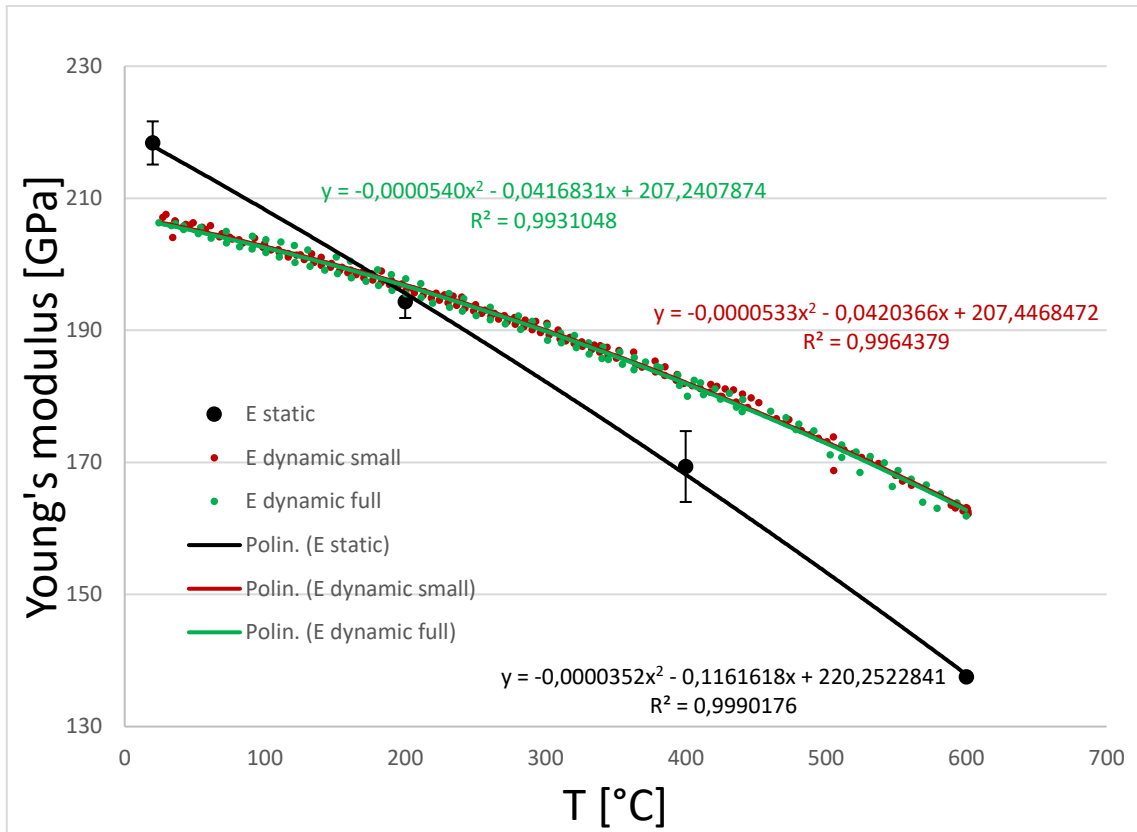


Figure 151: Static and dynamic Young's modulus as a function of the temperature for the steel 2

The trendlines are:

- $E_{\text{static}} = -0,0000352T^2 - 0,1161618T + 220,2522841$
- $E_{\text{dynamic small}} = -0,0000533T^2 - 0,0420366T + 207,4468472$
- $E_{\text{dynamic full}} = -0,0000540T^2 - 0,0416831T + 207,2407874$

The figure 152 shows the behavior of static Young's modulus (in black), dynamic Young's modulus of small specimen (in red) and dynamic Young's modulus of full size specimen (in green) as a function of the temperature for the steel 3.

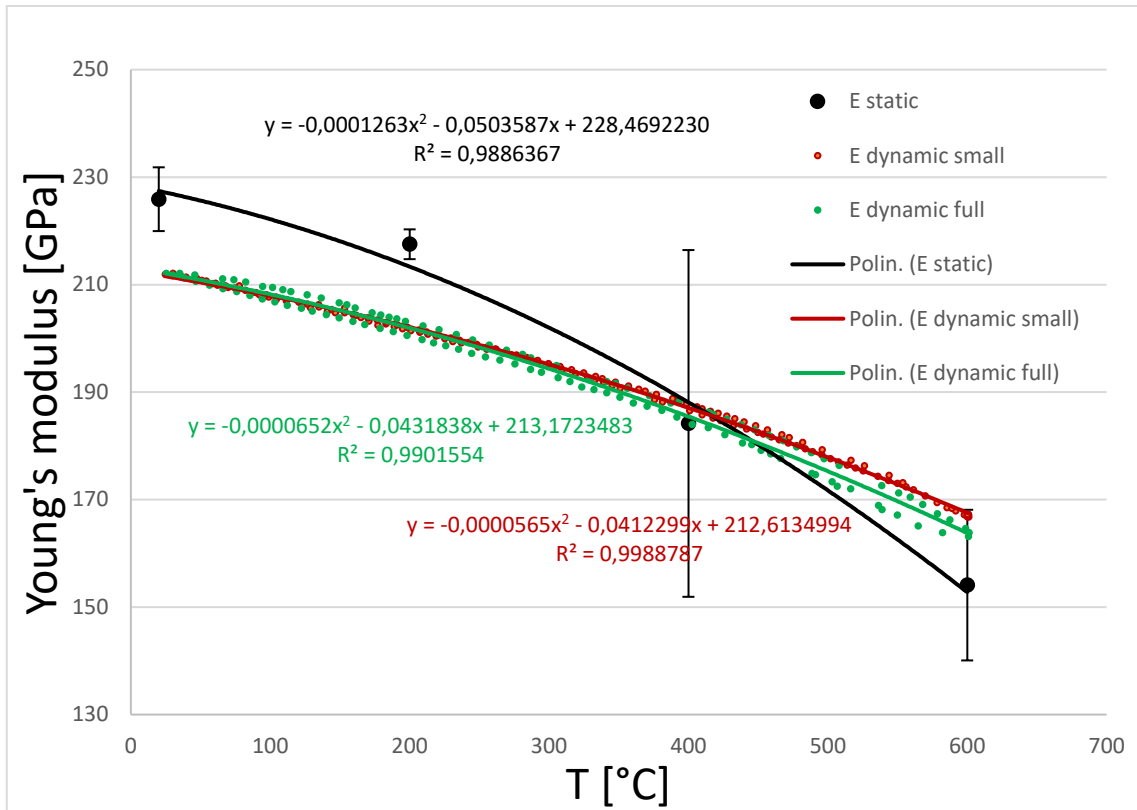


Figure 152: Static and dynamic Young's modulus as a function of the temperature for the steel 3

The trendlines are:

- $E_{\text{static}} = -0,0001263T^2 - 0,0503587T + 228,4692230$
- $E_{\text{dynamic small}} = -0,0000565T^2 - 0,0412299T + 212,6134994$
- $E_{\text{dynamic full}} = -0,0000652T^2 - 0,0431838T + 213,173483$

Regarding the steel 1, the gap between the two curves of dynamic Young's modulus may result from the mistakes in the measurements of the geometrical dimensions.

It is shown an example of how to a little variation in the geometrical dimensions can affect the results:

- the volumes of the two specimens are calculated how the product of the length times the thickness and the width. (The measured geometrical dimensions are in the table 48).
- The density is the ratio of the mass to volume; for the small specimen it is $7851,7 \text{ kg/m}^3$ and for the full size it is $7763,2 \text{ kg/m}^3$. This difference is not negligible because if it tries to calculate a second Young's modulus for the small specimen using the density of the full sizes specimen, the results is different.

- The formula to use is: $E = 0,9465 \left(\frac{mf_f^2}{b} \right) \left(\frac{L^3}{t^3} \right) T_1$, where f_f , L , b , t and T_1 are parameters of the small specimen and m is the product of the density of the full size specimen and the volume of small specimen. All of this leads to a new Young's modulus of 208,88 GPa against the previous value of 211,26 GPa; the difference of about 2,5 GPa. The same can be repeated for the full size specimen (f_f , L , b , t and T_1 of the full size specimen and density of the small specimen). In this situation the dynamic Young's modulus passes from 205,80 to 208,14 GPa; the difference is higher than 2 GPa.

Steel 1	Small	Full size
Mass (g)	7,057	198,1
length (mm)	29,982	80,056
width (mm)	9,95	35,036
thickness (mm)	3,013	9,096
flex freq (Hz)	17304,6	7210,83
T1	1,0665	1,0850
volume mm ³	898,841	25512,8
density (kg/m ³)	7851,7	7763,2
E (GPa)	211,26	205,80
With density 7851,7 kg/m³		
E' (GPa)		208,14
With density 7763,2 kg/m³		
E'' (GPa)	208,88	

Table 48: Mistakes in geometrical measurements can lead to a variation of Young's modulus

The comparison between static Young's modulus of the three steels is in figure 153:

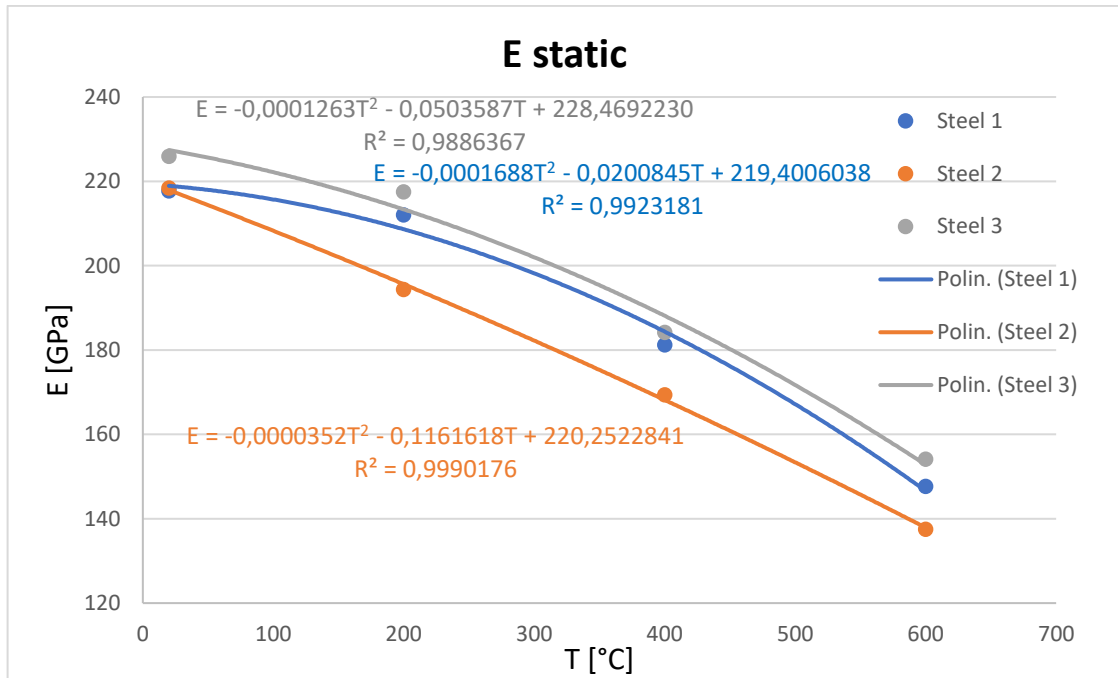


Figure 153: Comparison between static Young's modulus of three steels

The comparison between dynamic Young's modulus of the three steels is in figure 154:

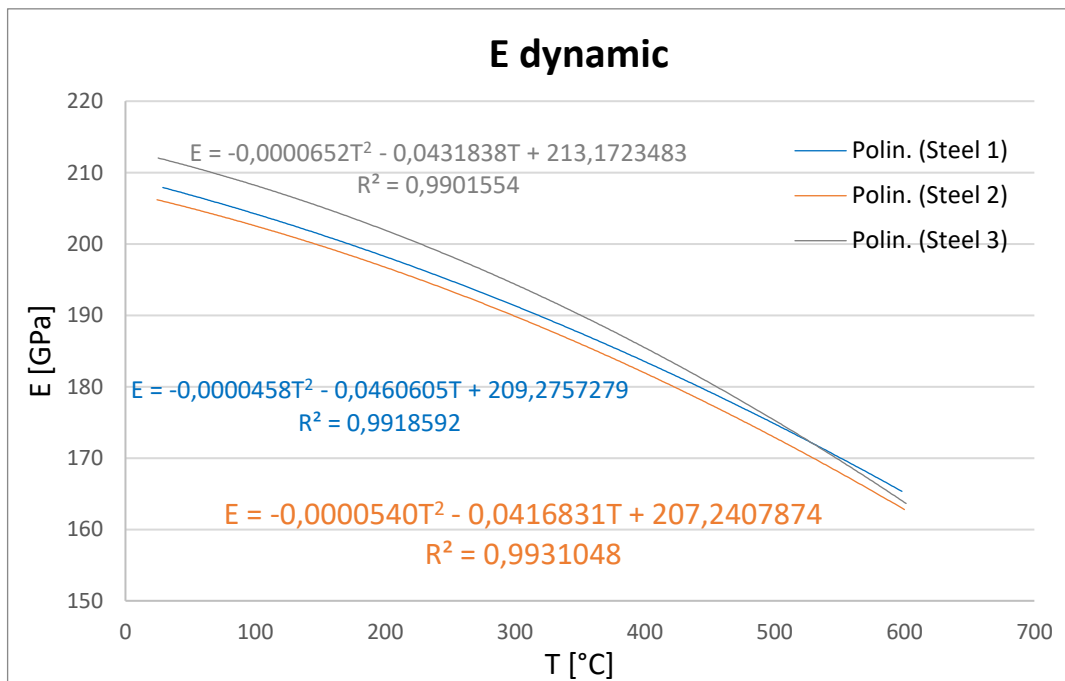


Figure 154: Comparison between dynamic Young's modulus of three steels

Dynamic Young's moduli of the three steel are grouped in a smaller range than static Young's moduli; moreover, the first ones present a more similar behavior than the seconds.

3.7 Relationships between dynamic and static Young's moduli for small and full size

For the steel 1, the relationship between dynamic and static Young's modulus is shown in the figure 155.

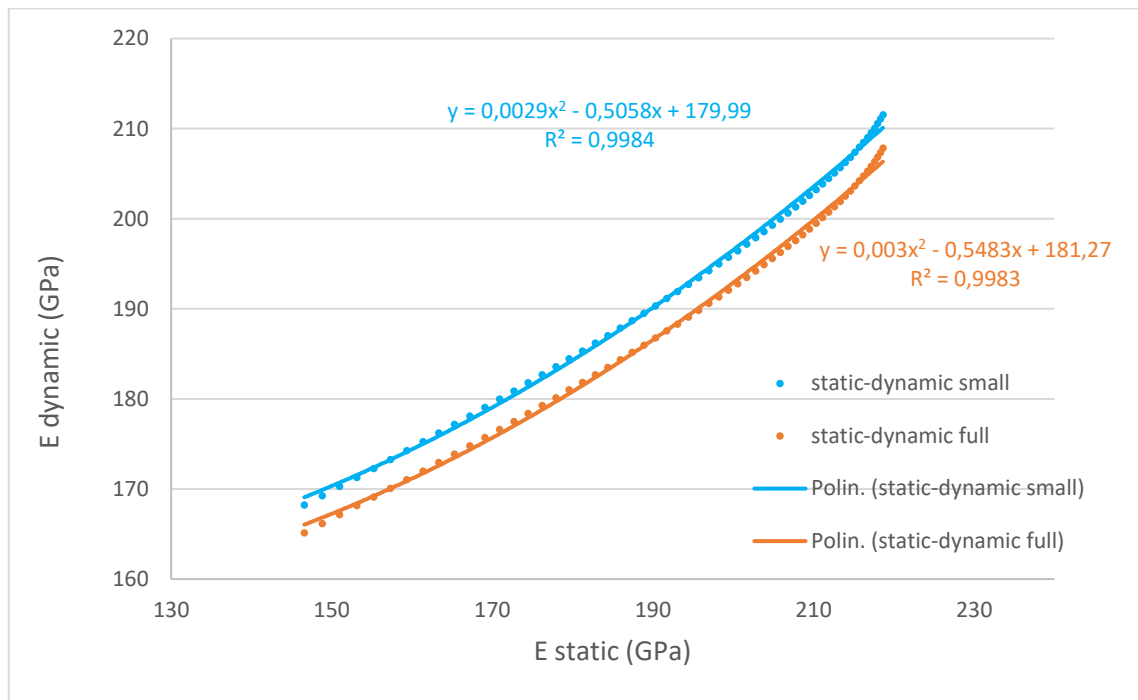


Figure 155: Relationship between static and dynamic Young's modulus (steel 1)

For the steel 1, the equations which relates dynamic Young's modulus of small specimen to static Young's modulus and dynamic Young's modulus of full size specimen to static Young's modulus are: (y is E_{dynamic} and x is E_{static})

- E_{dynamic} small specimens – E_{static} : $y = 0,0029x^2 - 0,5058x + 179,99$
- E_{dynamic} full size specimens – E_{static} : $y = 0,003x^2 - 0,5483x + 181,27$

For the steel 2, the relationship between dynamic and static Young's modulus is shown in the figure 156.

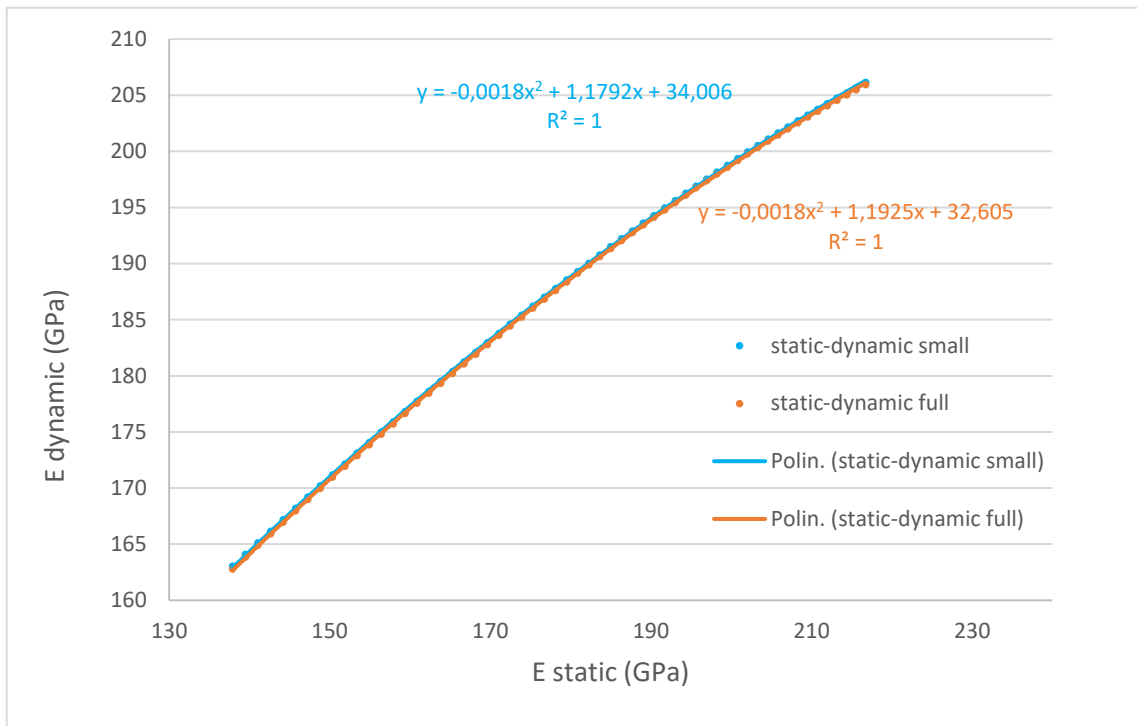


Figure 156: Relationship between static and dynamic Young's modulus (steel 2)

For the steel 2, the equations which relates dynamic Young's modulus of small specimen to static Young's modulus and dynamic Young's modulus of full size specimen to static Young's modulus are: (y is E_{dynamic} and x is E_{static})

- E_{dynamic} small specimens – E_{static} : $y = -0,0018x^2 + 1,1792x + 34,006$
- E_{dynamic} full size specimens – E_{static} : $y = -0,0018x^2 + 1,1925x + 32,605$

For the steel 3, the relationship between dynamic and static Young's modulus is shown in the figure 157.

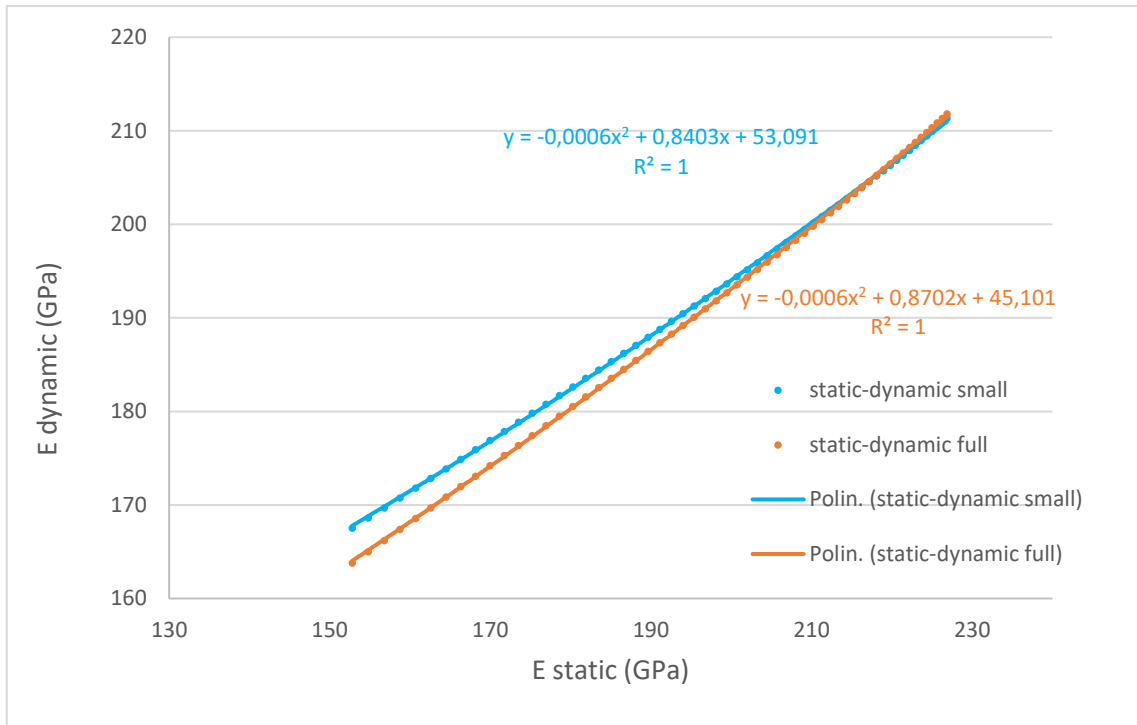


Figure 157: Relationship between static and dynamic Young's modulus (steel 2)

For the steel 3, the equations which relates dynamic Young's modulus of small specimen to static Young's modulus and dynamic Young's modulus of full size specimen to static Young's modulus are: (y is $E_{dynamic}$ and x is E_{static})

- $E_{dynamic}$ small specimens – E_{static} : $y = -0,0006x^2 + 0,8403x + 53,091$
- $E_{dynamic}$ full size specimens – E_{static} : $y = -0,0006x^2 + 0,8702x + 45,101$

Since the three steels are used for the turbine, a general linear trendline for the three steels is drawn in the figure 158:

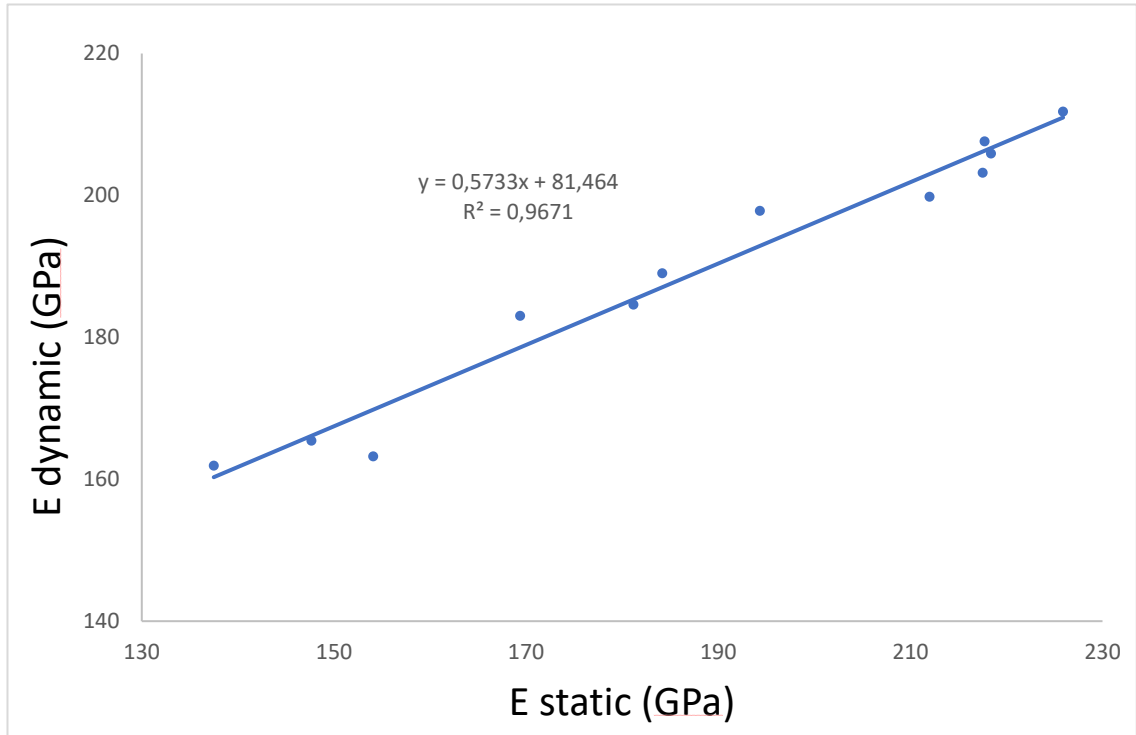


Figure 158: General equation for three steels which correlate static and dynamic Young's modulus of the three steels

Conclusion

The objectives of this work are:

- finding a relationship between Young's modulus and temperature;
- searching a correlation between static and dynamic Young's modulus.

The experimental techniques used are tensile test and impulse excitation. Impulse excitation is a quick, simple and non-destructive technique adopted to measure dynamic Young's modulus; it presents a good accuracy of the results, which do not depend on the operator and the laboratories where the tests are performed. Moreover, impulse excitation technique does not require standard specimens and can be used to calculate dynamic shear modulus and Poisson's ratio in just one test at high or cryogenic temperature.

A part of this work consists in finding a relationship between static and dynamic Young's modulus to pass, through an equation, from the dynamic modulus to the static modulus, which has several complex aspects in its calculation and high scatter in his results.

In this work, to determinate static Young's modulus, tensile tests are performed according with the standards BS EN ISO 6892-1:2016 and BS EN ISO 6892-2:2015 while for dynamic Young's modulus, impulse excitation technique is adopted according the standard ASTM1876-15.

The selected material are three turbine steels and for each of them the equations which link static and dynamic Young's modulus are in paragraph 3.7. Even if the desired results have been achieved the study of these and other turbine steels will continue and can be improved.

Regarding static Young's modulus, it would be useful to perform tests on more specimens, at different strain rates, and compare the results with those of other techniques as nanoindentation and three-point bending, while the results of impulse excitations technique could be compared with those of sonic resonance technique; moreover, using different specimens with different shapes (disks), in accordance with the standard ASTM E1876-15, would be useful for the purposes of this research.

Bibliography

- [1] <https://www.britannica.com/science/Youngs-modulus>
- [2] Marc Meyers, Krishan Chaw, “Mechanical Behavior of MATERIALS”, 2009, pagg. 120-125.
- [3] <https://www.nuclear-power.net/nuclear-engineering/materials-science/material-properties/strength/hookes-law/unit-of-youngs-modulus-of-elasticity/>
- [4] https://www.engineeringtoolbox.com/young-modulus-d_773.html
- [5] https://it.wikipedia.org/wiki/Modulo_di_elasticit%C3%A0#:~:text=Il%20modulo%20di%20elasticit%C3%A0%20%C3%A8,la%20deformazione%20che%20ne%20deriva.
- [6] BS EN ISO 6892-1:2016, “Part 1: Method of test at room temperature”, *Metallic materials — Tensile testing*.
- [7] ASTM E111 – 17, “Standard Test Method for Young’s Modulus, Tangent Modulus, and Chord Modulus”, 9.
- [8] BS EN ISO 6892-2:2015, “Part 2: Method of test at elevated temperature”, *Metallic materials — Tensile testing*.
- [9] ASTM E1876 – 15, “Standard Test Method for Dynamic Young’s Modulus, Shear Modulus, and Poisson’s Ratio by Impulse Excitation of Vibration”, 17.
- [10] RFDA Professional System 24 – User manual – v3.7.
- [11] C. K. Bullough, “The Determination of Uncertainties in Dynamic Young’s Modulus”, *SM&T Manual of Codes of*

Practice for the Determination of Uncertainties in Mechanical Tests on Metallic Materials n. 13, 2000.

- [12] ASTM E2769–18, “Standard Test Method for Elastic Modulus by Thermomechanical Analysis Using Three-Point Bending and Controlled Rate of Loading”.
- [13] Fischer-Cripps, “The IBIS Handbook of Nanoindentation”, 2013.
- [14] ASTM E1875-20a, “Standard Test Method for Dynamic Young’s Modulus, Shear Modulus, and Poisson’s Ratio by Sonic Resonance
- [15] <https://matmatch.com/materials/minfm32852-sew-555-grade-28crmoniv4-9-quenched-and-tempered-qt->
- [16] <https://search.totalmateria.com/MaterialDetails/MaterialDetail?vkKey=1046698&keyNum=1757&type=12&hs=0>
- [17] <https://wiam.de/en/sectors/>
- [18] <https://search.totalmateria.com/MaterialDetails/MaterialDetail?vkKey=1518383&keyNum=2&type=3&hs=0>
- [19] BS EN ISO 9513:2012, “Metallic materials — Calibration of the extensometer system used in uniaxial testing”.
- [20] RFDA HT650 (HT1050) – User manual v3.0.
- [21] R. Rahemi, D. Li, “Variation in electron work function with temperature and its effect on the Young's modulus of metals”, 5, 2015.
- [22] Bruno A. Latella, Samuel R. Humphries, “Young’s modulus of a 2.25Cr-1Mo steel at elevated temperature”, *Scripta materialia*, 20.
- [23] Wei-yong Wang, Bing Liu and Venkatesh Kodur, “Effect of Temperature on Strength and Elastic Modulus of High-Strength Steel”, 9, 2013.

